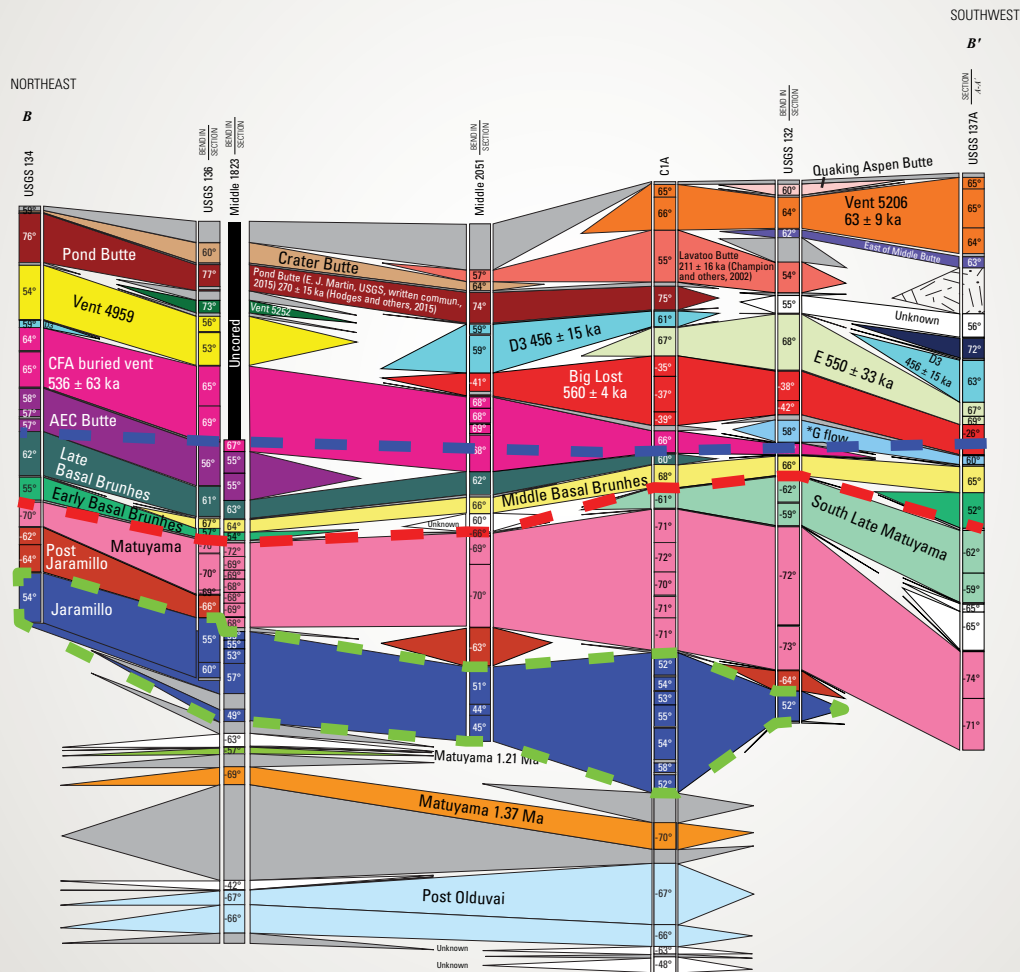


DOE/ID-22240

Prepared in cooperation with the U.S. Department of Energy

Paleomagnetic Correlation of Basalt Flows in Selected Coreholes near the Advanced Test Reactor Complex, the Idaho Nuclear Technology and Engineering Center, and along the Southern Boundary, Idaho National Laboratory, Idaho



Scientific Investigations Report 2016-5131

Cover: Subsurface cross section of stratigraphic units trending west of the Advanced Test Reactor Complex to the southern boundary of the Idaho National Laboratory, Idaho.

Paleomagnetic Correlation of Basalt Flows in Selected Coreholes near the Advanced Test Reactor Complex, the Idaho Nuclear Technology and Engineering Center, and along the Southern Boundary, Idaho National Laboratory, Idaho

By Mary K.V. Hodges and Duane E. Champion

DOE/ID-22240
Prepared in cooperation with the U.S. Department of Energy

Scientific Investigations Report 2016–5131

U.S. Department of the Interior
U.S. Geological Survey

U.S. Department of the Interior
SALLY JEWELL, Secretary

U.S. Geological Survey
Suzette M. Kimball, Director

U.S. Geological Survey, Reston, Virginia: 2016

For more information on the USGS—the Federal source for science about the Earth, its natural and living resources, natural hazards, and the environment—visit <http://www.usgs.gov> or call 1–888–ASK–USGS.

For an overview of USGS information products, including maps, imagery, and publications, visit <http://store.usgs.gov>.

Any use of trade, firm, or product names is for descriptive purposes only and does not imply endorsement by the U.S. Government.

Although this information product, for the most part, is in the public domain, it also may contain copyrighted materials as noted in the text. Permission to reproduce copyrighted items must be secured from the copyright owner.

Suggested citation:

Hodges, M.K.V., and Champion, D.E., 2016, Paleomagnetic correlation of basalt flows in selected coreholes near the Advanced Test Reactor Complex, the Idaho Nuclear Technology and Engineering Center, and along the southern boundary, Idaho National Laboratory, Idaho: U.S. Geological Survey Scientific Investigations Report 2016-5131 (DOE/ID-22240), 65 p., 1 pl., <http://dx.doi.org/10.3133/sir20165131>.

ISSN 2328-0328 (online)

Contents

Abstract.....	1
Introduction.....	1
Purpose and Scope	3
Previous Investigations.....	3
Geologic Setting.....	6
Sampling and Analytical Techniques	7
Geomagnetic Framework	8
Basalt Flow Labeling Conventions	8
Corehole USGS 137A.....	8
Correlation Techniques.....	8
Paleomagnetic Correlations of Basalt Flows	9
Cross Section <i>A–A'</i>	9
Cross Section <i>B–B'</i>	13
Cross Section <i>C–C'</i>	16
Summary and Conclusions.....	19
Acknowledgments.....	20
References Cited.....	20
Appendix A. Previously Unpublished Paleomagnetic Data.....	27

Plate

1. Map and subsurface stratigraphic cross sections interpreted from paleomagnetic inclination data from coreholes in the southern part of the Idaho National Laboratory, Idaho. download at <http://dx.doi.org/10.3133/sir20165131>

Figures

1. Map showing location of study area, selected facilities, volcanic vents, coreholes, and Arco-Big Southern Butte and Axial volcanic zones, Idaho National Laboratory, Idaho.....2
2. Diagram showing geomagnetic time scale.....4

Tables

1. Selected previous investigations on geology, paleomagnetism, and stratigraphy of the eastern Snake River Plain and Idaho National Laboratory, Idaho5

Conversion Factors

United States Customary Units to International System of Units

Multiply	By	To obtain
Length		
inch (in.)	2.54	centimeter (cm)
inch (in.)	25.4	millimeter (mm)
foot (ft)	0.3048	meter (m)
mile (mi)	1.609	kilometer (km)
Area		
square mile (mi ²)	2.590	square kilometer (km ²)
Volume		
cubic mile (mi ³)	4.168	cubic kilometer (km ³)

International System of Units to United States Customary Units

Multiply	By	To obtain
Length		
centimeter (cm)	0.3937	inch (in.)
meter (m)	3.281	foot (ft)
Volume		
square kilometer (km ²)	247.1	acre

Temperature in degrees Celsius (°C) may be converted to degrees Fahrenheit (°F) as:

$$^{\circ}\text{F} = (1.8 \times ^{\circ}\text{C}) + 32.$$

Datums

Vertical coordinate information is referenced to the National Geodetic Vertical Datum of 1929 (NGVD 29).

Horizontal coordinate information is referenced to the North American Datum of 1927 (NAD 27).

Altitude, as used in this report, refers to distance above the vertical datum.

Abbreviations

AEC	U.S. Atomic Energy Commission
AF	alternating field
Ar	argon
ARA	Auxiliary Reactor Area
ATR	Complex Advanced Test Reactor Complex
AVZ	Axial Volcanic Zone
CFA	Central Facilities Area
DOE	Department of Energy
EBB	Early Basal Brunhes
EMB	East of Middle Butte flow
ESRP	eastern Snake River Plain
INL	Idaho National Laboratory
INEL	Idaho National Engineering Laboratory
INEEL	Idaho National Engineering and Environmental Laboratory
IRM	isothermal remanent magnetization
K2O	potassium oxide
Ka	thousand years
LBB	Late Basal Brunhes
Ma	million years
MBB	Middle Basal Brunhes
NRTS	National Reactor Testing Station
RWMC	Radioactive Waste Management Complex
SCFABVU	South CFS Buried Vent Upper
SLM	South Late Matuyama
USGS	U.S. Geological Survey

Paleomagnetic Correlation of Basalt Flows in Selected Coreholes near the Advanced Test Reactor Complex, the Idaho Nuclear Technology and Engineering Center, and along the Southern Boundary, Idaho National Laboratory, Idaho

By Mary K.V. Hodges and Duane E. Champion

Abstract

The U.S. Geological Survey, in cooperation with the U.S. Department of Energy, used paleomagnetic data from 18 coreholes to construct three cross sections of subsurface basalt flows in the southern part of the Idaho National Laboratory (INL). These cross sections, containing descriptions of the subsurface horizontal and vertical distribution of basalt flows and sediment layers, will be used in geological studies, and to construct numerical models of groundwater flow and contaminant transport.

Subsurface cross sections were used to correlate surface vents to their subsurface flows intersected by coreholes, to correlate subsurface flows between coreholes, and to identify possible subsurface vent locations of subsurface flows. Correlations were identified by average paleomagnetic inclinations of flows, and depth from land surface in coreholes, normalized to the North American Datum of 1927. Paleomagnetic data were combined, in some cases, with other data, such as radiometric ages of flows. Possible vent locations of buried basalt flows were identified by determining the location of the maximum thickness of flows penetrated by more than one corehole.

Flows from the surface volcanic vents Quaking Aspen Butte, Vent 5206, Mid Butte, Lavatoo Butte, Crater Butte, Pond Butte, Vent 5350, Vent 5252, Tin Cup Butte, Vent 4959, Vent 5119, and AEC Butte are found in coreholes, and were correlated to the surface vents by matching their paleomagnetic inclinations, and in some cases, their stratigraphic positions.

Some subsurface basalt flows that do not correlate to surface vents, do correlate over several coreholes, and may correlate to buried vents. Subsurface flows which correlate across several coreholes, but not to a surface vent include the D3 flow, the Big Lost flow, the CFA buried vent flow, the

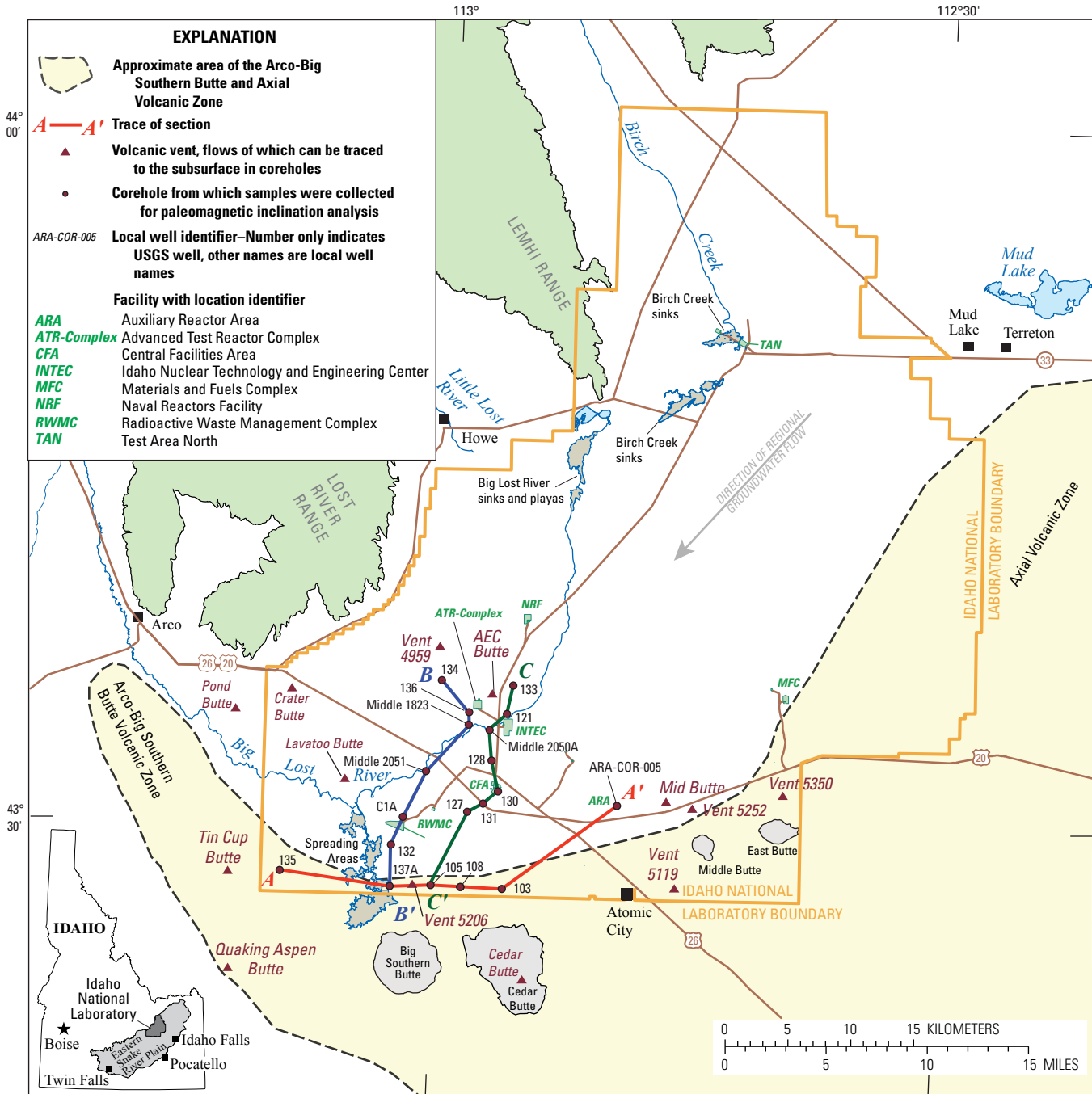
Early, Middle, and Late Basal Brunhes flows, the South Late Matuyama flow, the Matuyama flow, and the Jaramillo flow. The location of vents buried in the subsurface by younger basalt flows can be inferred if their flows are penetrated by several coreholes, by tracing the flows in the subsurface, and determining where the greatest thickness occurs.

Introduction

The U.S. Atomic Energy Commission ([AEC], now the U.S. Department of Energy [DOE]) established the National Reactor Testing Station (NRTS) overlying about 890 mi² of the eastern Snake River Plain (ESRP) in southeastern Idaho in 1949. The NRTS was established to develop peacetime atomic energy, nuclear safety research, defense programs, and advanced energy concepts. The name of the laboratory has been changed to reflect changes in the research focus of the laboratory. Names formerly used for the laboratory, from earliest to most recent, were the National Reactor Testing Station ([NRTS] 1949–74), the Idaho National Engineering Laboratory ([INEL] 1974–97), and the Idaho National Engineering and Environmental Laboratory ([INEEL] 1997–2005). The laboratory has been known as the Idaho National Laboratory (INL) (fig. 1) since 2005.

U.S. Geological Survey (USGS) scientists have been studying the geology, petrography, paleomagnetism, age of basalt flows, and hydrology of the ESRP for more than 100 years beginning with Russell (1902). Studies of the geologic framework of the ESRP at and near the INL intensified in 1949 when feasibility studies for siting of the NRTS began. Studies included evaluation of hydraulic properties of the aquifer, seismic and volcanic hazards, facility design and construction, and the evolution of basaltic volcanism on the ESRP.

2 Paleomagnetic Correlation of Basalt Flows in Coreholes, Idaho National Laboratory, Idaho



Base from U.S. Geological Survey digital data, 1:24,000 and 1:100,000
 Universal Transverse Mercator projection, Zone 12
 Datum is North American Datum of 1927

Figure 1. Location of study area, selected facilities, volcanic vents, coreholes, and Arco-Big Southern Butte and Axial volcanic zones, Idaho National Laboratory, Idaho.

Since activities at INL began wastewaters containing chemical and radiochemical wastes were discharged to ponds and wells, and solid and liquid wastes were buried in trenches and pits excavated in surficial sediments at the INL. Some wastewater continues to be disposed to infiltration and evaporation ponds. Concern about subsurface movement of contaminants from these wastes increased the number and kinds of studies of subsurface geology and hydrology to provide information for conceptual and numerical groundwater flow and contaminant transport models (Anderson and Lewis, 1989; Anderson, 1991; Anderson and Bartholomay, 1995; Anderson and Bowers, 1995; Anderson and Liszewski, 1997; Anderson, Ackerman, and others, 1996; Anderson, Liszewski, and Ackerman, 1996; Ackerman and others, 2006, 2010).

Basaltic lava flows, eruptive fissures and vents, and fluvial and eolian sediments differ greatly in hydraulic conductivity, and the three-dimensional distribution of these materials controls groundwater movement in the Snake River Plain aquifer (Welhan and others, 2002). Lava flows comprise more than 85 percent of the volume of the subsurface of the ESRP (Kuntz and others, 1992). Sedimentary interbeds comprise the rest. Paleomagnetic inclination and polarity studies on samples from subsurface drill cores and surface samples provide valuable data constraining the age and extent of basalt flows. Data from paleomagnetic studies at and near the INL (Champion and Greeley, 1978; Champion and others, 1981, 1988) also have been used to document paleomagnetic secular variation (Hagstrum and Champion, 2002) during late Pleistocene to Holocene time. The Big Lost Reversed Polarity Cryptochron (formerly referred to as the Big Lost Reversed Polarity Subchron [fig. 2; Champion and others, 1988]) of the Brunhes Normal Polarity Chron was first identified in subsurface ESRP basalts at the Idaho National Laboratory (Champion and others, 1981, 1988).

Paleomagnetic inclination data were used to correlate subsurface basalt flows based on similar inclination measurements and polarity. The subcore plugs collected from drill cores and used in this study yield only paleomagnetic inclination data, because the original declination of the drill cores is not preserved during drilling. Other data, such as lithology, petrology, geophysical logs, and geochemistry, can be used in conjunction with paleomagnetic inclination and age data to confirm or reject correlations.

Purpose and Scope

Knowledge about the surface and subsurface geologic framework of the ESRP is needed to aid in refining conceptual and numerical groundwater flow and contaminant transport models at and near the INL. The solid part of the aquifer below the INL is mostly composed of basalt and sediment, but sediment is volumetrically minimal, averaging 15 percent or less of the volume of the subsurface. Despite the small volume

of sediment, subsurface sediments have a great influence on groundwater movement. Nearly all subsurface sediments are loess, a fine-grained material deposited by wind. Sediment layers cannot be distinguished one from another, except by the basalt layers that overlie and underlie them, so sediment layers are illustrated in the cross sections, but not described.

Paleomagnetic data were used to correlate surface and subsurface stratigraphy, determine relative ages, and, in conjunction with previous studies, determine the absolute age of certain basalt flows. Samples were collected from coreholes at depths of a few feet to 1,653 ft. Drill core samples were selected from individual lava flow units based on identification of flow tops and bottoms in the coreholes. Correlations were made using average paleomagnetic inclinations, radiometric and relative ages, and stratigraphic position in the subsurface.

This report describes subsurface stratigraphy derived from paleomagnetic inclination data and selected ages of basalt flows from drill cores (six along and near the south INL boundary, seven from near the Advanced Test Reactor Complex [ATR-Complex] to the south boundary of INL, and eight from the Idaho Nuclear Technology and Engineering Center [INTEC] to the INL southern boundary). This report presents previously unpublished paleomagnetic data for basalt flows from coreholes drilled at and near the Advanced Test Reactor Complex (ATR-Complex), the Idaho Nuclear Technology and Engineering Center (INTEC) and along the southern boundary of the INL.

Previous Investigations

Numerous geologic, paleomagnetic, and stratigraphic investigations on surface and subsurface basalts have been conducted at and near the INL and the ESRP. Selected previous investigations and the areas of investigation are summarized in table 1. Paleomagnetic data record the Earth's magnetic field at the time of eruption, and basalt flows of different ages may have identical paleomagnetic inclinations. Other data such as lithology, petrology, geophysical logs, and geochemistry must be used in conjunction with paleomagnetic and age data to confirm or reject correlations.

The stratigraphic framework for the conceptual model for groundwater flow (Ackerman and others, 2006) was based on a limited number of cores and natural gamma geophysical logs from uncored wells (Anderson and Lewis, 1989; Anderson, 1991; Anderson and Bartholomay, 1995; Anderson and Bowers, 1995; Anderson, Ackerman, and others, 1996; Anderson, Liszewski, and Ackerman, 1996; Anderson and Liszewski, 1997; Anderson, Kuntz, and Davis, 1999). More recent paleomagnetic stratigraphy studies (Champion and others, 2011, 2013) have been used to confirm this stratigraphic framework. This report is a more detailed comparison of the stratigraphy through the south-central part of the INL, where groundwater contamination occurred (Bartholomay and others, 2015).

Geomagnetic Time Scale

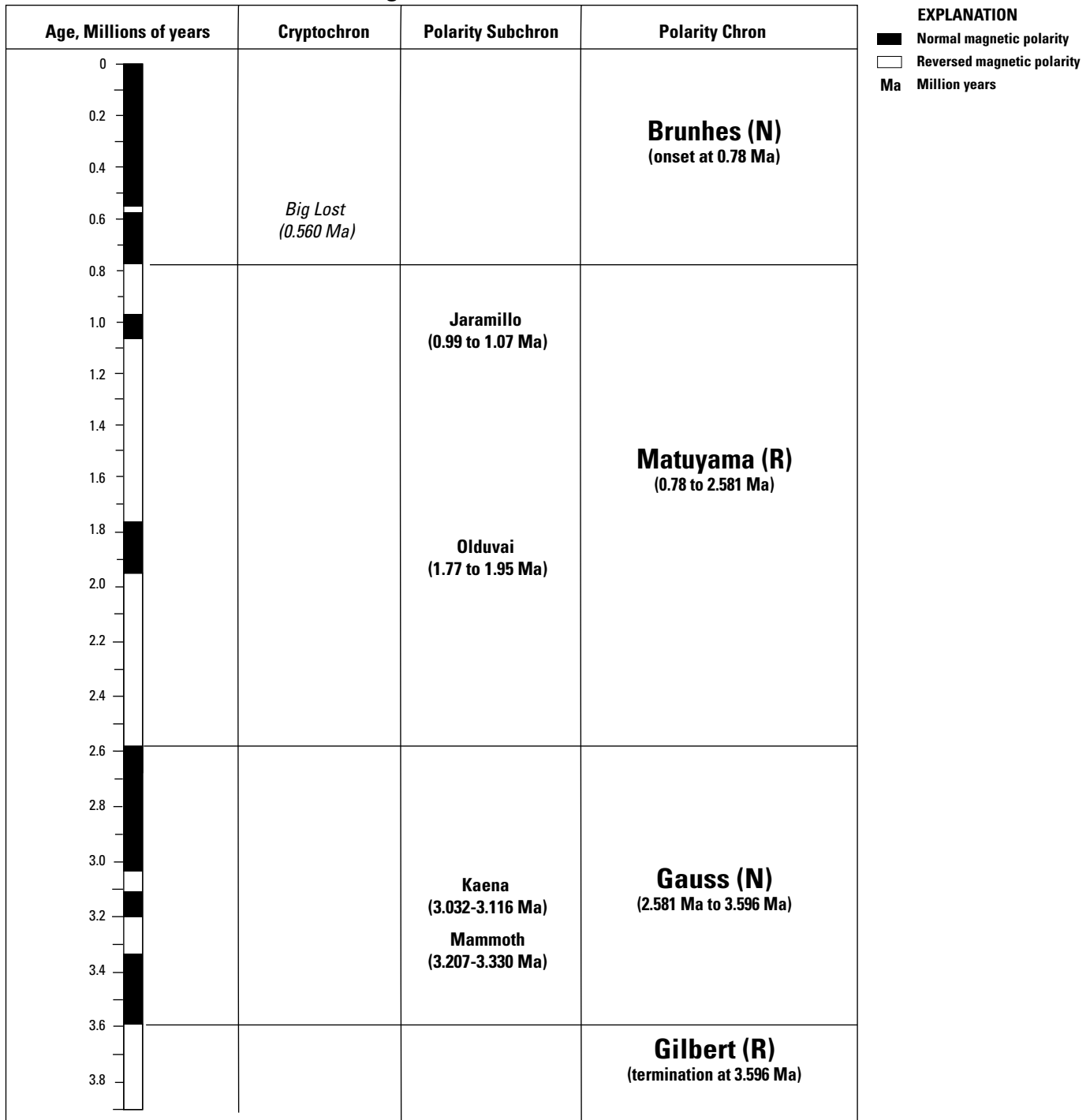


Figure 2. Geomagnetic time scale. Modified from Champion and others (1988), with new data from Ogg and Smith (2004).

Table 1. Selected previous investigations on geology, paleomagnetism, and stratigraphy of the eastern Snake River Plain and Idaho National Laboratory, Idaho.

[**Abbreviations:** CFA, Central Facilities Area; ESRP, eastern Snake River Plain; INL, Idaho National Laboratory; INTEC, Idaho Nuclear Technology and Engineering Center (also known as ICPP [Idaho Chemical Processing Plant]); K₂O, potassium oxide; NPR, New Production Reactor; NRF, Naval Reactors Facility; RWMC, Radioactive Waste Management Complex; SRP, Snake River Plain; TAN, Test Area North; USGS; U.S. Geological Survey]

Reference	Area of investigation	Reference summary
Anders and Sleep, 1992	ESRP	Thermal and mechanical effects of the Yellowstone hotspot
Anderson and Liszewski, 1997	INL	INL unsaturated and ESRP aquifer stratigraphy, based on core and natural gamma logs
Anderson, Ackerman, and others, 1996	INL	INL stratigraphy based on natural gamma logs
Anderson, Liszewski, and Ackerman, 1996	INL	INL surficial sediment thickness
Anderson and others, 1999	ESRP, INL, and vicinity	Geologic controls on hydraulic conductivity
Bestland and others, 2002	INL, Big Lost Trough	Sedimentary interbeds in the Big Lost Trough, corehole 2-2A
Braile and others, 1982	ESRP	Seismic profiling of ESRP
Champion and others, 1981	INL	Radiometric ages and paleomagnetism at corehole Site E (NPR Test)
Champion and others, 1988	INL	Radiometric ages and paleomagnetism at corehole Site E (NPR Test), description of Big Lost cryptochron
Champion and Herman, 2003	INL, INTEC area	Paleomagnetism of basalt from drill cores
Champion and others, 2002	INL and vicinity; ESRP	Accumulation and subsidence based on paleomagnetism and geochronology
Geslin and others, 2002	Big Lost Trough, INL	Pliocene and Quaternary river drainage and sediment
Grimm-Chadwick, 2004	INL, CFA	Stratigraphy, geochemistry, and descriptions of high K ₂ O flow in cores
Hackett and Smith, 1992	ESRP	Description of ESRP volcanism including development of Axial Volcanic Zone
Kuntz, 1978	INL, RWMC	Geology of RWMC area
Kuntz and others, 1980	INL, RWMC	Radiometric dating, paleomagnetism on cores from RWMC
Kuntz and others, 1986	ESRP	Radiocarbon dates on Pleistocene and Holocene basalt flows
Kuntz and others, 1992	ESRP	ESRP basaltic volcanism, including eruption styles, landforms, petrology, and geochemistry
Kuntz and others, 1994	INL	Geologic map of INL, including radiometric ages and paleomagnetism
Lanphere and others, 1994	INL, TAN cores	Petrography, age and paleomagnetism of basalt flows at and near TAN
Lanphere and others, 1993	INL, at and near NRF	Petrography, age and paleomagnetism of basalt flows at and near NRF
Mazurek, 2004	Central INL	Genetic alteration of basalt in SRP aquifer
Miller, 2007	INL, RWMC	Geochemistry, and descriptions of the B flow, and stratigraphy of corehole USGS 132
Morse and McCurry, 2002	INL	Base of the aquifer, alteration in basalts
Pierce and Morgan, 1992	ESRP	Age progression of Yellowstone hot spot
Pierce and others, 2002	ESRP	Age progression of Yellowstone hot spot
Reed and others, 1997	INL, ICPP	Geochemistry of lava flows in cores at ICPP
Rightmire and Lewis, 1987	INL, RWMC	Unsaturated zone geology, geochemistry of sediment and alteration products
Russell, 1902	Snake River Plain and aquifer	Geology and water resources of the Snake River Plain
Scarberry, 2003	INL, RWMC cores	Geochemistry of the F flow (now referred to as the Big Lost Reversed Polarity Cryptochron flows) and distribution in several coreholes at the INL
Shervais and others, 2006	INL, TAN cores	Cyclic geochemical variations in basalt in TAN drill cores
Stroup and others, 2008	INL	Statistical stationarity of sediment interbed thickness
Tauxe and others, 2004	SRP	Paleomagnetism of the Snake River Plain
Twining and others, 2008	INL	Construction diagrams, lithological, and geophysical logs for coreholes
Walker, 2000	ESRP	Volcanology of the Snake River Plain
Welhan and others, 2002	INL, ESRP	Morphology of inflated pahoehoe flows
Welhan and others, 2007	INL	Geostatistical modeling of sediment abundance
Wetmore and Hughes, 1997	INL	Model morphologies of subsurface lava flows
Wetmore and others, 1999	INL	Axial Volcanic Zone construction

Geologic Setting

The ESRP developed when the North American tectonic plate moved southwestward over a fixed upper mantle-melting anomaly beginning about 17 million years ago (Pierce and Morgan, 1992; Pierce and others, 2002; Morgan and McIntosh, 2005). Thermal disruption resulted in a time transgressive series of silicic volcanic fields, characterized by positive geoid anomalies, rhyolitic resurgent caldera eruptions, emplacement of a mid-crustal mafic sill, and subsidence with later basaltic plains magmatism (Braile and others, 1982; Anders and Sleep, 1992; Peng and Humphries, 1998; Rodgers and others, 2002; Shervais and others, 2006). Resurgent calderas of the Picabo volcanic field (10.2 ± 0.06 million years ago (Ma) to 7.9 ± 0.4 Ma (Kellogg and others, 1994; McCurry and Hughes, 2006)), and the Heise volcanic field (7.05 ± 0.04 Ma to 4.43 ± 0.08 Ma (Pierce and Morgan, 1992; Pierce and others, 2002; Morgan and McIntosh, 2005; McCurry and Hughes, 2006)) were active in the area now occupied by the INL.

The ESRP is subsiding in the wake of the Yellowstone hot spot calderas (Braile and others, 1982; Anders and Sleep, 1992; McQuarrie and Rodgers, 1998; Rodgers and others, 2002). The ESRP subsided as it was filled. Silicic material from the caldera eruptions, was followed by eastern Snake River Plain olivine tholeiite basalt, and eolian and fluvial sediments (Bestland and others, 2002; Blair, 2002; Geslin and others, 2002). Fluvial sediments can be identified, and correlated from corehole to corehole, in some cases, by detrital zircon analysis (Geslin and others, 2002). Eolian (loess) sediment layers cannot be distinguished from one another except by identifying the basalt flows that overlie and underlie them. The total volume of basalt filling the ESRP is estimated to be $9,600 \text{ mi}^3$ (Kuntz, 1992).

The ESRP is the type locality of basaltic plains volcanism (Greeley, 1982). This form of basaltic volcanism is intermediate in style between flood basalts, such as the Columbia River Basalt Group, and shield volcano eruptions, such as those in Hawaii and Iceland. Basaltic eruptions on the ESRP generated a land surface formed from coalesced shield volcanoes that produced voluminous tube-fed pahoehoe flows and fissure eruptions (Greeley, 1982). Basaltic plains volcanism is characterized by relatively low effusion rates, long recurrence intervals, low total volumes of lava erupted, and the prevalence of monogenetic volcanoes (Kuntz, 1992). ESRP shield volcanoes produce flows that range from about 3 to 131 ft thick. The extent of some ESRP flows may be as large as 155 mi^2 . Eastern Snake River Plain olivine tholeiite basalt flows may be as much as 22 mi long, and the accumulated volume of a shield volcano may be as large as 1.7 mi^3 (Kuntz and others, 1992). The flank areas of typical ESRP low shield volcanoes have slopes of less than 1 degree, and summit and vent areas have slopes of approximately 5 degrees (Greeley, 1982). Large, old vents are sometimes

preserved as low buttes surrounded by flows from younger vents; a good example is AEC Butte (fig. 1; Kuntz and others, 1994, 2003, 2007; Skipp and others, 2009).

More than 95 percent of the total volume of basalt in the ESRP is composed of tube-fed pahoehoe flows erupted from monogenetic shield volcanoes and lava cones (Kuntz and others, 1992). Basaltic lava fields, partially mantled with loess, cover the ESRP. The greatest numbers of eruptive centers are in the Axial Volcanic Zone ([AVZ]; fig. 1) (Hackett and Smith, 1992). The AVZ is a constructional volcanic highland that parallels the long axis of the ESRP (Hackett and Smith, 1992; Kuntz and others, 1992, 1994; Anderson and Liszewski, 1997; Anderson and others, 1999; Hughes and others, 1999; Wetmore and others, 1999).

Basaltic eruptions have occurred on the ESRP about every 32,000 to 140,000 years over the entire INL (Champion and others, 2002). Eruptions in the northern part of the INL occur at longer intervals, and the shortest recurrence interval eruptions occur on or near the axis of the ESRP in the AVZ. Accumulation rates are highest in and around the AVZ (fig. 1; Champion and others, 2002).

Most ESRP basalts are olivine tholeiites, the result of small quantities of magma that rise to the surface from subcrustal sources over short periods of time without significant fractionation or crustal contamination (Kuntz and others, 1992). Most basaltic lava flows at the INL are petrographically similar and contain olivine, plagioclase, clinopyroxene, ilmenite, magnetite, glass, and accessory apatite (Kuntz, 1978). Extrusive rocks of more evolved compositions also are found on the ESRP, but the volume of these rocks is small in comparison with the volume of olivine tholeiite basalts. Evolved composition lavas are exposed on the surface at the Cedar Butte eruptive center in the southern part of the INL and are found at depth in coreholes to the north and east of Cedar Butte (fig. 1, pl. 1) (Anderson, Ackerman, and others, 1996).

Most basalt flows and vents on the surface in the southern part of the INL have normal polarity. These basalt flows and vents erupted during the Brunhes Normal Polarity Chron, indicating that they are less than 0.78 Ma in age (fig. 2). Some surface basalt flows and vents in the northern part of the INL have reversed magnetic polarity and erupted during the Matuyama Reversed Polarity Chron (2.581–0.78 Ma) (fig. 2, modified from Champion and others, 1988, with new data from Ogg and Smith, 2004).

A young, reversed polarity basalt flow was detected at depths of 324–765 ft in coreholes C1A, ARA-COR-005, and USGS 127, 130, 131, 132, and 135 in the southern INL area. The geomagnetic polarity event that occurred during the eruption of this flow was named as the Big Lost Reversed Polarity Subchron (565 ± 14 thousand years [ka]) by Champion and others (1988) and revised to 560 ± 4 ka in Hodges and others (2015). The magnetic polarity cryptochron identified in this flow has since been reclassified as the Big Lost Reversed Polarity Cryptochron, and the flow, which

was labeled as the “F” flow in previous studies (Anderson, Ackerman, and others, 1996; Scarberry, 2003), and now is labeled the Big Lost flow. Big Lost flows that erupted during the Big Lost Reversed Polarity Cryptochron show rapidly changing magnetic inclinations, from -47 degrees in USGS 131 to -26 degrees in USGS 137A, coreholes that are roughly 5 mi apart (pl. 1). The stratigraphically lower Big Lost flows generally show steeper inclinations, and those flows emplaced above them show less steep inclinations, which may indicate that the ambient magnetic field present at the time of the Big Lost Reversed Polarity Cryptochron was changing rapidly (Champion and others, 1988).

Sampling and Analytical Techniques

The drill cores collected for this study were logged and sampled using INL Lithologic Core Storage Library protocols described in Davis and others (1997). Prior to sampling, the core materials were described and the tops and bottoms of lava flows and flow units were identified. A lava flow unit is defined herein as the minimum subdivision of a lava flow, possessing quenched bottom and top surfaces, and typically part of a nearly contemporaneous group of other lava flow units. Depths were measured by tape in feet and tenths of a foot from known marks recorded on wooden plugs or footage marked on the cores in the core boxes at the drill site. The wooden plugs are placed, or marks on cores are made by the drillers at the time of coring, and the recorded measured depths are logged at the end of each core run.

Attempts were made to take seven paleomagnetic samples from each identified lava flow or flow unit when enough core material was available. Using a drill press with a diamond-coring bit, a 1-in. diameter core plug was drilled at right angles to the vertical axis of the original core. This plug was drilled almost through the original core slug to maximize the amount of material to work with and to preserve the orientation and the precision of labeling of the plug. The drill cores are assumed to be vertical in their original drilling orientation to facilitate paleomagnetic study. Gyroscopic deviation logs of most wells were made at 10 ft intervals. Gyroscopic deviation logs document that there is usually less than 1 degree of corehole deviation from vertical, and thus, the deviations are no impediment to paleomagnetic remanent inclination interpretations. When deviations were greater than 1 degree, and occurred in a north–south vertical orientation, corrections to the data were applied ([appendix A](#)).

The core plugs were trimmed to 2.2-cm (0.87-in.) lengths, and the inclination, unoriented declination, and intensity of magnetizations were measured with a cryogenic magnetometer. Progressive alternating-field (AF) demagnetization using a commercial tumbling demagnetizer was performed on one sample from each core plug to remove any components of secondary magnetization. A common secondary magnetization is found on many core

plugs, imparted by the original drill string as a weak vertical downward isothermal remanent magnetization (IRM) and is easily removed. In rare instances, a much stronger IRM was imparted to a basalt flow by a lightning strike, while the flow was exposed on the land surface. The affected basalt flow was buried by subsequent basalt flows as the eastern Snake River Plain subsided. Lightning-induced secondary magnetization can penetrate 10 ft or more into the flow. Rare instances of a much stronger IRM imparted by a lightning strike to a previously exposed surface near the future corehole location also were observed. This lightning induced secondary magnetization can penetrate 10 ft or more along the vertical line of the corehole, and frequently cannot be removed. Average inclination measurements for each lava flow and 95 percent confidence limits about the average value were calculated using the method of McFadden and Reid (1982).

Following the preceding protocols and procedures, individual sample inclinations commonly are within ± 5 degrees of the average value of a single lava flow or flows of the same age. Above or below this depth interval, the inclination measurements obtained typically shift to center around a different steeper or shallower value. Notable exceptions to this common data distribution rule occur with samples collected from the uppermost parts of some lava flows as they are contacted with increasing depth. Samples with disparate inclination measurements typically are discarded and not included in the average inclination value of the lava flow(s).

The top of an underlying flow in a drill core may have been deformed, rotated, or both during emplacement, rendering the uppermost part of the flow unsuitable for paleomagnetic analysis ([fig. 2](#)). The depth range of samples near flow surfaces that need to be discarded typically is less than 3–7 ft.

The remanent magnetization of the top of any subsurface flow may be thermally remagnetized by subsequent eruption and emplacement of the overlying flow. Anomalous magnetizations because of this process are uncommon, but may be mistaken for rotation of the upper surface of a flow. Thermal remagnetization of flows is a minor process, probably because although molten basalt is erupted at about 1,100 °C, it will heat the surface of the underlying flow to half of this temperature (550 °C), less than the 585 °C Curie temperature of magnetite. Additionally, depending on the amount of time between eruptive events, even 1 ft of loess accumulation on the surface of the underlying flow may provide sufficient insulation to limit thermal remagnetization.

Thermal remagnetization frequently is detected on the contacts between flows of opposing polarity. Since 2000, the demagnetization protocol changed such that several samples below polarity boundaries were routinely thermally demagnetized. Formerly, samples were demagnetized using the AF protocol. Thermal demagnetization better separates the original magnetization from the secondary one imposed by the overlying flow.

8 Paleomagnetic Correlation of Basalt Flows in Coreholes, Idaho National Laboratory, Idaho

Every specimen collected from any flow recording the Big Lost Reversed Polarity Cryptochron was thermally demagnetized to remove the weak drill string IRM and to assess the relative declination orientations of overlying and underlying normal polarity flows, because they overprint and are overprinted, respectively, by subsequent flows. Assuming the bracketing normal polarity flows have declinations near 0 degree, an assessment of the declination of the Big Lost Reversed Polarity Cryptochron may be made. Champion and others (1988) provide further details of this analysis.

Geomagnetic Framework

The remanent magnetization recorded by ferrimagnetic minerals in basalt lava flows aligns with the geomagnetic field vector as the basalt crystallizes and cools. The local geomagnetic field vector varies with an average angular motion of 4–5 degrees per 100 years in latest Pleistocene and Holocene basalt flows, with extreme variance of 0–10 degrees per 100 years (Champion and Shoemaker, 1977). Snake River Plain monogenetic volcanic fields with volumes of 1 mi³ or more record a single direction of remnant magnetization, indicating that individual lava flows belonging to that flow erupted in a sufficiently brief period of time such that any change in the local geomagnetic field vector was too small to detect (less than 100 years). Each monogenetic volcano in this study most likely erupted for a few days to a few decades of time. The subcore plugs collected from drill cores and used in this study yielded only inclination data because the original declination was not preserved in the drill cores during drilling.

Basalt Flow Labeling Conventions

Champion and others (2011, 2013) used the term “basalt flow groups” to describe the eruptive products of a single monogenetic volcano, which have the same or related average paleomagnetic inclinations. However, the North American Stratigraphic Code states that “*A flow is the smallest formal lithostratigraphic unit of volcanic flow rocks. A flow is a discrete, extrusive, volcanic body distinguishable by texture, composition, order of superposition, paleomagnetism, or other objective criteria*” (North American Commission on Stratigraphic Nomenclature, 2005, p. 1,569). Therefore, this report will follow the terminology recommended by the Commission and use the term “basalt flow.”

Basalt flows are labeled for their vents, such as “Tin Cup Butte” (fig. 1), where a basalt flow can be traced from a vent exposed on the surface to core in the subsurface. Where surface to subsurface correlations are not possible, flows are labeled for chemical, spatial, or paleomagnetic identifiers. For example, a flow that has relatively large amounts of potassium oxide is labeled “High K₂O,” the reversed polarity flow that records the Big Lost Reversed Polarity Cryptochron

(Champion and others, 1981, 1988) is labeled “Big Lost,” a subsurface basalt flow that is thickest in the Central Facilities Area (CFA) is labeled the “CFA buried vent basalt flow” (modified from Champion and others, 2011), and a flow erupted during the Jaramillo Normal Polarity Subchron of the Matuyama Reversed Polarity Chron is labeled “Jaramillo” (fig. 2).

Many volcanoes on the ESRP do not have formal names. Informal names have been adopted for these vents, some of which have been in use at the INL and among ESRP researchers for many years. Some names came from spot elevations on 7.5' topographic maps, such as “Vent 5206.”

Corehole USGS 137A

Paleomagnetic data for corehole USGS 137A (appendix A), used in this report, represents data collected from USGS 137 and USGS 137A. USGS 137 was damaged during construction, the deepest core recovered was from 994 ft. USGS 137A is approximately 145 ft east northeast of USGS 137, and was air rotary drilled to the 984 ft, overlapping USGS 137 by approximately 10 ft. USGS 137A was then cored to the total depth of 1,317 ft. Paleomagnetic data was collected from USGS 137 and USGS 137A cores, and results were combined in one stratigraphic column. Data reported here from coreholes 137 and 137A are labeled 137A on cross sections (pl. 1).

Correlation Techniques

Following the protocol and procedures (see section, “[Sampling and Analytical Techniques](#)”), it is possible to subsample any drill core, obtain characteristic inclination and polarity data, and find an average for that data for any depth interval. The average inclination value may represent one flow unit over as little as 7 ft of depth, or represent data from a dozen or more flow units over more than about 300 ft of depth. In this report, the term “flow” refers to a package of flows from the same eruptive event (Kuntz and others, 1980). Basalt flows in each drill core can be characterized for polarity and average paleomagnetic inclinations over the entire length of the core. Basalt flows in nearby drill cores (hundreds of feet to a few miles apart) may be correlated at similar depth intervals having the same polarity and inclination measurements.

Correlation is less certain when coreholes are farther apart because flow similarities may be difficult to identify. Flows may pinch out before reaching the next drill core, or additional flows(s) may be present in that drill core. At distances of about 6 mi or greater, it still may be possible to correlate lava flows if they have the same petrography, polarity, and average inclination measurements, but the depths at which they correlate may be significantly different

(about \pm 50–100 ft) because of topographic or structural controls, or both, on flows during and after emplacement. Supporting data such as geophysical logs, geochemical analyses, and age dating experiments are necessary to make correlations when coreholes are far apart.

1. Basalt flow thicknesses in cross-section descriptions are from appendix A of Champion and others (2011). Paleomagnetic inclination data for coreholes USGS 131 (from 808 ft below land surface to total depth of 1,239 ft below land surface), USGS 136, USGS 137A, USGS 103, USGS 105, USGS 108 are in appendix A of this report.

Paleomagnetic Correlations of Basalt Flows

Correlations of basalt flows were established using subsurface cross sections through different areas of the INL. Stratigraphic units in the cross sections (pl. 1) represent similar paleomagnetic inclinations for units in that flow. The blocks represent the average paleomagnetic-inclination value of a flow, or flow unit, to the nearest whole degree (for example, 0.4 ft rounded down, 0.5 ft rounded up). A west to east cross-section line, *A–A'* (pl. 1), begins at corehole USGS 135, southwest of the Radioactive Waste Management Complex (RWMC), passes through coreholes USGS 137A, USGS 105, USGS 108, USGS 103, and ends at ARA-COR-005, near the Auxiliary Reactor Area [ARA], east of the CFA (fig. 1, pl. 1). Lithologic core logs and other data for coreholes USGS 135, USGS 105, USGS 108, and USGS 103 are available in Hodges and others (2012).

A north-northwest to southeast section line, *B–B'* (fig. 1, pl. 1), begins at corehole USGS 134 west of the ATR Complex, passes through coreholes USGS 136, Middle 1823, Middle 2051, C1A, USGS 132, and ends at USGS 137A on the southern INL boundary. Lithologic core logs and other data for USGS 134 and USGS 132 are available in Twining and others (2008).

Cross section *C–C'* begins at USGS 133, passes through USGS 121, Middle 2050A, USGS 128, USGS 130, USGS 127, USGS 131, and ends at corehole USGS 105. These cross sections represent the stratigraphy in the unsaturated zone and in the upper part of the ESRP aquifer. Lithologic core logs and other data for USGS 133, USGS 128, USGS 130, USGS 127, and USGS 131 are available in Twining and others (2008) and Hodges and others (2012).

Discussion of basalt flows in cross sections and coreholes proceed from the surface to the total depth of coreholes, that is, from youngest to oldest. Flows that appear in more than one cross section are presented in detail in the cross section description where first mentioned and noted in the other cross section descriptions. The cross sections are shown in figure 1 and on plate 1.

Cross Section *A–A'*

Three of the coreholes in cross section *A–A'*, USGS 105, USGS 108, and USGS 103 were not cored from the surface. These coreholes were air rotary drilled from land surface to 800, 760, and 760 ft below land surface, respectively, and cores begin at those depths. The uppermost flow in these coreholes is Vent 5206, which is exposed at the surface near the wellheads of these coreholes. Thicknesses of some uncored rock units, portrayed on cross section *A–A'* were inferred from natural gamma geophysical logs (Bartholomay, 1990; Anderson, Ackerman, and others, 1996; Hodges and others, 2012), and from the depths at which they occur in coreholes USGS 137A and ARA-COR-005 (pl. 1).

Vent 5206 Basalt Flow.—The youngest basalt flow in cross section *A–A'* erupted from Vent 5206, in the Arco-Big Southern Butte-Axial Volcanic Zone near USGS 137A, near the southern INL boundary (fig. 1; pl. 1). Vent 5206 is 63 ± 9 ka ($^{40}\text{Ar}/^{39}\text{Ar}$ age, Hodges and others, 2015). The Vent 5206 average paleomagnetic inclinations in corehole USGS 137A are 65, 65, and 64 degrees and thickness is 175 ft. The Vent 5206 flow overlies the East of Middle Butte flow (EMB) in USGS 137A. Coreholes USGS 105, USGS 108, and USGS 103 spud into Vent 5206 flows; the average paleomagnetic inclination of Vent 5206 on the surface is 64 degrees (Kuntz and others, 1994). The bottom depths of the Vent 5206 flow in the uncored parts of USGS 105, USGS 108, and USGS 103 were interpreted from natural gamma wireline geophysical logs (Anderson, Ackerman, and others, 1996). The base of Vent 5206 flows in the uncored parts of USGS 105, USGS 108, and USGS 103 was inferred from the large magnitude change in natural gamma signal, indicating the presence of the more felsic material from Big Southern Butte, similar to material collected from USGS 137A. Inferred thickness of Vent 5206 flows in USGS 105 is 235 ft, in USGS 108 is 182 ft, and in USGS 103 is 148 ft (Anderson, Ackerman, and others, 1996).

Vent 5206 is in cross section *B–B'* coreholes C1A, USGS 132, and USGS 137A and in cross section *C–C'* coreholes USGS 128, USGS 130, USGS 127, and USGS 131; USGS 105 spuds into a Vent 5206 flow at land surface, but no core was collected from land surface to 800 ft below land surface (pl. 1).

East of Middle Butte Basalt Flow.—The East of Middle Butte flow underlies the Vent 5206 flow in corehole USGS 137A where the average paleomagnetic inclination is 63 degrees, and the thickness is 32 ft (pl. 1). Material from the East of Middle Butte flow is in cross section *B–B'* coreholes in USGS 132 and USGS 137A, and in the cross section *C–C'* coreholes USGS 130, USGS 127, and USGS 131.

Mid Butte Basalt Flow.—The youngest basalt flow in basalt core from corehole ARA-COR-005 erupted from Mid Butte, where it overlies the High K_2O flow in cross section $A-A'$. The Mid Butte flow is 195 ± 39 ka (pl. 1; Hodges and others, 2015). The ARA-COR-005, Mid Butte flow units average paleomagnetic inclinations are 54 and 58 degrees, and thickness is approximately 85 ft. The Mid Butte flow also is in cross section $C-C'$ in coreholes Middle 2050A and USGS 128.

High K_2O Basalt Flow.—The High K_2O flow underlies the Mid Butte flow in ARA-COR-005 and overlies the Vent 5350 flow in cross section $A-A'$ (pl. 1). The High K_2O flow is 289 ± 8 ka (Hodges and others, 2015). The vent for the High K_2O flow has not yet been identified, but is probably exposed at the surface near the junction of Highways 20 and 26 (fig. 1). The corehole ARA-COR-005, High K_2O flow average paleomagnetic inclination is 55 degrees and thickness is approximately 85 ft. The High K_2O flow also is in cross section $C-C'$ coreholes USGS 121, Middle 2050A, USGS 128, USGS 130, USGS 127, and USGS 131.

Vent 5350 Basalt Flow.—The Vent 5350 flow erupted from Vent 5350, which is roughly 6 mi east of corehole ARA-COR-005 (fig. 1). Vent 5350 is older than the High K_2O flow and younger than the underlying Vent 5252 flow. The Vent 5350 flows exposed at the surface have an average paleomagnetic inclination of 63 degrees (Kuntz and others, 1994). A 6-ft thick flow from Vent 5350, with a paleomagnetic inclination of 64 degrees, underlies the High K_2O flow in ARA-COR-005 in cross section $A-A'$ (pl. 1).

Big Southern Butte Felsic Ash.—In corehole USGS 137A, an unwelded to welded, grey to light grey, aphyric, felsic, volcanic ash, probably from Big Southern Butte, underlies the East of Middle Butte flow, and overlies an uncorrelated 56-degree flow. This Big Southern Butte felsic ash layer is 309 ± 10 ka (Kuntz and others, 1994). In USGS 137A, the Big Southern Butte ash layer is 105 ft thick. Thicknesses derived from the large variation in natural gamma logs due to the higher radiogenic content of erupta from Big Southern Butte (Anderson, Ackerman, and others, 1996) are: USGS 105, 98 ft; USGS 108, 110 ft; and USGS 103, 87 ft. Average paleomagnetic inclination measurements were not made on this unit. The likely correlative stratigraphy of this unit in the uncored parts of coreholes USGS 105, USGS 108, and USGS 103, is shown with finely dashed contact lines in cross section $A-A'$ (pl. 1).

Vent 5252 Basalt Flow.—A basalt flow from Vent 5252 underlies the Vent 5350 flow and overlies an uncorrelated 53-degree flow in corehole ARA-COR-005 in cross section $A-A'$ (pl. 1). Vent 5252 is 350 ± 40 ka (K/Ar age, Champion and others, 1988), and is about 4 mi east-southeast of corehole ARA-COR-005 (fig. 1). The Vent 5252 basalt flow average paleomagnetic inclination is 69 degrees, and thickness is approximately 207 ft in ARA-COR-005. The average paleomagnetic inclination of the Vent 5252 basalt flows at the surface is 71 degrees (Kuntz and others, 1994). The Vent 5252

flow is in cross section $B-B'$ in corehole USGS 136, and in cross section $C-C'$ coreholes Middle 2050A, USGS 128, USGS 130, USGS 127, and USGS 131.

Unknown Source 56 Degrees Paleomagnetic Inclination Basalt Flow in USGS 137A.—This flow underlies a rhyolitic tuffaceous sediment probably derived from Big Southern Butte, in corehole USGS 137A (pl. 1). The average paleomagnetic inclination is 56 degrees, and thickness is approximately 61 ft in USGS 137A. This flow also is in cross section $B-B'$ in USGS 132.

Unknown Sources 53- and 60-Degree Paleomagnetic Inclination Basalt Flows in ARA-COR-005.—These uncorrelated flows are only in corehole ARA-COR-005, and average paleomagnetic inclinations and thicknesses are 53 degrees and 62 ft; 60 degrees and 14 ft, respectively (pl. 1). These flows are older than the Vent 5252 flow, and overlie the D3 flow, which is 456 ± 15 ka (Hodges and others, 2015).

Tin Cup Butte Basalt Flow.—Tin Cup Butte flow is the uppermost basalt flow in corehole USGS 135, and is 352 ± 5 ka ($^{40}Ar/^{39}Ar$ age, B. Turrin, Rutgers University, written commun., 2013). Tin Cup Butte is 2 mi west of USGS 135 (fig. 1). In USGS 135, the Tin Cup Butte flow has three flow units with paleomagnetic inclinations of 72, 71, and 72 degrees, and thickness is 120 ft. Tin Cup Butte underlies the unknown 56-degree flow in USGS 137A. The average paleomagnetic inclination is 72 degrees and thickness is 47 ft.

Unknown 51-Degree Paleomagnetic Inclination Basalt Flow in USGS 135.—This uncorrelated 51-degree flow underlies the Tin Cup Butte flow units and overlies the 456 ± 15 ka D3 flow in USGS 135 (pl. 1). It is approximately 51 ft thick.

Cedar Butte Felsic Intervals in USGS 108 and USGS 103 from Natural Gamma Wireline Logs.—Natural gamma wireline logs of the uncored upper parts of coreholes USGS 108 and USGS 103 (pl. 1) show a correlative high natural gamma response at depths of 356–428 ft in USGS 108, and 364–454 ft in USGS 103 (Anderson, Ackerman, and others, 1996). A natural gamma response is not present in corehole USGS 105 at similar depths (Anderson, Ackerman, and others, 1996).

This interval is deeper and therefore older than the previously described interval attributed to rhyolitic tuff derived from the 309 ± 10 ka eruption of Big Southern Butte (Kuntz and others, 1994). Anderson, Ackerman, and others (1996) attributed the greater natural gamma log response to andesite and sediment in the depth description of natural gamma logs.

Coreholes USGS 108 and USGS 103 are located directly downslope from the andesite to rhyolite lava flows from Cedar Butte (pl. 1; McCurry and others, 1992). The buried high natural gamma rock in coreholes USGS 108 and USGS 103 is correlated to the compositionally evolved vent of Cedar Butte, using data from Anderson, Ackerman, and others (1996). Kuntz and others (1994) published a K/Ar age date for

Cedar Butte of 400 ± 19 ka. This unit is identified as sediment and andesite in USGS 108, with a thickness of 72 ft, and as andesite in USGS 103, with a thickness of 90 ft (Anderson, Ackerman, and others, 1996).

D3 Basalt Flow, and the Basalt Flow Formerly Labeled South CFA Buried Vent Lower.—A sample of the D3 flow collected from *A–A'* corehole USGS 135 is 456 ± 15 ka (Hodges and others, 2015; pl. 1, cross section *A–A'*, black asterisk), and a sample collected from the South CFA buried vent lower flow from USGS 128 was dated in at 452 ± 88 ka (Hodges and others, 2015; pl. 1, cross section *C–C'*, asterisk). The ages of these two flows are the same within uncertainty, the flows have similar average paleomagnetic inclinations, depths, and thicknesses, so they are the product of one eruption. The vent from which the D3 flow erupted has not been identified; however, it may be buried.

The D3 flow underlies an uncorrelated 51-degree flow in corehole USGS 135, the Tin Cup Butte flow in USGS 137A, and an uncorrelated 60-degree flow in ARA-COR-005. The D3 flow overlies the E flow in USGS 135 and USGS 137A, and an uncorrelated 45-degree flow in ARA-COR-005. The D3 flow is present in coreholes USGS 137A and ARA-COR-005, which are located to either side of USGS 105, USGS 108, and USGS 103, it is inferred to be present in the uncored parts of USGS 105, USGS 108, and USGS 103 (cross section *A–A'*, pl. 1). The natural gamma wireline logs for the uncored parts of these coreholes show a single flow at correlative depths in USGS 105, USGS 108, and USGS 103 (Bartholomay, 1990; Anderson, Ackerman, and others, 1996; Hodges and others, 2012). Correlations inferred from natural gamma wireline logs are shown in cross section *A–A'* (pl. 1) with dashed contacts constrained to a common horizontal depth interval underlying younger andesitic flows from Cedar Butte. The average paleomagnetic inclinations and thicknesses of the D3 flow in cross section *A–A'* coreholes are USGS 135, 60 degrees, 80 ft; USGS 137A, 63 degrees, 96 ft; USGS 105, no paleomagnetic data; USGS 108, no paleomagnetic data; USGS 103, no paleomagnetic data; and ARA-COR-005, 60 degrees, 142 ft.

The D3 flow is in cross section *B–B'* coreholes Middle 2051, C1A, and USGS 137A (pl. 1), and in cross section *C–C'* coreholes Middle 2050A, USGS 128, USGS 130, USGS 127, USGS 131, and USGS 105 (pl. 1).

Unknown Source 45-Degrees and 60-Degrees Basalt Flows in ARA-COR-005.—These flows underlie the D3 flow in ARA-COR-005, have paleomagnetic inclinations of 45 degrees and 60 degrees, and are 65 and 46 ft thick, respectively.

E Basalt Flow.—The E basalt flow (550 ± 33 ka, Hodges and others, 2015) underlies the D3 flow and overlies the Big Lost flow in USGS 135 and USGS 137A. A vent has not been identified for the E flow; however, it may be buried. The E flow average paleomagnetic inclinations and thicknesses in cross section *A–A'* are USGS 135, 67 degrees, 60 ft; and USGS 137A, 69 and 67 degrees, 51 ft. The E flow also may

occur in USGS 105, USGS 108, or USGS 103, but natural gamma logs do not show a clear correlation at depths similar to its occurrence in USGS 137A. The E flow is not found in ARA-COR-005. The E flow is found in cross section *B–B'* in coreholes C1A, USGS 132, and USGS 137A.

Big Lost Basalt Flow.—The Big Lost flow underlies the E flow in USGS 135 and USGS 137A, and underlies an uncorrelated 60-degree flow in ARA-COR-005. The Big Lost flow overlies the G flow in USGS 135, USGS 137A, and USGS 108. The Big Lost flow overlies the Vent 5119 flow in USGS 105, USGS 103, and ARA-COR-005. The Big Lost flow is 560 ± 4 ka (Hodges and others, 2015). No surface vent or surface lava flows for the Big Lost flow have been identified. The thickest Big Lost flows are beneath the RWMC, which probably indicates that the Big Lost vent is in the subsurface beneath the RWMC (fig. 1, pl. 1; Anderson and others, 1997; Wetmore, 1998; Scarberry, 2003). The Big Lost flow has slightly more K_2O than most eastern Snake River Plain olivine tholeiite basalts (Anderson and Bartholomay, 1995), and shows a slightly greater natural gamma log response in wireline logs. Formation tops of the Big Lost flow were interpreted from natural gamma logs in USGS 105 and USGS 108, and the entire thickness of the Big Lost flow was interpreted from the natural gamma log of USGS 103 (Anderson, Ackerman, and others, 1996).

The Big Lost flow was erupted during the Big Lost Cryptochron (Champion and others, 1988; Ogg and Smith, 2004), and the average paleomagnetic inclinations and thicknesses in cross section *A–A'* coreholes are USGS 135, -40 degrees, 38 ft; USGS 137A, -26 degrees, 68 ft; USGS 105, -35 degrees, 138 ft (123 ft, Anderson, Ackerman and others, 1996; 15 ft, this report); USGS 108, -39 degrees, 87 ft (86 ft; Anderson, Ackerman, and others, 1996; 1 ft, this report); USGS 103, no paleomagnetic data, 54 ft (Anderson, Ackerman and others, 1996); and ARA-COR-005, -35 degrees, 53 ft.

The Big Lost flow is in cross section *B–B'* in coreholes Middle 2051, C1A, USGS 132, and USGS 137A. The Big Lost flow is in cross section *C–C'* in coreholes USGS 130, USGS 127, USGS 131, and USGS 105.

G Basalt Flow.—The G flow underlies the Big Lost flow in USGS 135, USGS 137A, and USGS 108 in cross section *A–A'*. The G flow overlies the Vent 5119 flow in USGS 108. The vent for the G flow has not been identified; however, it may be buried. The G flow average paleomagnetic inclinations and thicknesses in cross section *A–A'* coreholes are USGS 135, 59, 58, 59, and 60 degrees, 233 ft; USGS 137A, 60 degrees, 21 ft; and USGS 108, 62 degrees, 37 ft. The G flow also is present in cross section *B–B'* in coreholes USGS 132 and USGS 137A.

Vent 5119 Basalt Flow.—Vent 5119 is 572 ± 43 ka (B. Turrin, Rutgers University, written commun., 2012), and is exposed at the surface approximately 9 mi east of USGS 103, east of Atomic City, Idaho (fig. 1). The Vent 5119 flow underlies the Big Lost flow in USGS 105 and ARA-COR-005, the G flow in USGS 108, and is the uppermost-cored flow in

USGS 103 (pl. 1). The Vent 5119 flow overlies the Middle Basal Brunhes flow in USGS 105 and USGS 108, and an uncorrelated 60-degree flow in USGS 103, and is the deepest flow contacted in corehole ARA-COR-005, which was not cored through the bottom of the flow. Vent 5119 flow average paleomagnetic inclinations and thicknesses in cross section *A–A'* coreholes are USGS 105, 49 and 53 degrees, 53 ft; USGS 108, 57 and 54 degrees, 75 ft; USGS 103, 46, 50, and 52 degrees, 91 ft; and ARA-COR-005, 56 degrees, 89 ft.

Unknown 60- and 58-Degrees Paleomagnetic Inclination Basalt Flows in USGS 103.—These flows underlie the Vent 5119 flow in USGS 103, and overlie the Middle Basal Brunhes basalt flow. The average paleomagnetic inclinations and thicknesses are 60 degrees, 49 ft; and 58 degrees, 27 ft.

Middle Basal Brunhes Basalt Flow.—The Middle Basal Brunhes flow underlies the G flow in USGS 135 and USGS 137A, and the Vent 5119 flow in USGS 105, and USGS 108. The MBB underlies the uncorrelated 58-degree flow in USGS 103. The MBB flow overlies the South Late Matuyama flow in USGS 135, the Early Basal Brunhes flow in USGS 137A, USGS 105, USGS 108, and USGS 103; ARA-COR-005 was not drilled deep enough to contact the MBB. The MBB flow average paleomagnetic inclinations and thicknesses in the cross section *A–A'* coreholes are USGS 135, 66 degrees, 36 ft; USGS 137A, 65 degrees, 62 ft; USGS 105, 62 degrees, 66 ft; USGS 103, 66 degrees, 29 ft. A thin flow unit (average paleomagnetic inclination, 63 degrees, thickness 3 ft) that may be part of the Middle Basal Brunhes, is just above the labeled Middle Basal Brunhes unit in corehole USGS 105, but it did not yield a statistically robust average paleomagnetic-inclination measurement. There is a thin flow unit (18 ft thick) that is interpreted to be part of the Middle Basal Brunhes in USGS 108 with an average paleomagnetic inclination of 66 degrees, but it is too thin to provide enough samples to obtain a statistically reliable average paleomagnetic-inclination measurement. The Middle Basal Brunhes flow also is in cross section *B–B'* coreholes USGS 136, Middle 1823, Middle 2051, C1A, USGS 132, and USGS 137A, and in cross section *C–C'* coreholes USGS 128, USGS 130, USGS 131, and USGS 105 (pl. 1). USGS 127 was not drilled deep enough to penetrate the Middle Basal Brunhes flow, which likely underlies that corehole.

Early Basal Brunhes Flow.—The Early Basal Brunhes flow underlies the Middle Basal Brunhes flow in USGS 137A, USGS 105, USGS 108, and USGS 103, and overlies the South Late Matuyama flow in the same coreholes. The Early Basal Brunhes flow average paleomagnetic inclination measurements and thicknesses in cross section *A–A'* coreholes are USGS 137A, 52 degrees, 81 ft; USGS 105, 53 degrees; 47 ft; USGS 108, 55, 55, and 53 degrees, 108 ft; USGS 103, 55 and 55 degrees, 67 ft. ARA-COR-005 was not drilled deep enough to penetrate the Early Basal Brunhes flow, which may underlie that corehole. The EBB flow is also in cross section *B–B'* in coreholes USGS 134, USGS 136, Middle

1823, and USGS 137A, and in cross section *C–C'* in coreholes USGS 121, Middle 2050A, USGS 128, USGS 131, and in USGS 105.

South Late Matuyama Basalt Flow.—The South Late Matuyama (SLM) flow is a reversed polarity flow, and is older than 780 ka, the onset of the Brunhes Normal Polarity Chron (Ogg and Smith, 2004). The vent for the South Late Matuyama basalt flow has not been identified; however, it is probably buried. The South Late Matuyama basalt flow underlies the MBB flow in USGS 135, the EBB in USGS 137A, USGS 105, USGS 108, and USGS 103. The South Late Matuyama basalt flow overlies the Matuyama flow in USGS 135, USGS 108, and USGS 103, and overlies an unknown source -65-degree flow in USGS 137A, and an unknown source -67-degree flow in USGS 105. The SLM average paleomagnetic inclination measurements and thicknesses in cross section *A–A'* coreholes are USGS 135, -61, -59, and -59 degrees, 225 ft; USGS 137A, -62 and -59 degrees, 166 ft; USGS 105, -62, -60, and -59 degrees, 137 ft; USGS 108, -61 degrees, 98 ft; USGS 103, -59 and -59 degrees, 135 ft.

The South Late Matuyama basalt flow is in cross section *B–B'* in coreholes C1A, USGS 132, and 137A, and in cross section *C–C'* in coreholes USGS 131 and USGS 105.

Unknown Source -65-, -65-, and -67-Degrees Basalt Flow in USGS 137A and USGS 105.—This unknown source flow underlies the South Late Matuyama basalt flow in USGS 137A and USGS 105, and overlies the Matuyama flow in coreholes USGS 137A and USGS 105. The unknown source 65-, -65-, and -67-degree flow average paleomagnetic inclinations and thicknesses in cross section *A–A'* coreholes are USGS 137A, -65 and -65 degrees, 106 ft; and USGS 105, -67 degrees, 116 ft.

Matuyama Basalt Flow.—The reversed polarity Matuyama flow underlies the South Late Matuyama basalt flow, and its vent is not at the surface. The Matuyama flow overlies the Post Jaramillo flow in USGS 135, USGS 105, and USGS 103; it also may be below the deepest depths of USGS 137A, USGS 108 and ARA-COR-005. The Matuyama flow average paleomagnetic inclinations and thicknesses in cross section *A–A'* coreholes are USGS 135, -72, -73, -70, -70, and -73 degrees, 268 ft; USGS 137A, -74 and -71 degrees, 229 ft; USGS 105, -71 and -69 degrees, 111 ft; USGS 108, -70 and -70 degrees, 111 ft; and USGS 103, -67, 32 ft.

The Matuyama basalt flow is also in the cross section *B–B'* coreholes USGS 134, USGS 136, Middle 1823, Middle 2051, C1A, USGS 132, and USGS 137A. The Matuyama flow is in the cross section *C–C'* coreholes USGS 133, Middle 2050A, USGS 131, and USGS 105.

Post Jaramillo Basalt Flow.—The Post Jaramillo flow underlies the Matuyama flow in USGS 135, USGS 105, and USGS 103 (pl. 1). The Post-Jaramillo flow overlies an unknown source, -71-degree average paleomagnetic inclination flow in USGS 135. The Post Jaramillo flow average paleomagnetic inclinations and thicknesses in cross section *A–A'* coreholes are USGS 135, -66 degrees, 31 ft;

USGS 105, -67 degrees, 48 ft; USGS 103, -66, -66, and -69 degrees, 93 ft. The Post Jaramillo flow in USGS 105 and USGS 103 is probably thicker than the stated thickness because those coreholes were not drilled through the flow to the underlying unit. Coreholes USGS 137A and USGS 108 were not drilled deep enough to contact the Post Jaramillo flow, which may underlie their locations.

The Post Jaramillo basalt flow is in cross section *B–B'* coreholes USGS 134, 136, Middle 2051, and USGS 132, and in cross section *C–C'* corehole USGS 105.

Unknown -71-Degree Basalt Flow at the Base of USGS 135.—This flow is 22 ft thick and overlies a sediment layer at the base of corehole USGS 135.

Cross Section *B–B'*

Quaking Aspen Butte Basalt Flow.—The youngest flow in cross section *B–B'* erupted from Quaking Aspen Butte, which is 60 ± 16 ka (Hodges and others, 2015), and is found only in corehole USGS 132; the average paleomagnetic inclination is 60 degrees and thickness is 23 ft (pl. 1). Quaking Aspen Butte is about 6 mi southwest of USGS 135 (fig. 1).

Vent 5206 Basalt Flow.—The Vent 5206 flow is 63 ± 9 ka (Hodges and others, 2015), and is near the southern INL border, 1.1 mi northeast of corehole USGS 137A (fig. 1). Corehole C1A and USGS 137 A spud into Vent 5206 flows, which underlie Quaking Aspen Butte flow in USGS 132, and USGS 137A. Vent 5206 flows overlie a Lavatoo Butte flow in C1A, and East of Middle Butte basalt flows in USGS 132 and USGS 137A. Vent 5206 flows paleomagnetic inclinations and thicknesses in cross section *B–B'* coreholes are C1A, 65 and 66 degrees, 102 ft; USGS 132, 64 degrees, 72 ft; and USGS 137A, 65, 65, and 64 degrees, 175 ft. Vent 5206 flows also are in cross section *A–A'* (see section, “[Cross Section A–A'](#)”) and in the cross section *C–C'* coreholes USGS 128, USGS 130, USGS 127, USGS 131, and USGS 105 (pl. 1).

East of Middle Butte Basalt Flow.—The East of Middle Butte flow underlies Vent 5206 flows in USGS 132 and USGS 137A. The East of Middle Butte overlies a thick sediment and Lavatoo Butte in USGS 132, and the Big Southern Butte felsic ash in USGS 137A. The East of Middle Butte flow average paleomagnetic inclinations and thicknesses in cross section *B–B'* coreholes are USGS 132, 62 degrees, 18 ft; USGS 137A, 63 degrees, 32 ft. East of Middle Butte flows also occur in cross section *C–C'*, in coreholes USGS 130, USGS 127, and USGS 131.

Lavatoo Butte Basalt Flow.—Lavatoo Butte is 211 ± 16 ka [K/Ar age] (Champion and others, 2002), and is 4 mi west of Middle 2051 (fig. 1). The Lavatoo Butte flow is the top flow in Middle 2051, underlies Vent 5206 flows in C1A, and underlies the EMB and a sediment layer in USGS 132. The Lavatoo Butte flow overlies the Crater Butte flow in Middle 2051, a sediment layer and the Pond Butte flow in C1A, and a sediment layer and a 55 degree unknown source flow. The Lavatoo Butte flow average paleomagnetic inclinations

and thicknesses in cross section *B–B'* coreholes are Middle 2051, 57 degrees, 6 ft; C1A, 55 degrees, 118 ft; and USGS 132, 54 degrees, 71 ft. Lavatoo Butte is in cross section *C–C'* coreholes USGS 121, USGS 127, and USGS 131.

Crater Butte Basalt Flow.—Crater Butte is 7 mi west of USGS 134 (fig. 1). Crater Butte is the top flow in coreholes USGS 134 and USGS 136 (pl. 1), and underlies Lavatoo Butte in corehole Middle 2051. Crater Butte may be in the uncored upper 500 ft of Middle 1823. Crater Butte overlies Pond Butte in USGS 134, USGS 136, and Middle 2051. The Crater Butte flow average paleomagnetic inclinations and thicknesses in cross section *B–B'* coreholes are USGS 134, 59 degrees, 4 ft; USGS 136, 60 degrees, 46 ft ([appendix A](#), this report); and Middle 2051, 64 degrees, 15 ft. A Crater Butte flow is also in cross section *C–C'* in corehole USGS 121.

Pond Butte (WATR-Complex Vent) Flow.—The flow labeled “WATR-Complex Vent flow” in previous subsurface stratigraphic studies (Champion and others, 2011, 2013), is correlated to flows erupted from the Pond Butte vent through paleomagnetic field studies and bulk rock x-ray fluorescence geochemistry studies (E.J. Martin, U.S. Geological Survey, written commun., 2015). The Pond Butte vent is 10 mi west of USGS 134 (fig. 1), and is 270 ± 15 ka (Hodges and others, 2015). Pond Butte flow underlies the Crater Butte flows in coreholes USGS 134, 136, and Middle 2051, and Lavatoo Butte in C1A. Pond Butte flows overlie Vent 4959 flows in USGS 134, Vent 5252 flows in USGS 136, and the D3 flow in Middle 2051 and C1A (pl. 1). Pond Butte is probably in the uncored upper 500 ft of Middle 1823. The Pond Butte flows average paleomagnetic inclinations and thicknesses in cross section *B–B'* coreholes are USGS 134, 76 degrees, 113 ft; USGS 136, 77 degrees, 50 ft ([appendix A](#), this report); Middle 2051, 74 degrees, 72 ft; and C1A, 75 degrees, and 50 ft. Pond Butte is in the *C–C'* coreholes USGS 133, USGS 121, and Middle 2050A.

Big Southern Butte Felsic Ash (309 ± 10 ka [K–Ar age]).—Big Southern Butte (309 ± 10 ka, Kuntz and others, 1994) ash underlies the East of Middle Butte flow in USGS 137A. Average paleomagnetic inclination data are not reported for this unit (see section, “[Cross Section A–A'](#)”).

Unknown Source 55–56-Degrees Paleomagnetic Inclination Basalt Flow in USGS 132 and USGS 137A.—This unknown source flow is found in two coreholes, USGS 132 and USGS 137A. It underlies Lavatoo Butte in USGS 132, and the Big Southern Butte felsic ash in USGS 137A, and overlies The E flow in USGS 132, and Tin Cup Butte in USGS 137A (pl. 1). The average paleomagnetic inclinations and thicknesses for the unknown source 55–56-degrees flow in cross section *B–B'* coreholes are USGS 132, 55 degrees, 40 ft; and USGS 137A, 56 degrees, 54 ft ([appendix A](#)).

Vent 5252 Basalt Flow.—The Vent 5252 flow (350 ± 40 ka, [K/Ar age], Champion and others, 1988) underlies the Pond Butte flow and a sediment in USGS 136, and overlies the Vent 4959 flow in USGS 136. The Vent 5252 flow average paleomagnetic inclination is 73 degrees and thickness is 29

ft in USGS 136. This flow likely is also in the uncored part of Middle 1823. The Vent 5252 flow also is in cross section *C–C'* in coreholes Middle 2050A, USGS 128, USGS 130, USGS 127, and USGS 131.

Vent 4959 Basalt Flow (Formerly Labeled ATR Complex Unknown Vent).—Vent 4959 is a kipuka surrounded by younger flows, about 2 mi north of corehole USGS 134 (fig. 1). Flows formerly labeled ATR Complex Unknown Vent in stratigraphic studies of the subsurface (Champion and others, 2011, 2013) are correlated to flows erupted from Vent 4959 through paleomagnetic field studies and x-ray fluorescence bulk rock geochemical studies (E.J. Martin, written commun., 2015). Vent 4959 flows are older than Vent 5252, in USGS 136 (Champion and others, 2011, pl. 1). A Vent 4959 flow underlies a Pond Butte flow in USGS 134 and Vent 5252 in USGS 136, and overlies the D3 flow in USGS 134 and a CFA buried vent flow in USGS 136. A Vent 4959 flow also may be in the uncored upper 500 ft of Middle 1823. The Vent 4959 flows average paleomagnetic inclinations and thicknesses in cross section *B–B'* coreholes are USGS 134, 54 degrees, 124 ft; USGS 136, 56 and 53 degrees, 35 and 75 ft. Vent 4959 flows likely are in the uncored part of Middle 1823. Vent 4959 also is in cross section *C–C'* coreholes USGS 133 and USGS 121 (pl. 1).

D3 Basalt Flow, and the Basalt Flow Formerly Labeled South CFA Buried Vent Lower.—The D3 flow and the formerly labeled South CFA buried vent lower flow (Champion and others, 2011) are the same age within uncertainty; the D3 flow is 456 ± 15 ka (Hodges and others, 2015), from a sample collected at 225 ft depth in corehole USGS 135 (pl. 1, cross section *A–A'*, USGS 135, black asterisk); the South CFA buried vent lower flow is 452 ± 88 ka (Hodges and others, 2015), from a sample collected at 312 ft depth in corehole USGS 128 (pl. 1, cross section *C–C'*, USGS 128, asterisk) (Hodges and others, 2015). The D3 flow and the South CFA buried vent lower flow have similar average paleomagnetic inclinations, depths, and thicknesses. The D3 age from USGS 135 has a smaller uncertainty than the South CFA buried vent lower basalt flow age, so the D3 age from USGS 135 is used in this report.

The D3 flow underlies a Vent 4959 flow in corehole USGS 134, below a thin sediment, Pond Butte in Middle 2051 and C1A, and the Tin Cup Butte flow in USGS 137A. The D3 flow overlies the CFA buried vent flow in corehole USGS 134, the Big Lost flow in Middle 2051, and the E flow in C1A and 137A. The D3 flow average paleomagnetic inclinations and thicknesses in cross section *B–B'* coreholes are USGS 134, 59 degrees, 17 ft; Middle 2051, 59 and 59 degrees, 112 ft; C1A, 61 degrees, 38 ft; USGS 137A, 63 degrees, 96 ft. The D3 flow is in cross section *C–C'* in coreholes Middle 2050A, USGS 128, USGS 130, USGS 127, USGS 131, and inferred to be in USGS 105.

E Basalt Flow.—The 550 ± 33 ka (Hodges and others, 2015) E flow underlies a D3 flow in corehole C1A, an unknown source 55-degree flow in USGS 132, and the D3 flow in USGS 137A. The E flow overlies the Big Lost flow in C1A, USGS 132, and USGS 137A. The E flow average paleomagnetic inclinations and thicknesses in cross section *B–B'* coreholes are C1A, 67 degrees, 65 ft; USGS 132, 68 degrees, 129 ft; USGS 137A, 67 and 69 degrees, 73 ft.

Big Lost Basalt Flow.—The Big Lost flow is a reversed polarity flow, erupted during the Big Lost Reversed Polarity Cryptochron of the Brunhes Normal Polarity Chron (Ogg and Smith, 2004), and is 560 ± 4 ka (Hodges and others, 2015). The Big Lost flow underlies the D3 flow in corehole Middle 2051, and the E flow in C1A, USGS 132, and USGS 137A. The Big Lost flow average paleomagnetic inclinations and thicknesses in cross section *B–B'* coreholes are Middle 2051, -41 degrees, 43 ft; C1A, -35, -37, and -39 degrees, 159 ft; USGS 132, -38 and -42 degrees, 102 ft; USGS 137A, -26 degrees, 68 ft. The Big Lost Flow is in cross section *C–C'* coreholes USGS 130, USGS 127, USGS 131, and USGS 105.

G Flow.—The G flow is present in cross section *B–B'* in coreholes USGS 132 and USGS 137A, underlying the Big Lost flows in both coreholes. The G flow overlies the CFA buried vent flow in USGS 132, and overlies the Middle Basal Brunhes flow in USGS 137A.

The G flow average paleomagnetic inclinations and thicknesses in cross section *B–B'* coreholes are USGS 132, 58 degrees, 50 ft and USGS 137A, 60 degrees, 21 ft (appendix A).

CFA Buried Vent Basalt Flow.—The 536 ± 63 ka CFA buried vent flow (Hodges and others, 2015) underlies the D3 flow in corehole USGS 134, the Vent 4959 flow in USGS 136, the Big Lost flow in Middle 2051 and C1A, and the G flow in USGS 132. The CFA buried vent flow overlies the AEC Butte flow in USGS 134, USGS 136, Middle 1823, the Late Basal Brunhes flow in Middle 2051 and C1A, and the Middle Basal Brunhes flow in USGS 132. The CFA buried vent flow average paleomagnetic inclinations and thicknesses in cross section *B–B'* coreholes are USGS 134, 64 and 65 degrees, 136 ft; USGS 136, 65 and 69 degrees, 170 ft; Middle 1823, 67 degrees, 27 ft (the upper 500 ft of Middle 1823, is not cored; the CFA buried vent flow likely is in the uncored part of Middle 1823, and is thicker than 27 ft); Middle 2051, 68, 68, 69, and 68 degrees, 175 ft; C1A, 66 degrees, 50 ft; USGS 132, 65 degrees, 25 ft. The CFA buried vent flow is in the *C–C'* coreholes USGS 133, USGS 121, Middle 2050A, USGS 128, USGS 130, USGS 127, and USGS 131.

AEC Butte Basalt Flow.—AEC Butte is exposed at the surface near the Advanced Test Reactor Complex (ATR-Complex), 3 mi east-southeast of USGS 134 (fig. 1). AEC Butte is 637 ± 35 ka ([K/Ar age] Champion and others, 2002). The AEC Butte flow underlies the CFA buried vent flow in USGS 134, USGS 136, and Middle 1823, and overlies the Late Basal Brunhes flow in USGS 134, USGS 136, and

Middle 1823 (pl. 1). The AEC Butte flow inclinations and thicknesses in cross section $B-B'$ coreholes are USGS 134, 58, 57, and 57 degrees, 99 ft; USGS 136, 56 degrees; 102 ft, and Middle 1823, 55 and 55 degrees, 101 ft. The AEC Butte flow is in cross section $C-C'$ coreholes USGS 133, USGS 121, Middle 2050A, and USGS 128.

Late Basal Brunhes Basalt Flow.—The Late Basal Brunhes flow underlies the AEC Butte flows in USGS 134, USGS 136, and Middle 1823, the CFA buried vent flow in Middle 2051, and C1A (pl. 1). The Late Basal Brunhes flow overlies the Early Basal Brunhes flow in USGS 134, the Middle Basal Brunhes flow in USGS 136, Middle 1823, Middle 2051 and C1A. The Late Basal Brunhes flow average paleomagnetic inclinations and thicknesses in cross section $B-B'$ coreholes are USGS 134, 62 degrees, 103 ft, USGS 136, 61 degrees, 54 ft; Middle 1823, 63 degrees, 44 ft; Middle 2051, 62 degrees, 50 ft; and C1A, 60 degrees, 25 ft. The Late Basal Brunhes flow is in cross section $C-C'$ coreholes USGS 133, USGS 121, and Middle 2050A.

Middle Basal Brunhes Basalt Flow.—The Middle Basal Brunhes (MBB) flow underlies the Late Basal Brunhes flow in USGS 136, Middle 1823, Middle 2051, C1A, the CFA buried vent flow in USGS 132, and the G flow in USGS 137A. The Middle Basal Brunhes flow overlies the Early Basal Brunhes flow in USGS 136, Middle 1823, and USGS 137A, an unknown 60-degree flow in Middle 2051, the South Late Matuyama in C1A and USGS 132. The Middle Basal Brunhes flow average paleomagnetic inclinations and thicknesses in cross section $B-B'$ coreholes are USGS 136, 67 degrees, 43 ft; Middle 1823, 64 degrees, 29 ft; Middle 2051, 66 degrees, 37 ft; C1A, 68 degrees, 53 ft; USGS 132, 66 degrees, 50 ft; and USGS 137A, 65 degrees, 62 ft. The Middle Basal Brunhes flow is in cross section $C-C'$ coreholes USGS 128, USGS 130, USGS 131, and USGS 105.

Unknown 60-Degree Basalt Flow.—This flow underlies the Middle Basal Brunhes flow in corehole Middle 2051. The average paleomagnetic inclination is 60 degrees average and thickness is 42 ft (pl. 1).

Early Basal Brunhes Basalt Flow.—The Early Basal Brunhes basalt flow underlies the Late Basal Brunhes flow in USGS 134, the Middle Basal Brunhes flow in coreholes USGS 136, Middle 1823, and USGS 137A. The Early Basal Brunhes overlies the Matuyama flow in USGS 134, USGS 136, and Middle 1823, and the South Late Matuyama flow in USGS 137A. The Early Basal Brunhes flow average paleomagnetic inclinations and thicknesses in cross section $B-B'$ coreholes are USGS 134, 55 degrees, 52 ft, USGS 136, 57 degrees, 21 ft; Middle 1823, 54 degrees, 11 ft; USGS 137A, 52 degrees, 81 ft.

The Early Basal Brunhes flow is in cross section $C-C'$ coreholes USGS 121, Middle 2050A, USGS 128, USGS 131, and USGS 105 (pl. 1).

South Late Matuyama Basalt Flow.—The South Late Matuyama (SLM) flow underlies the Middle Basal Brunhes flow in coreholes C1A and USGS 132, and the Early Basal

Brunhes flow in USGS 137A. The South Late Matuyama flow overlies the Matuyama flow in coreholes C1A and USGS 132, and an unknown source -65-degree flow in USGS 137A. The South Late Matuyama flow average paleomagnetic inclinations and thicknesses in cross section $B-B'$ are C1A, -61 degrees, 47 ft; USGS 132, -62 and -59 degrees, 111 ft; and USGS 137A, -62 and -59 degrees, 166 ft. The South Late Matuyama flow is in cross section $C-C'$ coreholes USGS 131 and USGS 105.

Unknown -65- and -67-Degrees Basalt Flow in USGS 137A.—The unknown -65- and -65-degrees flow underlies the South Late Matuyama flow in $B-B'$ corehole USGS 137A, and overlies the Matuyama flow. The unknown flow average paleomagnetic inclinations are -65 and -65 in cross section $B-B'$ corehole USGS 137A and thickness is 106 ft. This flow correlates to a flow with a similar average paleomagnetic inclination at a similar depth in cross section $C-C'$ corehole USGS 105.

Matuyama Basalt Flow.—The Matuyama basalt flow underlies the early Basal Brunhes flow in USGS 134, USGS 136, Middle 1823, the unknown source 60-degree flow in Middle 2051, the South Late Matuyama flow in C1A, and USGS 132, and the unknown source -65 and -65 flow in USGS 137A. The Matuyama flow overlies the Post Jaramillo flow in USGS 134, USGS 136, Middle 2051 and USGS 132, and the Jaramillo flow in Middle 1823 and C1A. The Matuyama flow average paleomagnetic inclinations and thicknesses in cross section $B-B'$ coreholes are USGS 134, -70 degrees, 56 ft; USGS 136, -70, -70, and -69 degrees, 126 ft; Middle 1823, -72, -69, -69, -68, -68, -69, and -68 degrees, 193 ft; Middle 2051, -66, -69, and -70 degrees, 214 ft; C1A, -71, -72, -70, -71, and -71 degrees, 322 ft; USGS 132, -72 and -73, 327 ft; USGS 137A, and -74 and -71 degrees, 229 ft. The Matuyama flow is in cross section $C-C'$ coreholes USGS 133, Middle 2050A, USGS 131, and USGS 105.

Post Jaramillo Flow.—The Post Jaramillo flow underlies the Matuyama flow in USGS 134, USGS 136, Middle 2051, and USGS 132, and overlies the Jaramillo flow in these same coreholes, and may exist below the total depth of USGS 137A. The Post Jaramillo flow average paleomagnetic inclinations and thicknesses in cross section $B-B'$ coreholes are USGS 134, -62 and -64 degrees, 102 ft; USGS 136, -66 degrees, 55 ft; Middle 2051, -63 degrees, 88 ft; and USGS 132, -64 degrees, 46 ft. The Post-Jaramillo flow is in cross section $C-C'$ corehole USGS 105.

Jaramillo Basalt Flow.—The normal polarity Jaramillo flow erupted during the Jaramillo normal polarity subchron of the Matuyama Chron, which lasted from 1.072 Ma to 0.988 Ma. The Jaramillo flow underlies, and overlies sediment and the Unknown -61- and -63-Degrees Flow in Middle 1823, and a thick sediment in C1A. The Jaramillo flow average paleomagnetic inclinations and thicknesses in cross section $B-B'$ coreholes are USGS 134, 54 degrees, 104 ft; USGS 136, 55 and 60 degrees, 138 ft; Middle 1823, 55, 55, 53, 57, and 49 degrees, 203 ft; Middle 2051, 51, 44, and 45 degrees,

169 ft; C1A, 52, 54, 53, 55, 54, 58, and 52 degrees, 321 ft; and USGS 132, 52 degrees, 69 ft. The Jaramillo flow also may be beneath the bottom of USGS 137A. The Jaramillo flow is in the C–C' coreholes Middle 2050A, and USGS 131.

Unknown -61- and -63-Degrees Basalt Flow.—This flow is in Middle 1823, where it underlies the Jaramillo flow and a sediment, and overlies the Matuyama 1.21 Ma flow. The unknown flow average paleomagnetic inclination is -63 degrees and thickness is 31 ft. This flow also is in the cross section C–C' corehole Middle 2050A (Champion and others, 2011).

Matuyama 1.21 Ma Basalt Flow in Middle 1823.—The Matuyama 1.21 Ma flow (Champion and Lanphere, 1997) is in the deep part of corehole Middle 1823, where it overlies a thick sediment and the Matuyama 1.37 Ma flow, and underlies the unknown source -63-degrees flow. The Matuyama 1.21 Ma flow average paleomagnetic inclination is -57 degrees and thickness is 16 ft. The Matuyama 1.21 Ma flow also is in the cross section C–C' in corehole Middle 2050A.

Matuyama 1.37 Ma Basalt Flow [⁴⁰Ar/³⁹Ar Age, (Champion and Lanphere, 1997)].—The Matuyama 1.37 Ma flow (Champion and Lanphere, 1997) underlies the Matuyama 1.21 Ma flow in corehole Middle 1823, and the Jaramillo flow in C1A. It overlies a thick sediment, the -42-degree unknown flow, and the Post Olduvai flow in Middle 1823. In C1A, it overlies a thick sediment, and the Post Olduvai flow. The Matuyama 1.37 Ma flow average paleomagnetic inclinations and thicknesses in cross section B–B' corehole are Middle 1823, 69 degrees 38 ft; and C1A, -70 degrees, 61 ft. The Matuyama 1.37 Ma flow is in the cross section C–C' corehole Middle 2050A.

Unknown -42-Degree Basalt Flow in Middle 1823.—This flow underlies the Matuyama 1.37 Ma flow and a very thick sediment (399 ft) in Middle 1823, and overlies the Post Olduvai flows. The average paleomagnetic inclination is -42 degrees and thickness is 22 ft.

Post Olduvai Basalt Flow.—The Post Olduvai flow underlies a very thick sediment and the unknown -42-degree flow in Middle 1823, and a sediment in C1A, and overlies a sediment in Middle 1823, and an unknown -63-degree flow in C1A. The paleomagnetic inclinations are -67 and -66 degrees in two flow units in coreholes Middle 1823 and C1A thicknesses are 89 ft and 190 ft, respectively.

Unknown -63-Degree Basalt Flow in C1A.—The unknown -63-degree flow underlies the Post Olduvai flows in C1A, and overlies a thin sediment and the unknown -48-degree flow. This unknown source flow is near the base of C1A, and the average paleomagnetic inclination is -63 degrees and thickness is 17 ft.

Unknown -48-Degree Basalt Flow in C1A.—The unknown -48-degree flow underlies a thin sediment and the unknown -63-degree flow in C1A. This unknown source flow is at the base of C1A, and the average paleomagnetic inclination is -48 degrees and thickness is at least 34 ft; corehole C1A did not penetrate the base of this flow.

Cross Section C–C'

Cross section C–C' begins at USGS 133, north of the Idaho Nuclear Technology and Engineering Center, and extends to the southwest through USGS 121, Middle 2050A, USGS 128, USGS 130, USGS 127, USGS 131, and ends at USGS 105 (fig. 1). Basalt flows are discussed from land surface to depth, that is, from youngest to oldest, and, generally, from north to south (pl. 1).

Vent 5206 Basalt Flow (63 ± 9 ka).—The Vent 5206 basalt flow is the youngest flow in cross section C–C', at 63 ± 9 ka (Hodges and others, 2015). Vent 5206 overlies Mid Butte in USGS 128, the East of Middle Butte flow in USGS 130, USGS 127, and USGS 131, and USGS 105 spuds into a Vent 5206 flow (pl. 1; Kuntz and others, 1994). Vent 5206 flow average paleomagnetic inclinations and thicknesses in cross section C–C' coreholes are USGS 128, 65 degrees, 26 ft; USGS 130, 65 degrees, 39 ft; USGS 127, 65 and 63 degrees, 58 ft; USGS 131, 64 degrees, 83 ft; and USGS 105, 64 degrees (from Kuntz and others, 1994 surface measurement), 235 ft (Anderson, Ackerman, and others, 1996).

East of Middle Butte Basalt Flow.—The East of Middle Butte basalt flow underlies the Vent 5206 flow and a sediment in USGS 130, USGS 127, and USGS 131. The East of Middle Butte flow overlies the High K₂O flow in USGS 130, and the Lavatoo Butte flow in USGS 127, and USGS 131. The East of Middle Butte flow paleomagnetic inclinations and thicknesses in cross section C–C' coreholes are USGS 130, 60 degrees, 68 ft; USGS 127, 58 degrees, 20 ft; and USGS 131, 61 degrees, 26 ft (Champion and others, 2011, appendix A).

Mid Butte Basalt Flow.—The youngest basalt flow in Middle 2050A is the 195 ± 39 ka Mid Butte flow, and overlies Pond Butte (fig. 1; Hodges and others, 2015). A Mid Butte flow underlies the Vent 5206 flow, and overlies the High K₂O flow in USGS 128. The Mid Butte flow average paleomagnetic inclinations and thicknesses in cross section C–C' coreholes are Middle 2050A, 53 degrees, 41 ft; and USGS 128, 52 and 53 degrees, 121 ft (L. Matson, written commun., 2003; Champion and others, 2011).

Lavatoo Butte Basalt Flow.—Corehole USGS 121 spuds into a 57-degree flow, which may correlate to Lavatoo Butte. It overlies a Crater Butte flow and a Pond Butte flow. Crater Butte and Pond Butte are near Lavatoo Butte (fig. 1), and are older than Lavatoo Butte. Lavatoo Butte underlies East of Middle Butte flows in USGS 127 and USGS 131, and overlies the High K₂O flow in USGS 127 and USGS 131. The Lavatoo Butte flow average paleomagnetic inclinations and thicknesses in cross section C–C' coreholes are USGS 121, 57 degrees 18 ft; USGS 127, 54 degrees, 39 ft; and USGS 131, 55 degrees, 62 ft (appendix A; Champion and others, 2011).

Crater Butte Basalt Flow.—Crater Butte underlies the probable Lavatoo Butte flow in corehole USGS 121, and overlies the Pond Butte flow. The Crater Butte flow in USGS 121 average paleomagnetic inclination is 62 degrees and thickness is 27 ft.

Pond Butte Basalt Flow (West of ATR Complex; 270 ± 15 ka [$^{40}\text{Ar}/^{39}\text{Ar}$ age]).—Pond Butte is the top flow in corehole USGS 133, and underlies Crater Butte in USGS 121, and the Mid Butte flow in Middle 2050A. The Pond Butte flow overlies the Vent 4959 flow in USGS 133, and the High K_2O flow in USGS 121 and Middle 2050A. The Pond Butte flow average paleomagnetic inclination and thicknesses in cross section C–C' coreholes are USGS 133, 75 degrees, 111 ft; USGS 121, 75 degrees, 22 ft; and Middle 2050A, 72 degrees (with an uncertainty of 26.3 degrees), 9 ft.

High K_2O Basalt Flow.—The 289 ± 8 ka High K_2O basalt flow (Hodges and others, 2015) underlies Pond Butte in coreholes USGS 121 and Middle 2050A, underlies Mid Butte in USGS 128, East of Middle Butte in USGS 130, and underlies Lavatoo Butte in USGS 127 and USGS 131. The High K_2O flow overlies the Vent 4959 flow in USGS 121, Vent 5252 in Middle 2050A, USGS 128, USGS 130, USGS 127, and USGS 131. The High K_2O flow average paleomagnetic inclinations and thicknesses in cross section C–C' coreholes are USGS 121, 53 degrees, 14 ft; Middle 2050A, 51 degrees, 29 ft; USGS 128, 51 degrees, 34 ft; USGS 130, 49 degrees, 47 ft; USGS 127, 50 degrees, 55 ft; and USGS 131, 53 degrees, 16 ft.

Big Southern Butte Felsic Ash, Inferred in USGS 105.—See the description of this unit in section, “Cross Section A–A'.”

Vent 5252 Flow.—The Vent 5252 flow (350 ± 40 ka, [K/Ar age] Champion and others, 1988) underlies the High K_2O flow in Middle 2050A, USGS 128, USGS 130, USGS 127, and USGS 131. The Vent 5252 flow overlies the D3 flow in Middle 2050A, the South CFA buried vent upper flow in USGS 128, USGS 130, USGS 127, and USGS 131. The Vent 5252 flow average paleomagnetic inclinations and thicknesses in cross section C–C' coreholes are Middle 2050A, 70 degrees, 46 ft; USGS 128, 70 degrees, 49 ft; USGS 130, 70 degrees, 82 ft; USGS 127, 70 degrees, 22 ft; and USGS 131, 73 degrees, 11 ft.

Vent 4959 Basalt Flow (formerly labeled ATR Complex Unknown Vent).—A Vent 4959 basalt flow underlies a Pond Butte basalt flow in USGS 133, and the High K_2O flow in USGS 121. The Vent 4959 flow overlies the North INTEC buried vent flow in USGS 133 and USGS 121. The Vent 4959 flow average paleomagnetic inclinations and thicknesses in cross section C–C' coreholes are USGS 133, 51 and 54 degrees, 101 ft; and USGS 121, 54 and 55 degrees, 110 ft.

South CFA Buried Vent Upper Basalt Flow.—The South CFA Buried Vent Upper flow is 309 ± 13 ka (Hodges and others, 2015). The South CFA Buried Vent Upper Basalt Flow underlies the Vent 5252 flow in USGS 128, USGS 130, USGS 127, and USGS 131, and overlies the D3 flow in USGS 128, USGS 130, USGS 127, and USGS 131. The South CFA Buried Vent Upper Basalt Flow paleomagnetic inclinations and thicknesses in cross section C–C' coreholes are USGS 128, 64 degrees, 39 ft; USGS 130, 70 and 63 degrees (the upper South CFA Buried Vent Upper Basalt Flow unit in corehole USGS 130 is so heavily overprinted by

the overlying Vent 5252 flow that it could not be corrected), 43 ft; USGS 127, 57 and 63 degrees, 63 ft; and USGS 131, 62 degrees, 21 ft.

D3 Basalt Flow, and the basalt flow formerly labeled South CFA Buried Vent Lower.—A sample of the D3 flow from cross section A–A' corehole USGS 135 was $^{40}\text{Ar}/^{39}\text{Ar}$ dated at 456 ± 15 ka (Hodges and others, 2015), and a sample collected from the South CFA buried vent lower flow from cross section C–C' corehole USGS 128 was $^{40}\text{Ar}/^{39}\text{Ar}$ dated at 452 ± 88 ka (Hodges and others, 2015). All samples collected from the D3 and South CFA buried vent flows have similar average paleomagnetic inclinations. The ages are the same within uncertainty and the D3 and South CFA buried vent upper flow occur at similar depths, so it is most probable that the flow in USGS 135, USGS 128, and all the other coreholes where it occurs are the same flow, herein labeled “D3.”

The D3 basalt flow paleomagnetic inclinations and thicknesses in cross section C–C' coreholes are Middle 2050A, 59, 59, and 61 degrees, 87 ft; USGS 128, 60 degrees, 63 ft; USGS 130, 59 and 60 degrees, 121 ft; USGS 127, 61, 57, and 62 degrees, 129 ft; and USGS 131, 60 degrees, 121 ft. The D3 flow is inferred to exist in the uncored part of USGS 105, although interpretation of natural gamma wireline logs does not allow precise judgment as to its depth and thickness.

Unknown 47-Degree Basalt Flow in Middle 2050A.—This 10 ft flow underlies the D3 flow and overlies the North INTEC buried vent flow in Middle 2050A. The average paleomagnetic inclination is 47 degrees.

North INTEC Buried Vent Basalt Flow.—The North INTEC Buried Vent flow underlies the Vent 4959 flow in USGS 133 and USGS 121, the unknown 47-degree flow in Middle 2050A, the D3 flow in USGS 128. The North INTEC Buried Vent overlies the CFA buried vent flow in USGS 133, the low K_2O flow in USGS 121, the CFA buried vent flow in Middle 2050A and USGS 128. The North INTEC Buried Vent flow paleomagnetic inclinations and thicknesses in cross section C–C' coreholes are USGS 133, 55 degrees, 70 ft; USGS 121, 53 and 54 degrees, 144 ft; Middle 2050A, 53 degrees, 38 ft; and USGS 128, 57 degrees, 56 ft (Champion and others, 2011).

Low K_2O Basalt Flow.—The Low K_2O flow is only in USGS 121 in this study, where it underlies the North INTEC buried vent flow and overlies the CFA buried vent flow. The average paleomagnetic inclination is 62 degrees, and thickness is 11 ft.

Big Lost Basalt Flow.—The Big Lost flow underlies the D3 flow in USGS 130, USGS 127, USGS 131, and overlies the CFA buried vent flow in USGS 130, USGS 127, USGS 131, and Vent 5119 in USGS 105. The Big Lost flow average paleomagnetic inclinations and thicknesses in cross section C–C' coreholes are USGS 130, -30 and -32 degrees, 50 ft; USGS 127, -34 and -35 degrees, 67 ft; and USGS 131, -35, -44, and -47, 121 ft. Twelve feet of core was recovered in USGS 105 from bottom of the Big Lost flow. The average paleomagnetic inclination in USGS 105 is -35 degrees and total thickness, inferred from natural gamma logs, is 138 ft (Anderson, Ackerman, and others, 1996).

CFA Buried Vent Basalt Flow.—The CFA buried vent flow underlies the low K_2O flow in USGS 121, the North INTEC buried vent flow in USGS 133, Middle 2050A, and USGS 128, and the Big Lost flow in USGS 130, USGS 127, and USGS 131. The CFA buried vent flow average paleomagnetic inclinations and thicknesses in cross section *C–C'* coreholes are USGS 133, 67 and 65 degrees, 62 ft; USGS 121, 66, 68, and 65 degrees, 113 ft; Middle 2050A, 66, 66, 60, and 65 degrees, 177 ft; USGS 128, 67, 69, and 69 degrees, 189 ft; USGS 130, 67, 67, 67, and 69 degrees, 150 ft; USGS 127, 68 and 67 degrees, 57 ft (USGS 127 does not penetrate the base of the CFA buried vent flow); USGS 131, 66 and 67 degrees, 128 ft.

Vent 5119 Basalt Flow.—The Vent 5119 flow underlies the Big Lost flow and overlies the Middle Basal Brunhes flow in USGS 105. The Vent 5119 flow average paleomagnetic inclinations are 49 and 53 degrees, and thickness is 51 ft (pl. 1).

AEC Butte Basalt Flow.—AEC Butte is exposed at the surface, 1 mi southwest of corehole USGS 133 (fig. 1). The AEC Butte flow underlies the CFA buried vent flow in cross section *C–C'* coreholes USGS 133, USGS 121, Middle 2050A, and USGS 128. The AEC Butte flow overlies the Late Basal Brunhes flow in USGS 133, USGS 121, Middle 2050A, and the Middle Basal Brunhes flow in USGS 128. The AEC Butte flow average paleomagnetic inclinations and thicknesses in cross section *C–C'* coreholes are USGS 133, 50, 52, and 54 degrees, 185 ft; USGS 121, 58, 51, and 58 degrees, 105 ft; Middle 2050A, 52 and 53 degrees, 118 ft; USGS 128, 55, 55, and 53 degrees, 66 ft (pl. 1).

Late Basal Brunhes Basalt Flow.—The Late Basal Brunhes underlies the AEC Butte flow in cross section *C–C'* coreholes USGS 133, USGS 121, and Middle 2050A, and overlies the North Late Matuyama flow in USGS 133, and the Early Basal Brunhes flow in USGS 121 and Middle 2050A. The Late Basal Brunhes flow average paleomagnetic inclinations and thicknesses in cross section *C–C'* coreholes are USGS 133, 64 degrees, 63 ft; USGS 121, 66 degrees, 62 ft; and Middle 2050A 62 degrees, 33 ft (pl. 1).

Middle Basal Brunhes Basalt Flow.—The Middle Basal Brunhes flow underlies the AEC Butte flow in USGS 128, the CFA buried vents flow in USGS 130, USGS 131, and Vent 5119 in USGS 105. USGS 127 was not drilled deep enough to penetrate the Middle Basal Brunhes flow, but the Middle Basal Brunhes flow may exist below the total depth of USGS 127. The Middle Basal Brunhes flow overlies the Early Basal Brunhes flow in USGS 128, USGS 131, and USGS 105. The Middle Basal Brunhes flow average paleomagnetic inclinations and thicknesses in cross section *C–C'* coreholes are USGS 128, 65 degrees, 32 ft; USGS 130, 64 degrees, 17 ft; USGS 131, 66, 65, and 68 degrees, 92 ft; and USGS 105, 63, 62 degrees, 71 ft (pl. 1).

Early Basal Brunhes Basalt Flow.—The Early Basal Brunhes flow underlies the Late Basal Brunhes in USGS 121 and Middle 2050A, the Middle Basal Brunhes in USGS 128, USGS 131, and USGS 105. The Early Basal Brunhes overlies the Matuyama flow in Middle 2050A, and the South Late Matuyama in USGS 131 and USGS 105. The Early Basal Brunhes flow average paleomagnetic inclinations and thicknesses in cross section *C–C'* coreholes are USGS 121, 58 degrees, 24 ft; USGS 2050A, 52 and 53 degrees, 74 ft; USGS 128, 58 degrees, 19 ft; USGS 131, 54 degrees, 14 ft; and USGS 105, 53 degrees, 47 ft (pl. 1). The Early Basal Brunhes flow may underlie USGS 130 and USGS 127, which were not drilled deep enough for contact.

South Late Matuyama Basalt Flow.—The South Late Matuyama (SLM) flow underlies the Early Basal Brunhes flow in USGS 131 and USGS 105. The South Late Matuyama basalt flow overlies the Matuyama flow in USGS 131, and the unknown source -67-degree flow in USGS 105. The South Late Matuyama basalt flow average paleomagnetic inclinations and thicknesses in cross section *C–C'* coreholes are USGS 131, -65 and -61 degrees, 88 ft; USGS 105, -62, -60, and -59 degrees, 136 ft (pl. 1).

Unknown -65- and -67-Degrees Basalt Flow.—The Unknown -65- and -67-Basalt Flow underlies the South Late Matuyama basalt flow in cross section *C–C'* corehole USGS 105, and overlies the Matuyama basalt flow. It has average paleomagnetic inclination of -67 in cross section *C–C'* corehole USGS 105, and is 116 ft thick (pl. 1). This basalt flow correlates to a -65-degree flow in USGS 137, at a similar depth and thickness, seen in cross section *A–A'*, described in section “[Cross Section A–A'](#).”

North Late Matuyama Basalt Flow.—The North Late Matuyama flow underlies a thick sediment and the Late Basal Brunhes flow, and overlies the Matuyama flow in USGS 133. The North Late Matuyama flow average paleomagnetic inclination in USGS 133 is -47 degrees and thickness is 36 ft (pl. 1).

Matuyama Basalt Flow.—The Matuyama basalt flow underlies the North Late Matuyama flow in USGS 133, the Early Basal Brunhes flow in Middle 2050A, the South Late Matuyama flow in USGS 131, and the unknown -65 and -67 degrees flow in USGS 105. The Matuyama flow also may exist in the subsurface below the total depths of USGS 121, USGS 128, USGS 130, and USGS 127, none of which were drilled deep enough to contact the Matuyama basalt flow. The Matuyama flow average paleomagnetic inclinations and thicknesses in cross section *C–C'* coreholes are USGS 133, -72 and -69 degrees, 112 ft; USGS 2050A, -72, -67, -68, and -69 degrees, 147 ft; USGS 131, -72 degrees, 25 ft; and USGS 105, -71 and -69 degrees, 111 ft (pl. 1).

Post Jaramillo Basalt Flow.—The Post Jaramillo basalt flow underlies the Matuyama flow in USGS 105. The average paleomagnetic inclination is -67 degrees, and the corehole penetrated the Post Jaramillo basalt flow in USGS 105 to a depth of 48 ft; the total thickness of the flow in USGS 105 is likely greater than 48 ft, because the corehole was not drilled through this flow to the underlying unit.

Jaramillo Basalt Flow (990 ka to 1.070 Ma).—The Jaramillo basalt flow is so labeled because it is a normal polarity flow overlain and underlain by reversed polarity flows, which indicate that it erupted during the Jaramillo Normal Polarity Subchron of the Matuyama Reversed Polarity Chron (fig. 2). The Jaramillo basalt flow is in coreholes Middle 2050A and USGS 131. The normal polarity Jaramillo flow average paleomagnetic inclinations and thicknesses in cross section *C–C'* coreholes are Middle 2050A, 53, 52, 51, 58, 49, and 53 degrees, 195 ft; USGS 131, 51, 51, and 54 degrees, 303 ft minimum. USGS 131 was not drilled through the base of the Jaramillo flow.

Unknown -61- and -63-Degrees Basalt Flow.—The basalt flow labeled Unknown -61- and -63-Degrees Flow underlies the Jaramillo flow in Middle 2050A, and overlies the Matuyama 1.21 Ma flow. The Unknown -61 and -63-Degrees Flow average paleomagnetic inclination is -61 degrees in Middle 2050A, and thickness is 19 ft. The Unknown -61- and -63-Degrees Flow is in the cross section *B–B'* corehole Middle 1823.

Matuyama 1.21 Ma Flow The Matuyama 1.21 Ma flow is in corehole Middle 2050A, where it underlies the unknown -61- and -63-degrees flow and overlies the Matuyama 1.37 Ma flow. The average paleomagnetic inclination is -56 degrees and the thickness is 52 ft. The Matuyama 1.21 Ma flow is also in the *B–B'* corehole Middle 1823.

Matuyama 1.37 Ma Flow.—The Matuyama 1.37 Ma flow is in corehole Middle 2050A, where it underlies the Matuyama 1.21 Ma flow and overlies a very thick sediment. The average paleomagnetic inclination is -66 degrees and the thickness is 87 ft. The Matuyama 1.37 Ma flow is also in the *B–B'* coreholes Middle 1823 and C1A.

Unknown 11-Degree Flow in Middle 2050A.—The unknown 11-degree flow underlies a thick sediment, below the Matuyama 1.37 Ma flow in corehole Middle 2050A. The average paleomagnetic inclination is 11 degrees and the thickness is 11 ft.

Summary and Conclusions

Paleomagnetic inclination data were used to correlate surface and subsurface basalt stratigraphy, and to determine relative ages. Results demonstrate that coreholes a few miles apart have stratigraphic successions that correlate over tens to hundreds of feet of depth. Correlations between coreholes separated by greater distances are less consistent because some stratigraphic sequences may be missing, added, or are at different depths.

Basalt flows were correlated from surface vents to subsurface flows in coreholes in cross sections *A–A'*, *B–B'*, and *C–C'*. Correlations included:

- Quaking Aspen Butte (erupted 60 ± 16 ka [$^{40}\text{Ar}/^{39}\text{Ar}$ age]) is exposed at the surface, and is in the subsurface in USGS 132, 10.2 mi northeast of the Quaking Aspen Butte vent, where it overlies Vent 5206 flows.
- Vent 5206, (erupted 63 ± 9 ka [$^{40}\text{Ar}/^{39}\text{Ar}$ age]) is exposed at the surface, and is in the subsurface in coreholes USGS 137A, USGS 105, USGS 108, and USGS 103 to the south, USGS 132, C1A, USGS 128, USGS 130, USGS 127, and USGS 131 to the north.
- Mid Butte, (erupted 195 ± 39 ka [$^{40}\text{Ar}/^{39}\text{Ar}$ age]) is exposed at the surface, and is in the subsurface in corehole ARA-COR-005 west of the Mid Butte vent, and coreholes Middle 2050A and USGS 128, which are west-northwest of the Mid Butte vent.
- Lavatoo Butte (erupted 211 ± 16 ka [K/Ar age]) is exposed at the surface, and is in the subsurface in coreholes Middle 2051, C1A, and USGS 132 southeast of Lavatoo Butte, and probably in USGS 121, USGS 127, and USGS 131.
- Crater Butte (older than Lavatoo Butte, and younger than Pond Butte) is exposed at the surface, and is in the subsurface in coreholes USGS 134, USGS 136, and Middle 2051 to the southeast, and in USGS 121 to the east.
- Pond Butte (erupted 270 ± 15 ka [$^{40}\text{Ar}/^{39}\text{Ar}$ age]) is exposed at the surface, and is in the subsurface in coreholes USGS 134, USGS 136, Middle 2051, and C1A to the east and southeast, and in USGS 133, USGS 121, and Middle 2051, to the east and southeast.
- Vent 5350 is older than Mid Butte and younger than Vent 5252 and is in corehole ARA-COR-005 to the east.
- Big Southern Butte felsic ash (erupted 309 ± 10 ka [K/Ar age] is in core from corehole USGS 137A, and detectable in wireline geophysical logs in the uncored parts of coreholes USGS 105, USGS 108, and USGS 103.
- Vent 5252 (erupted 350 ± 40 ka [K/Ar age] is exposed at the surface, and is in the subsurface in coreholes ARA-COR-005 to the west, USGS 136 to the west-northwest, and Middle 2050A, USGS 128, USGS 130, USGS 127, and USGS 131 to the west.
- Tin Cup Butte (erupted 352 ± 5 ka [$^{40}\text{Ar}/^{39}\text{Ar}$ age]) is exposed at the surface and is in USGS 135 and USGS 137A to the east.

- Vent 4959 is older than Vent 5252 (350 ± 40 ka [K/Ar age]) and younger than CFA buried vent (536 ± 63 ka, [$^{40}\text{Ar}/^{39}\text{Ar}$ age]), is exposed at the surface, and is in coreholes USGS 134 and USGS 136 to the south and south-southeast, and in USGS 133 and USGS 121 to the east and south.
- Vent 5119 (erupted 572 ± 43 ka [$^{40}\text{Ar}/^{39}\text{Ar}$ age]) is exposed on the surface east of Atomic City and is in USGS 105, USGS 108, USGS 103, to the east, and ARA-COR-005 to the north.
- AEC Butte (erupted 637 ± 35 ka, [K/Ar]) is exposed at the surface, and is in USGS 134, USGS 136, and Middle 1823 to the south and west, USGS 133, to the northeast, USGS 121, Middle 2050A, and USGS 128 to the east and south.

Possible subsurface vent locations in this study area include:

- The D3 flow is thickest in corehole ARA-COR-005, thins towards the west and north, and may have come from the Axial Volcanic Zone. The D3 flow is much larger than previously reported; it now includes the flow previously labeled South CFA buried vent (lower).
- The Big Lost flow is thickest in the RWMC area, its vent probably lies beneath RWMC.
- The G flow thickens to the south and its vent is probably south of corehole USGS 135, in the Arco-Big Southern Butte volcanic rift zone.
- The CFA buried vent flow is probably located in the subsurface below CFA.
- The North INTEC buried vent is thickest beneath corehole USGS 121 and, as the name implies, probably originates somewhere north of INTEC.
- The South Late Matuyama flow thickens toward the southwest. This vent likely is south and west of corehole USGS 135, in the Arco-Big Southern Butte volcanic rift zone.
- The Matuyama flow is thickest in the subsurface between coreholes C1A and USGS 132 so its vent is probably under the RWMC.
- The Jaramillo flow is thickest in the subsurface at USGS 131, so the Jaramillo vent is probably underground near corehole USGS 131.

Basalt shield volcanoes and their lava flows have a wide range of eruptive volumes and lateral extents. Examination of the cross sections shows that flows may end rather abruptly, in steep fronts, as seen in cross section C–C', where the Vent 4959 flow ends against the older D3 flows, or they may

resemble the “pinch outs” seen in sedimentary successions, as seen in cross section C–C', where the High K_2O flow “pinches out” above the Vent 4959 flow, and below the younger, overlying Pond Butte flow. Flows may also pinch out in some areas, and end in steep fronts in other areas, depending on the underlying topography, and the effusion rate of the eruption.

The relief with which lava flow ends influences the emplacement of subsequent flows. Where flows end in an abrupt, steep front, subsequent flows may not overtop the flow, and will be forced laterally and downslope. Where a laterally continuous lava flow ends in a thin, uninflated margin, it will be easily overtopped by a subsequent flow. These variations may account for the sometimes discontinuous nature of basalt stratigraphy in the eastern Snake River Plain.

Acknowledgments

The authors would like to acknowledge Linda C. Davis, USGS retired, for her dedicated work in helping to create and continue the Idaho National Laboratory Lithologic Core Storage Library, which made these studies possible.

References Cited

- Ackerman, D.J., Rattray, G.W., Rousseau, J.P., Davis, L.C., and Orr, B.R., 2006, A conceptual model of ground-water flow in the eastern Snake River Plain aquifer at the Idaho National Laboratory and vicinity with implications for contaminant transport: U.S. Geological Survey Scientific Investigations Report 2006-5122 (DOE/ID-22198), 62 p., accessed February 25, 2016, at <http://pubs.usgs.gov/sir/2006/5122/>.
- Ackerman, D.J., Rousseau, J.P., Rattray, G.W., and Fisher, J.C., 2010, Steady-state and transient models of groundwater flow and advective transport, Eastern Snake River Plain aquifer, Idaho National Laboratory and vicinity, Idaho: U.S. Geological Survey Scientific Investigations Report 2010-5123, (DOE/ID-22209), 220 p., accessed February 25, 2016, at <http://pubs.usgs.gov/sir/2010/5123/>.
- Anders, M.H., and Sleep, N.H., 1992, Magmatism and extension—The terminal and mechanical effects of the Yellowstone hotspot: *Journal of Geophysical Research*, v. 97, no. B11, p. 15,379–15,393.
- Anderson, S.R., 1991, Stratigraphy of the unsaturated zone and uppermost part of the Snake River Plain aquifer at the Idaho Chemical Processing Plant and Test Reactor Area, Idaho National Engineering Laboratory, Idaho: U.S. Geological Survey Water-Resources Investigations Report 91-4010 (DOE/ID 22095), 71 p., accessed February 25, 2016, at <https://pubs.er.usgs.gov/publication/wri914010>.

- Anderson, S.R., Ackerman, D.J., Liszewski, M.J., and Freiburger, R.M., 1996, Stratigraphic data for wells at and near the Idaho National Engineering Laboratory, Idaho: U.S. Geological Survey Open-File Report 96-248 (DOE/ID-22127), 27 p. and 1 diskette, accessed February 25, 2016, at <https://pubs.er.usgs.gov/publication/ofr96248>.
- Anderson, S.R., and Bartholomay, R.C., 1995, Use of natural gamma logs and cores for determining the stratigraphic relations of basalt and sediment at the Radioactive Waste Management Complex, Idaho National Engineering Laboratory, Idaho: *Journal of the Idaho Academy of Science*, v. 31, issue 1, p. 1–10.
- Anderson, S.R., and Bowers, Beverly, 1995, Stratigraphy of the unsaturated zone and uppermost part of the Snake River Plain aquifer at Test Area North, Idaho National Engineering Laboratory, Idaho: U.S. Geological Survey Water-Resources Investigations Report 95-4130 (DOE/ID-22122), 47 p.
- Anderson, S.R., Kuntz, M.A., and Davis, L.C., 1999, Geologic controls of hydraulic conductivity in the Snake River Plain aquifer at and near the Idaho National Engineering and Environmental Laboratory, Idaho: U.S. Geological Survey Water-Resources Investigations Report 99-4033 (DOE/ID-22155), 38 p., accessed February 25, 2016, at <https://pubs.er.usgs.gov/publication/wri994033>.
- Anderson, S.R., and Lewis, B.D., 1989, Stratigraphy of the unsaturated zone at the Radioactive Waste Management Complex, Idaho National Engineering Laboratory, Idaho: U.S. Geological Survey Water-Resources Investigations Report 89-4065 (DOE/ID-22080), 54 p., accessed February 25, 2016, at <https://pubs.er.usgs.gov/publication/wri894065>.
- Anderson, S.R., and Liszewski, M.J., 1997, Stratigraphy of the unsaturated zone and the Snake River Plain aquifer at and near the Idaho National Engineering Laboratory, Idaho: U.S. Geological Survey Water-Resources Investigations Report 97-4183 (DOE/ID-22142), 65 p., accessed February 25, 2016, at <https://pubs.er.usgs.gov/publication/wri974183>.
- Anderson, S.R., Liszewski, M.J., and Ackerman, D.J., 1996, Thickness of surficial sediment at and near the Idaho National Engineering Laboratory, Idaho: U.S. Geological Survey Open-File Report 96-330 (DOE/ID-22128), 16 p.
- Anderson, S.R., Liszewski, M.J., and Cecil, L.D., 1997, Geologic ages and accumulation rates of basalt-flow groups and sedimentary interbeds in selected wells at the Idaho National Engineering Laboratory, Idaho: U.S. Geological Survey Water-Resources Investigations Report, 97-4010 (DOE/ID-22134), 39 p., accessed April 5, 2016, at <http://pubs.usgs.gov/wri/1997/4010/report.pdf>.
- Bartholomay, R.C., 1990, Digitized geophysical logs for selected wells on or near the Idaho National Engineering Laboratory, Idaho: U.S. Geological Survey Open-File Report 90-366, 347 p., accessed April 19, 2016, at <http://pubs.usgs.gov/of/1990/0366/report.pdf>.
- Bartholomay, R.C., Hopkins, C.B., and Maimer, N.V., 2015, Chemical constituents in groundwater from multiple zones in the eastern Snake River Plain aquifer, Idaho National Laboratory, Idaho, 2009–13: U.S. Geological Survey Scientific Investigations Report 2015–5002 (DOE/ID-22232), 110 p., accessed February 25, 2016, at <https://pubs.er.usgs.gov/publication/sir20155002>.
- Bestland, E.A., Link, P.K., Lanphere, M.A., and Champion, D.E., 2002, Paleoenvironments of sedimentary interbeds in the Pliocene and Quaternary Big Lost Trough (eastern Snake River Plain, Idaho), *in* Link, P.K., and Mink, L.L., eds., *Geology, hydrogeology and environmental remediation*, Idaho National Engineering and Environmental Laboratory, Eastern Snake River Plain, Idaho: Boulder, Colo., Geological Society of America Special Paper 353, p. 27–44.
- Blair, J.J., 2002, Sedimentology and stratigraphy of sediments of the Big Lost trough subsurface from selected coreholes at the Idaho National Engineering and Environmental Laboratory: Idaho State University, Master's thesis, 148 p.
- Braile, L.W., Smith, R.B., Anson, J., Baker, M.R., Sparlin, M.A., Prodehl, C., Schilly, M.M., Healy, J.H., Mueller, S., and Olsen, K.H., 1982, The Yellowstone-Snake River Plain seismic profiling experiment—Crustal structure of the Eastern Snake River Plain: *Journal of Geophysical Research*, v. 87, no. B4, p. 2,597–2,609.
- Champion, D.E., Dalrymple, G.B., and Kuntz, M.A., 1981, Radiometric and paleomagnetic evidence for the Emperor reversed polarity event at 0.46 ± 0.05 m. y. in basalt lava flows from the eastern Snake River Plain, Idaho: *Geophysical Research Letters*, v. 8, no. 10, p. 1,055–1,058.
- Champion, D.E., Davis, L.C., Hodges, M.K.V., and Lanphere, M.A., 2013, Paleomagnetic correlation and ages of basalt flow groups in coreholes at and near the Naval Reactors Facility, Idaho National Laboratory, Idaho: U.S. Geological Survey Scientific Investigations Report 2013-5012 (DOE/ID-22223), 48 p.
- Champion, D.E., and Greeley, R., 1978, Geology of the Wapi Lava Field, Idaho, *in* Greeley, R., and King, J.S., eds., *Volcanism of the Snake River Plain, a comparative planetary geology guidebook*: Washington, D.C., Office of Planetary Geology, National Aeronautics and Space Administration, p. 133–152.

- Champion, D.E., and Herman, T.C., 2003, Paleomagnetism of basaltic lava flows in coreholes ICPP-213, ICPP-214, ICPP-215, and USGS 128 near the vadose zone research park, Idaho Nuclear Technology and Engineering Center, Idaho National Engineering and Environmental Laboratory, Idaho: U.S. Geological Survey Open-File Report 2003-483 (DOE/ID 22189), 21 p.
- Champion, D.E., Hodges, M.K.V., Davis, L.C., and Lanphere, M.A., 2011, Paleomagnetic correlation of surface and subsurface basaltic lava flows and flow groups in the southern part of the Idaho National Laboratory, Idaho, with paleomagnetic data tables for drill cores: U.S. Geological Survey Scientific Investigations Report 2011-5049, 34 p., 1 pl. (DOE/ID 22214), accessed February 25, 2016, at <https://pubs.er.usgs.gov/publication/sir20115049>.
- Champion, D.E., and Lanphere, M.A., 1997, Age and paleomagnetism of basaltic lava flows in corehole ANL-OBS-AQ-014 at Argonne National Laboratory-West, Idaho National Engineering and Environmental Laboratory. U.S. Geological Survey Open-File Report 97-700, 34 p., accessed April 25, 2016, at <http://pubs.usgs.gov/of/1997/0700/report.pdf>.
- Champion, D.E., Lanphere, M.A., Anderson, S.R., and Kuntz, M.A., 2002, Accumulation and subsidence of late Pleistocene basaltic lava flows of the eastern Snake River Plain, Idaho, *in* Link, P.K., and Mink, L.L., eds., *Geology, hydrogeology, and environmental remediation—Idaho National Engineering and Environmental Laboratory, Eastern Snake River Plain, Idaho*: Boulder, Colo., Geological Society of America Special Paper 353, p. 175–192.
- Champion, D.E., Lanphere, M.A., and Kuntz, M.A., 1988, Evidence for a new geomagnetic reversal from lava flows in Idaho—Discussion of short polarity reversals in the Brunhes and late Matuyama polarity chrons: *Journal of Geophysical Research*, v. 93, no. B10, p. 11,667–11,680.
- Champion, D.E., and Shoemaker, E.M., 1977, Paleomagnetic evidence for episodic volcanism on the Snake River Plain: National Aeronautics and Space Administration Technical Memorandum 78 436, p. 7–9.
- Davis, L.C., Hannula, S.R., and Bowers, Beverly, 1997, Procedures for use of, and drill cores and cuttings available for study at the Lithologic Core Storage Library, Idaho National Engineering Laboratory, Idaho: U.S. Geological Survey Open-File Report 97-124 (DOE/ID-22135), 31 p., accessed February 25, 2016, at <https://pubs.er.usgs.gov/publication/ofr97124>.
- Geslin, J.K., Link, P.K., Riesterer, J.W., Kuntz, M.A., and Fanning, C.M., 2002, Pliocene and Quaternary stratigraphic architecture and drainage systems of the Big Lost Trough, northeastern Snake River Plain, Idaho, *in* Link, P.K., and Mink, L.L., eds., *Geology, hydrogeology, and environmental remediation—Idaho National Engineering and Environmental Laboratory, Eastern Snake River Plain, Idaho*: Boulder, Colo., Geological Society of America Special Paper 353, p. 11–26.
- Greeley, Ronald, 1982, The style of basaltic volcanism in the eastern Snake River Plain, Idaho, *in* Bonnicksen, Bill, and Breckinridge, R.M., eds., *Cenozoic geology of Idaho*: Idaho Bureau of Mines and Geology Bulletin 26, p. 407–421.
- Grimm-Chadwick, Claire, 2004, Petrogenesis of an evolved olivine tholeiite and chemical stratigraphy of cores USGS 127, 128, and 129, Idaho National Engineering and Environmental Laboratory: Idaho State University, Master's thesis, 100 p., plus apps.
- Hackett, W.R., and Smith, R.P., 1992, Quaternary volcanism, tectonics, and sedimentation in the Idaho National Engineering Laboratory area, *in* Wilson, J.R., ed., *Field guide to geologic excursions in Utah and adjacent areas of Nevada, Idaho, and Wyoming*: Utah Geological Survey Miscellaneous Publication 92-3, p. 1–18.
- Hagstrum, J.T., and Champion, D.E., 2002, A Holocene paleosecular variation record from ¹⁴C-dated volcanic rocks in western North America: *Journal of Geophysical Research*, v. 107, no. B1, 2,025, 14 p. (doi:10.1029/2001JB000524).
- Hodges, M.K.V., Orr, S.M., Potter, K.E., and LeMaitre, Tynan, 2012, Construction diagrams, geophysical logs, and lithologic descriptions for boreholes USGS 103, 105, 108, 131, 135, NRF-15, and NRF-16, Idaho National Laboratory, Idaho: U.S. Geological Survey Data Series 660, 34 p., accessed February 25, 2016, at <https://pubs.er.usgs.gov/publication/ds660>.
- Hodges, M.K.V., Turrin, B.D., Champion, D.E., and Swisher, C.C., III, 2015, New argon-argon (⁴⁰Ar/³⁹Ar) radiometric age dates from selected subsurface basalt flows at the Idaho National Laboratory, Idaho: U.S. Geological Survey Scientific Investigations Report 2015-5028 (DOE/ID 22234), 25 p., accessed February 25, 2016, at <https://pubs.er.usgs.gov/publication/sir20155028>.
- Hughes, S.S., Smith, R.P., Hackett, W.R., and Anderson, S.R., 1999, Mafic volcanism and environmental geology of the eastern Snake River Plain *in* Hughes, S.S., and Thackray, G.D., eds., *Guidebook to the geology of eastern Idaho*: Pocatello, Idaho, Idaho Museum of Natural History, p. 143–168.

- Kellogg, K.S., Harlan, S.S., Mehnert, H.H., Snee, L.W., Pierce, K.S., Hackett, W.R., and Rodgers, D.W., 1994, Major 10.2-Ma rhyolitic volcanism in the eastern Snake River Plain, Idaho—Isotopic age and stratigraphic setting of the Arbon Valley Tuff Member of the Starlight Formation: U.S. Geological Survey Bulletin 2091, 18 p., accessed February 25, 2016, at <https://pubs.er.usgs.gov/publication/b2091>.
- Kuntz, M.A., 1978, Geology of the Big Southern Butte area, eastern Snake River Plain, and potential volcanic hazards to the Radioactive Waste Management Complex, and other waste storage and reactor facilities at the Idaho National Engineering Laboratory, Idaho, *with a section on* Statistical treatment of the age of lava flows, by John O. Kork: U.S. Geological Survey Open-File Report 78-691, 70 p.
- Kuntz, M.A., 1992, A model-based perspective of basaltic volcanism, eastern Snake River Plain, Idaho *in* Link, P.K., Kuntz, M.A., and Platt, L.B., Regional geology of eastern Idaho and western Wyoming: Geological Society of America Memoir 179, p. 289–304.
- Kuntz, M.A., Anderson, S.R., Champion, D.E., Lanphere, M.A., and Grunwald, D.J., 2002, Tension cracks, eruptive fissures, dikes, and faults related to late Pleistocene-Holocene basaltic volcanism and implications for the distribution of hydraulic conductivity in the eastern Snake River Plain, *in* Link, P.K., and Mink, L.L., eds., Geology, hydrogeology, and environmental remediation—Idaho National Engineering and Environmental Laboratory, eastern Snake River Plain, Idaho: Boulder, Colo., Geological Society of America Special Paper 353, p. 111–133.
- Kuntz, M.A., Covington, H.R., and Schorr, L.J., 1992, An overview of basaltic volcanism of the eastern Snake River Plain, Idaho, *in* Link, P.K., Kuntz, M.A., and Platt, L.B., Regional geology of eastern Idaho and western Wyoming: Geological Society of America Memoir 179, p. 227–267.
- Kuntz, M.A., Dalrymple, G.B., Champion, D.E., and Doherty, D.J., 1980, An evaluation of potential volcanic hazards at the Radioactive Waste Management Complex, Idaho National Engineering Laboratory, Idaho: U.S. Geological Survey Open-File Report 80-388, 63 p., 1 map, accessed February 25, 2016, at <https://pubs.er.usgs.gov/publication/ofr80388>.
- Kuntz, M.A., Link, P.K., Boyack, D.L., Geslin, J.K., Mark, L.E., Hodges, M.K.V., Kauffman, M.E., Champion, D.E., Lanphere, M.R., Rodgers, D.W., and Anders, M.H., 2003, Geologic map of the northern and central parts of the Idaho National Engineering and Environmental Laboratory, Eastern Idaho: Idaho Geological Survey Publication GM-35, color map with 14 page booklet, scale 1:50,000, accessed March 3, 2016, at <http://www.idahogeology.org/Products/MapCatalog/default.asp?switch=title&value=GM-35>.
- Kuntz, M.A., Skipp, Betty, Lanphere, M.A., Scott, W.E., Pierce, K.L., Dalrymple, G.B., Champion, D.E., Embree, G.F., Page, W.R., Morgan, L.A., Smith, R.P., Hackett, W.R., and Rodgers, D.W., 1994, Geologic map of the Idaho National Engineering Laboratory and adjoining area, eastern Idaho: U.S. Geological Survey Miscellaneous Investigations Series I-2330, scale 1:100,000. [Also available at http://ngmdb.usgs.gov/Prodesc/proddesc_10237.htm.]
- Kuntz, M.A., Skipp, Betty, Champion, D.E., Gans, P.B., Van Sistine, D.P., and Snyders, S.R., 2007, Geologic map of the Craters of the Moon 30' x 60' quadrangle, Idaho: U.S. Geological Survey Scientific Investigations Map 2969, 64-p. pamphlet, 1 plate, scale 1:100,000, accessed July 27, 2016, at <http://pubs.usgs.gov/sim/2007/2969/>.
- Kuntz, M.A., Spiker, E.C., Rubin, Meyer, Champion, D.E., and Lefebvre, R.H., 1986, Radiocarbon studies of latest Pleistocene and Holocene lava flows of the Snake River Plain, Idaho—Data, lessons, interpretations: Quaternary Research, v. 25, no. 2, p. 163–176.
- Lanphere, M.A., Champion, D.E., and Kuntz, M.A., 1993, Petrography, age, and paleomagnetism of basalt lava flows in coreholes Well 80, NRF 89-04, NRF 89-05, and ICPP 123, Idaho National Engineering Laboratory: U.S. Geological Survey Open-File Report 93-0327, 40 p.
- Lanphere, M.A., Kuntz, M.A., and Champion, D.E., 1994, Petrography, age, and paleomagnetism of basaltic lava flows in coreholes at Test Area North (TAN), Idaho National Engineering Laboratory: U.S. Geological Survey Open-File Report 94-686, 49 p.
- Mazurek, John, 2004, Genetic controls on basalt alteration within the eastern Snake River Plain aquifer system, Idaho: Idaho State University, Master's thesis, 132 p. and apps.
- McCurry, M., Hackett, W.R., and Hayden, K., 1999, Cedar Butte and cogenetic Quaternary rhyolite domes of the eastern Snake River Plain, *in* Hughes, S.S., and Thackray, G.D., eds., Guidebook to the Geology of Eastern Idaho: Idaho Museum of Natural History, p. 169–179.
- McCurry, M.O., and Hughes, S.S., 2006, Rhyolite volcanic fields of the Yellowstone-Snake River Plain hot spot track—Does the Picabo Field exist?: Eos, Transactions, American Geophysical Union, v. 87, no. 52, Suppl. 26, Abstract V51D-1705.
- McFadden, P.L., and Reid, A.B., 1982, Analysis of paleomagnetic inclination data: Geophysical Journal of the Royal Astronomical Society, v. 69, no. 2, p. 307–319.
- McQuarrie, Nadine, and Rodgers, D.W., 1998, Subsidence of a volcanic basin by flexure and lower crustal flow—The eastern Snake River Plain, Idaho: Tectonics, v. 17, p. 203–220.

- Miller, M.L., 2007, Basalt stratigraphy of corehole USGS-132 with correlations and petrogenetic interpretations of the B Flow Group, Idaho National Laboratory, Idaho: Idaho State University, Master's thesis, 69 p., app., and 1 pl.
- Morgan, L.A., and McIntosh, W.C., 2005, Timing and development of the Heise volcanic field, Snake River Plain, Idaho, western USA: Geological Society of America Bulletin, v. 117, no. 3 of 4, p. 288–306.
- Morse, L.H., and McCurry, M.O., 2002, Genesis of alteration of Quaternary basalts within a portion of the eastern Snake River Plain aquifer, *in* Link, P.K., and Mink, L.L., eds., Geology, hydrogeology, and environmental remediation—Idaho National Engineering and Environmental Laboratory, eastern Snake River Plain, Idaho: Boulder, Colo., Geological Society of America Special Paper 353, p. 213–224.
- North American Commission on Stratigraphic Nomenclature, 2005, North American Stratigraphic Code: The American Association of Petroleum Geologists Bulletin, v. 89, no. 11, p. 1,547–1,591, accessed July 27, 2016, at http://ngmdb.usgs.gov/Info/NACSN/05_1547.pdf.
- Ogg, J.G., and Smith, A.G., 2004, The geomagnetic polarity time scale, *in* Gradstein, F.M., Ogg, J.G., and Smith, A.G., eds., 2004, A geologic time scale 2004: New York, Cambridge University Press, 589 p.
- Peng, Xiaohua, and Humphreys, E.D., 1998, Crustal velocity structure across the eastern Snake River Plain and the Yellowstone Swell: Journal of Geophysical Research, v. 103, no. B4, p. 7,171–7,186.
- Pierce, K.L., and Morgan, L.A., 1992, The track of the Yellowstone hot spot, *in* Link, P.K., Kuntz, M.A., and Platt, L.B., eds., Regional geology of eastern Idaho and western Wyoming: Geological Society of America Memoir 179, p. 1–53.
- Pierce, K.L., Morgan, L.A., and Saltus, R.W., 2002, Yellowstone plume head—Postulated tectonic relations to the Vancouver Slab, continental boundaries, and climate, *in* Bonnichsen, Bill, White, C.M., and McCurry, M.O., eds., Tectonic and magmatic evolution of the Snake River Plain volcanic province: Idaho Geological Survey Bulletin 30, p. 5–29.
- Reed, M.F., Bartholomay, R.C., and Hughes, S.S., 1997, Geochemistry and stratigraphic correlation of basalt lavas beneath the Idaho Chemical Processing Plant, Idaho National Engineering Laboratory: Berlin, Germany, Environmental Geology, v. 30, no. 1–2, p. 108–118.
- Rightmire, C.T., and Lewis, B.D., 1987, Geologic data collected and analytical procedures used during a geochemical investigation of the unsaturated zone, Radioactive Waste Management Complex, Idaho National Engineering Laboratory, Idaho: U.S. Geological Survey Open-File Report 87-0246 (DOE/ID-22072), 83 p.
- Rodgers, D.W., Ore, H.T., Bobo, R.T., McQuarrie, Nadine, and Zentner, Nick, 2002, Extension and subsidence of the eastern Snake River Plain, Idaho, *in* Bonnichsen, Bill, White, C.M., and McCurry, Michael, eds., Tectonic and Magmatic Evolution of the Snake River Plain Volcanic Province: Idaho Geological Survey Bulletin 30, p. 121–155.
- Russell, I.C., 1902, Geology and water resources of the Snake River plains of Idaho: U.S. Geological Survey Series Bulletin Report Number 199, 192 p.
- Scarberry, K.C., 2003, Volcanology, geochemistry, and stratigraphy of the F Basalt Flow Group, eastern Snake River Plain, Idaho: Idaho State University, Master's thesis, 139 p., 1 pl.
- Shervais, J.W., Vetter, S.K., and Hanan, B.B., 2006, A layered mafic sill complex beneath the eastern Snake River Plain—Evidence from cyclic geochemical variations in basalt: Geology, v. 34, no. 5, p. 365–368.
- Skipp, Betty, Snider, L.G., Janecke, S.U., and Kuntz, M.A., 2009, Geologic map of the Arco 30 x 60 minute quadrangle, south-central Idaho: Idaho Geological Survey Geologic Map GM-47, map scale 1:100,000 and 42 p. booklet, accessed March 3, 2016, at <http://www.idahogeology.org/Products/MapCatalog/default.asp?switch=title&value=GM-47>.
- Stroup, C.N., Welhan, J.A., and Davis, L.C., 2008, Statistical stationarity of sediment interbed thicknesses in a basalt aquifer, Idaho National Laboratory, eastern Snake River Plain, Idaho: U.S. Geological Survey Scientific Investigations Report 2008-5167 (DOE/ID-22204), 20 p.
- Tauxe, Lisa, Luskin, Casey, Selkin, Peter, Gans, Phillip, and Calvert, Andy, 2004, Paleomagnetic results from the Snake River Plain—Contribution to the time-and field global database: G3, Geochemistry, Geophysics, and Geosystems, American Geophysical Union and the Geochemical Society, v. 5, no. 8, 19 p.
- Twining, B.V., Hodges, M.K.V., and Orr, Stephanie, 2008, Construction diagrams, geophysical logs, and lithologic descriptions for boreholes USGS 126a, 126b, 127, 128, 129, 130, 131, 132, 133, and 134, Idaho National Laboratory, Idaho: U.S. Geological Survey Data Series Report 350 (DOE/ID-22205), 27 p., and apps., accessed February 25, 2016, at <http://pubs.usgs.gov/ds/350/>.

- Walker, G.P.L., 2000, Basaltic volcanoes and volcanic systems, *in* Sigurdsson, H., ed., *Encyclopedia of volcanoes*: New York, Academic Press, p. 283–289.
- Welhan, J.A., Farabaugh, R.L., Merrick, M.J., and Anderson, S.R., 2007, Geostatistical modeling of sediment abundance in a heterogeneous basalt aquifer at the Idaho National Laboratory, Idaho: U.S. Geological Survey Scientific Investigations Report 2006-5316 (DOE/ID-22201), 32 p.
- Welhan, J.A., Johannesen, C.M., Davis, L.L., Reeves, K.S., and Glover, J.A., 2002, Overview and synthesis of lithologic controls on aquifer heterogeneity in the eastern Snake River Plain, Idaho, *in* Bonnicksen, Bill., White, C.M., and McCurry, M.O., eds., *Tectonic and magmatic evolution of the Snake River Plain Volcanic Province*: Idaho Geological Survey Bulletin 30, p. 435–460.
- Wetmore, P.H., 1998, An assessment of physical volcanology and tectonics of the central Eastern Snake River Plain based on the correlation of subsurface basalts at and near the Idaho National Engineering and Environmental Laboratory, Idaho: Pocatello, Idaho State University, Master's thesis, 118 p.
- Wetmore, P.H., and Hughes, S.S., 1997, Change in magnitude of basaltic magmatism determined from model morphologies of subsurface quaternary lavas at the Idaho National Engineering and Environmental Laboratory, Idaho: Geological Society of America Abstracts with Programs, v. 29, no. 6, p. 365.
- Wetmore, P.H., Hughes, S.S., Rodgers, D.W., and Anderson, S.R., 1999, Late Quaternary constructional development of the Axial Volcanic Zone, eastern Snake River Plain, Idaho: Geological Society of America Abstracts with Programs, v. 31, no. 4, p. 61.

This page intentionally left blank.

Appendix A. Previously Unpublished Paleomagnetic Data

Previously unpublished depth and paleomagnetic inclination data from coreholes USGS 103, USGS 105, USGS 108, USGS 131 (from 808 to 1,239 ft), USGS 136, and USGS137A. are presented in [table A1](#). Tables are organized numerically by corehole name. Paleomagnetic data for USGS 131 from land surface to 808 ft, and other coreholes in this report were published in Champion and others (2011).

Information in the tables includes sample depth and identification of sample groups that were used to determine the average inclination for flows and 95 percent uncertainty. Each sample has a characteristic remanent inclination in degrees and an alternating field demagnetization level in milliTeslas or an alternative demagnetization approach. Positive inclination values indicate normal paleomagnetic polarity, and negative inclination values indicate reversed paleomagnetic polarity.

Some coreholes are not vertical. In cases where the corehole deviates from vertical to the north or south, deviation correction values were obtained from geophysical deviation logs and applied to the paleomagnetic inclination data obtained from deviated samples to account for this variation from the vertical. Paleomagnetic inclination data, which were corrected for borehole deviation are in parentheses, and the corrected values presented in the column to the right of the

measured values. Deviation corrections were applied to the average paleomagnetic inclination of sample groups.

Petrographic boundaries denote a significant change in mineralogy in a flow. Unrecovered core and sediment intervals were also recorded in the depth column. Samples that are labeled “NIIA,” were not included in the average. NIIA samples may have been thermally overprinted by overlying flows, tilted by endogenous inflation, struck by lightning when on the surface, or otherwise had their orientations disturbed so that they do not yield usable paleomagnetic inclination data.

Stepwise thermal demagnetizations were done only on samples of particular interest.

The designation “Li” stands for values derived from a line fit performed from a vector component diagram using a sequence, or all of the demagnetizations steps from each sample from that site.

The designation “TO” stands for “thermal overprinting.” Samples that are thermally overprinted may require extra processing to discover their original orientation. If thermal overprinting was extensive, the sample may not yield useful paleomagnetic data, and those samples were not included in averages. Measurements are in feet and milliTeslas because the raw data were collected using these units of measure.

Table A1. Paleomagnetic inclination values for basalt samples from coreholes at and near the Idaho National Laboratory, Idaho.

[See figure 1 and plate 1 for corehole locations. Sample depth measured to nearest 1 foot; shading delimits groups of samples used to determine the average flow inclination and 95 percent uncertainty level. For additional information see, appendix A text. **Characteristic remanent inclination:** In degrees down (negative value) or up (positive value) from the horizontal obtained by demagnetization. Petrographic boundary, indicates noted change in mineralogy. **Alternating-field:** Deviation corrected inclination, average inclination corrected for corehole deviation from vertical orientation, blank if not corrected. Li, values derived from a line fit from a vector component diagram. Therm, stepwise thermal demagnetization was applied to the sample. **Average flow inclination:** OP, overprint; NIA, the sample was not included in the group average inclination. Parenthesis indicate that the deviation in this corehole was great enough in the north-south direction to warrant correction. **Abbreviations:** Alt, altitude above National Geodetic Vertical Datum of 1929 (NGVD 29); ft, foot; mT, milliTesla; N, north; N/A, not applicable; TO, sample was thermally overprinted by overlying flow; W, west; WL, water level below land surface, in feet, approximate]

NAD 27

N 43°27'13.57"

W 112°56'06.53

Alt 5,007.42 ft

NGVD 29

TD 1,307 ft

WL 588.09 ft

Corehole USGS 103

Sample depth (ft)	Characteristic remanent inclination (degrees)	Alternating field demagnetization level (mT) or alternative demagnetization approach	Average flow inclination and 95 percent uncertainty level for sample groupings (degrees)	Deviation corrected inclination for sample groupings (degrees)
763	39.8	40		
765	41.9	40	(39.2 ± 1.9)	45.5
767	41.6	40		
771	38.0	30		
773	37	40		
774	36.2	30		
777	38.1	30		
779	41.3	40		
Petrographic boundary at 779 ft				
782	41.8	40	(43.1 ± 1.9)	50
783	43.3	40		
786	42.7	40		
788	42.3	30		
789	45.2	40		
Petrographic boundary at 790 ft				
791	40.0	40	(42.2 ± 2.8)	49
794	44.4	40		
796	38.9	30		
797	42.2	30		
799	45.4	40		
801	42	40		
Sediment and unrecovered core between 801 and 803 ft				
804	49.9	30	(44.8 ± 2.7)	51.5
807	46.4	40		
810	48.1	30		
813	49.8	40		
819	52.4	30		
824	40.3	30		
827	41.6	30		
830	41.2	40		
835	46.6	40		
839	44.5	30		
844	39.5	30		
846	39.4	10		
849	42.2	30		

Table A1. Paleomagnetic inclination values for basalt samples from coreholes at and near the Idaho National Laboratory, Idaho.—
Continued

NAD 27				
N 43°27'13.57"				
W 112°56'06.53				
Alt 5,007.42 ft				
NGVD 29				
TD 1,307 ft				
WL 588.09 ft				
Corehole USGS 103				
Sample depth (ft)	Characteristic remanent inclination (degrees)	Alternating field demagnetization level (mT) or alternative demagnetization approach	Average flow inclination and 95 percent uncertainty level for sample groupings (degrees)	Deviation corrected inclination for sample groupings (degrees)
Sediment and unrecovered core between 850 and 856 ft				
859	52.9	40	(53.9 ± 1.7)	60
864	55.5	40		
869	54.9	40		
874	551.7	40		
880	49.4	40		
884	56.1	30		
889	56.8	40		
894	55.9	30		
899	53.3	30		
904	52.2	40		
Petrographic boundary at 905 ft				
909	55.5	40	(51.8 ± 2.6)	58
911	51.7	40		
914	51.7	40		
920	54.3	40		
924	52.1	40		
928	50.0	40		
932	47.5	40		
Sediment and unrecovered core between 932 and 939 ft				
941	69.2	40	Not included in average	
948	59.1	40	(60.0 ± 1.5)	65.5
951	62.3	40		
953	60.1	40		
958	61.8	40		
959	56.9	40		
961	57.6	10		
964	60.8	30		
967	60.4	20		
Sediment between 968 and 969 ft				
972	61.3	Therm		
975	56.6	Therm	Not included in average	
979	49.9	40	(48.8 ± 1.8)	54.5
983	46.6	40		
986	47.2	30		
990	48	30		
991	51.7	40		
994	49.2	30		
997	51.3	40		
1,000	46.5	40		

30 Paleomagnetic Correlation of Basalt Flows in Coreholes, Idaho National Laboratory, Idaho

Table A1. Paleomagnetic inclination values for basalt samples from coreholes at and near the Idaho National Laboratory, Idaho.—
Continued

Corehole USGS 103				
Sample depth (ft)	Characteristic remanent inclination (degrees)	Alternating field demagnetization level (mT) or alternative demagnetization approach	Average flow inclination and 95 percent uncertainty level for sample groupings (degrees)	Deviation corrected inclination for sample groupings (degrees)
NAD 27				
N 43°27'13.57"				
W 112°56'06.53				
Alt 5,007.42 ft				
NGVD 29				
TD 1,307 ft				
WL 588.09 ft				
Petrographic boundary at 1,002 ft				
1,002	46.9	40	(49.2 ± 1.2)	55
1,006	49.4	40		
1,010	50.1	40		
1,014	51.0	30		
1,019	47.1	40		
1,024	49.3	40		
1,028	51.0	40		
1,032	50.2	40		
1,036	48.0	40		
Sediment and unrecovered core between 1,036 and 1,043 ft				
1,045	-56.9	40	(-52.4 ± 1.1)	-58.5
1,048	-52.1	40		
1,051	-51.1	40		
1,054	-55.0	40		
1,056	-56.4	40		
1,059	-56.1	40		
1,060	-51.7	40		
1,063	-51.3	30		
1,066	-54.9	40		
1,070	-49.5	40		
1,074	-45.8	40		
1,076	-47.6	40		
1,079	-53.7	40		
1,081	-52.4	40		
1,084	-52.1	40		
1,086	-52.7	40		
1,090	-48.9	40		
1,094	-51.4	30		
1,095	-52.5	40		
1,098	-52.7	40		
1,101	-53.5	30		
1,104	-54.7	40		
1,108	-54.5	40		
1,111	-5.5	40		
1,115	-51.6	40		
1,118	-55.7	40		
1,121	-51.6	40		
1,124	-48.7	40		

Table A1. Paleomagnetic inclination values for basalt samples from coreholes at and near the Idaho National Laboratory, Idaho.—
Continued

NAD 27					
N 43°27'13.57"					
W 112°56'06.53					
Alt 5,007.42 ft					
NGVD 29					
TD 1,307 ft					
WL 588.09 ft					
Corehole USGS 103					
Sample depth (ft)	Characteristic remanent inclination (degrees)	Alternating field demagnetization level (mT) or alternative demagnetization approach	Average flow inclination and 95 percent uncertainty level for sample groupings (degrees)	Deviation corrected inclination for sample groupings (degrees)	
Petrographic boundary at 1,126 ft					
1,127	-51.4	40	(-51.9 ± 1.1)	-58.5	
1,131	-52.0	40			
1,135	-51.2	40			
1,140	-51.6	40			
1,143	-50.0	40			
1,147	-50.3	30			
1,153	-52.0	40			
1,159	-54.4	40			
1,165	-54.6	40			
1,169	-48.0	40			
1,174	-53.9	30			
1,177	-51.6	40			
Petrographic boundary at 1,178 ft					
1,181	-54.1	therm	(-61.4 ± 2.6)	-67	
1,184	-54.0	therm			
1,188	-50.0	40			
1,191	-58.9	30			
1,197	-61.4	40			
1,200	-63.7	40			
1,204	-58.0	40			
1,206	-50.3	40			Not included in average
1,209	-65.3	40			
1,211	-59.7	40			
1,213	-62.9	40			
Sediment between 1,214 and 1,215 ft					
1,216	-60.9	40	(-60.0 ± 1.9)	-66	
1,219	-61.1	40			
1,223	-64.0	30			
1,225	-55.4	30			
1,228	-65.4	30			
1,232	-64.1	30			
1,235	-62.9	40			
1,238	-62.1	40			
1,243	-59.7	40			
1,248	-57.9	40			
1,254	-58.9	30			
1,259	-58.8	30			
1,263	-58.0	40			
1,269	-56.5	40			
1,275	-54.4	40			

Table A1. Paleomagnetic inclination values for basalt samples from coreholes at and near the Idaho National Laboratory, Idaho.—
Continued

Corehole USGS 103				
Sample depth (ft)	Characteristic remanent inclination (degrees)	Alternating field demagnetization level (mT) or alternative demagnetization approach	Average flow inclination and 95 percent uncertainty level for sample groupings (degrees)	Deviation corrected inclination for sample groupings (degrees)
Petrographic boundary at 1,277 ft				
1,279	-62.2	40	(-59.7 ± 2.4)	-65.5
1,282	-55.3	30		
1,285	-57.9	40		
1,286	-62.1	30		
1,288	-60.7	40		
1,291	-60.6	40		
1,292	-58.9	40		
Petrographic boundary at 1,294 ft				
1,294	-61.9	30	(-62.9 ± 1.7)	-68.5
1,297	-63.1	40		
1,298	-62.9	30		
1,300	-61.1	40		
1,302	-61.2	40		
1,304	-65.8	40		
1,307	-64.3	30		

Table A1. Paleomagnetic inclination values for basalt samples from coreholes at and near the Idaho National Laboratory, Idaho.—Continued

[See figure 1 and plate 1 for corehole locations. Sample depth measured to nearest 1 foot; shading delimits groups of samples used to determine the average flow inclination and 95 percent uncertainty level. For additional information see, appendix A text. **Characteristic remanent inclination:** In degrees down (negative value) or up (positive value) from the horizontal obtained by demagnetization. Petrographic boundary, indicates noted change in mineralogy. **Alternating-field:** Deviation corrected inclination, average inclination corrected for corehole deviation from vertical orientation, blank if not corrected. Li, values derived from a line fit from a vector component diagram. Therm, stepwise thermal demagnetization was applied to the sample. **Average flow inclination:** OP, overprint; NIIA, the sample was not included in the group average inclination. Parenthesis indicate that the deviation in this corehole was great enough in the north-south direction to warrant correction. **Abbreviations:** Alt, altitude above National Geodetic Vertical Datum of 1929 (NGVD 29); ft, foot; mT, milliTesla; N, north; N/A, not applicable; TO, sample was thermally overprinted by overlying flow; W, west; WL, water level below land surface, in feet, approximate]

NAD 27
N 43°27'13.40"
W 113°00'17.78
NGVD 29
Alt 5,095.12 ft
TD 1,409 ft
WL 490.55 ft

Corehole USGS 105

Sample depth (ft)	Characteristic remanent inclination (degrees)	Alternating field demagnetization level (mT) or alternative demagnetization approach	Average flow inclination and 95 percent uncertainty level for sample groupings (degrees)	Deviation corrected inclination for sample groupings (degrees)
802	-31.9	Therm		
805	-33.5	Therm	(-34.9 ± 1.7)	-34.5
807	-33.5	Therm		
809	-35.6	Therm		
812	-35.8	Therm		
814	-35	Therm		
Sediment between 815 and 817 ft				
819	51.4	30	(49.7 ± 1.5)	49.0
822	49.9	40		
825	51.1	30		
830	49.2	40		
834	47	30		
839	49	40		
843	48.1	40		
847	52.1	40		
Petrographic boundary at 848 ft				
850	54.1	30	(53.7 ± 2.3)	53.0
854	50.1	40		
858	50.7	40		
860	55.0	40		
863	55.6	40		
867	55.7	10		
870	55	40		
Sediment between 870 and 873 ft				
873	59.4	Therm		
874	65.3	Therm	(63.4 ± 25.5)	
875	65.4	Therm		

Table A1. Paleomagnetic inclination values for basalt samples from coreholes at and near the Idaho National Laboratory, Idaho.—Continued

NAD 27				
N 43°27'13.40"				
W 113°00'17.78				
NGVD 29				
Alt 5,095.12 ft				
TD 1,409 ft				
WL 490.55 ft				
Corehole USGS 105				
Sample depth (ft)	Characteristic remanent inclination (degrees)	Alternating field demagnetization level (mT) or alternative demagnetization approach	Average flow inclination and 95 percent uncertainty level for sample groupings (degrees)	Deviation corrected inclination for sample groupings (degrees)
Sediment between 876 and 878 ft				
881	62.6	40	(62.6 ± 1.2)	62
885	59.6	30		
889	64.4	40		
892	65.3	40		
895	64.7	40		
900	65.6	40		
904	64.2	40		
908	64	40		
912	61.5	40		
917	61.2	40		
920	60.7	40		
825	61.7	40		
929	59.7	40		
933	57.4	Therm		
935	64.2	Therm		
942	64.1	Therm		
944	65.0	Therm		
Petrographic boundary at 944 ft				
946	55.7	Therm	(53.3 ± 1.4)	52.5
950	53.1	Therm		
955	49.8	30		
960	53.4	40		
966	58.2	40		
971	54.5	40		
976	56.3	40		
981	52.9	40		
985	48.8	40		
991	53.0	40		
Sediment between 991 and 993 ft				
996	51.0	Therm		
997	51.8	Therm		
999	51.3	Therm		
1,003	54.4	Therm		
1,001	-61.2	Therm		
1,011	-66.1	Therm	(-62.9 ± 20.7)	-62.0
1,015	-61.3	40		

Table A1. Paleomagnetic inclination values for basalt samples from coreholes at and near the Idaho National Laboratory, Idaho.—Continued

NAD 27				
N 43°27'13.40"				
W 113°00'17.78				
NGVD 29				
Alt 5,095.12 ft				
TD 1,409 ft				
WL 490.55 ft				
Corehole USGS 105				
Sample depth (ft)	Characteristic remanent inclination (degrees)	Alternating field demagnetization level (mT) or alternative demagnetization approach	Average flow inclination and 95 percent uncertainty level for sample groupings (degrees)	Deviation corrected inclination for sample groupings (degrees)
Petrographic boundary at 1,015 ft				
1,017	-60.5	30		
1,018	-63.5	40	(-60.7 ± 0.9)	-60
1,019	-61.3	40		
1,021	-60.6	40		
1,022	-63.2	40		
1,025	-57.3	40		
1,028	-60.4	40		
1,031	-62.0	40		
1,034	-60.0	40		
1,036	-59.4	40		
1,039	-64.3	40		
1,041	-60.5	40		
1,043	-58.4	40		
1,045	-60.0	30		
1,048	-60.3	40		
1,049	-60.0	40		
1,051	-58.9	40		
1,056	-57.8	40		
1,060	-63.2	40		
1,064	-62.6	40		
1,066	59.5	40		
Petrographic boundary at 1,066 ft				
1,068	-63.1	30	(-59.2 ± 1.1)	-59.0
1,070	-63.1	40		
1,074	-59.4	40		
1,076	-58.4	30		
1,078	-61.6	30		
1,080	-61.5	40		
1,085	-59.4	40		
1,090	-55.2	40		
1,095	-58.6	30		
1,100	-59.1	30		
1,105	-58.2	30		
1,109	-57.4	40		
1,112	-56.2	20		
1,115	-60.5	40		
1,119	-57.8	40		
1,121	-58.3	40		
1,123	-58	40		
1,125	-60.6	30		
1,129	-53.6	40		

Table A1. Paleomagnetic inclination values for basalt samples from coreholes at and near the Idaho National Laboratory, Idaho.—Continued

NAD 27				
N 43°27'13.40"				
W 113°00'17.78				
NGVD 29				
Alt 5,095.12 ft				
TD 1,409 ft				
WL 490.55 ft				
Corehole USGS 105				
Sample depth (ft)	Characteristic remanent inclination (degrees)	Alternating field demagnetization level (mT) or alternative demagnetization approach	Average flow inclination and 95 percent uncertainty level for sample groupings (degrees)	Deviation corrected inclination for sample groupings (degrees)
Sediment and unrecovered core between 1,129 and 1,133 ft				
1,135	-65	Therm	(-67.7 ± 1.0)	-67
1,138	-67.5	30		
1,140	-66.2	40		
1,142	-66.2	40		
1,145	-62.4	40		
1,148	-64.8	40		
1,150	-67.9	40		
1,154	-63.8	40		
1,163	-65.3	20		
1,169	-64.3	40		
1,170	-65.7	40		
1,174	-67.2	40		
1,176	-66.4	40		
1,179	-66	30		
1,182	-67.3	40		
1,185	-73.9	20		
1,187	-73.4	40		
1,190	-64	40		
1,195	-68.7	40		
1,201	-69	40		
1,205	-69.2	40		
1,208	-69.2	40		
1,210	-68.9	40		
1,214	-67.6	40		
1,218	-70.4	30		
1,222	-70.6	40		
1,226	-68.2	40		
1,229	-72.9	30		
1,232	-70.6	40		
1,238	-67.7	40		
1,240	-69.6	40		
1,242	-67.6	40		
1,248	-67.1	40		

Table A1. Paleomagnetic inclination values for basalt samples from coreholes at and near the Idaho National Laboratory, Idaho.—Continued

NAD 27				
N 43°27'13.40"				
W 113°00'17.78				
NGVD 29				
Alt 5,095.12 ft				
TD 1,409 ft				
WL 490.55 ft				
Corehole USGS 105				
Sample depth (ft)	Characteristic remanent inclination (degrees)	Alternating field demagnetization level (mT) or alternative demagnetization approach	Average flow inclination and 95 percent uncertainty level for sample groupings (degrees)	Deviation corrected inclination for sample groupings (degrees)
Sediment between 1,249 and 1,250 ft				
1,252	-78.5	40	(-71.6 ± 1.0)	-71
1,256	-75.6	40		
1,260	-73.8	30		
1,264	-71.3	40		
1,266	-70.8	40		
1,268	-70.3	40		
1,271	-71.9	40		
1,275	-71.6	30		
1,279	-71.5	30		
1,286	-69.3	40		
1,288	-74.2	40		
1,290	-73.3	30		
1,292	-73.1	40		
1,293	-66.7	40		
1,295	-68.2	30		
1,298	-68.5	40		
1,300	-73.9	40		
1,303	-71.2	40		
1,305	-72.8	40		
1,308	-72.3	40		
1,309	-72.1	30		
1,312	-67.4	40		
1,313	-73.4	40		
1,315	-73.2	40		
1,317	-71.0	40		
Petrographic boundary at 1,318 ft				
1,320	-72.6	40	(-69.5 ± 1.4)	-68.5
1,323	-69.4	40		
1,325	-72.5	40		
1,329	-71.7	40		
1,333	-72.1	40		
1,335	-70.3	40		
1,338	-67.4	40		
1,340	-70.1	40		
1,343	-64.6	40		
1,348	-67.6	40		
1,350	-70.5	40		
1,354	-68.0	30		
1,357	-67.3	30		
1,361	-68.8	40		

Table A1. Paleomagnetic inclination values for basalt samples from coreholes at and near the Idaho National Laboratory, Idaho.—Continued

NAD 27				
N 43°27'13.40"				
W 113°00'17.78				
NGVD 29				
Alt 5,095.12 ft				
TD 1,409 ft				
WL 490.55 ft				
Corehole USGS 105				
Sample depth (ft)	Characteristic remanent inclination (degrees)	Alternating field demagnetization level (mT) or alternative demagnetization approach	Average flow inclination and 95 percent uncertainty level for sample groupings (degrees)	Deviation corrected inclination for sample groupings (degrees)
Petrographic boundary at 1,361 ft				
1,363	-68.9	40	(-67.6 ± 1.3)	-66.5
1,366	-71.8	40		
1,368	-66.9	40		
1,374	-66.8	40		
1,378	-68.8	40		
1,382	-67.1	40		
1,386	-65.7	40		
1,390	-66.9	40		
1,395	-68.2	40		
1,399	-67.9	40		
1,409	-64.7	30		

Table A1. Paleomagnetic inclination values for basalt samples from coreholes at and near the Idaho National Laboratory, Idaho.—Continued

[See figure 1 and plate 1 for corehole locations. Sample depth measured to nearest 1 foot; shading delimits groups of samples used to determine the average flow inclination and 95 percent uncertainty level. For additional information see, appendix A text. **Characteristic remanent inclination:** In degrees down (negative value) or up (positive value) from the horizontal obtained by demagnetization. Petrographic boundary, indicates noted change in mineralogy. **Alternating-field:** Deviation corrected inclination, average inclination corrected for corehole deviation from vertical orientation, blank if not corrected. Li, values derived from a line fit from a vector component diagram. Therm, stepwise thermal demagnetization was applied to the sample. **Average flow inclination:** OP, overprint; NIIA, the sample was not included in the group average inclination. **Abbreviations:** Alt, altitude above National Geodetic Vertical Datum of 1929 (NGVD 29); ft, foot; mT, milliTesla; N, north; N/A, not applicable; TO, sample was thermally overprinted by overlying flow; W, west; WL, water level below land surface, in feet, approximate]

NAD 27**N 43°26'58.79"****W 112°58'26.34****NGVD 29****Alt 5,031.36 ft****TD 1,218 ft**

Corehole USGS 108				
Sample depth (ft)	Characteristic remanent inclination (degrees)	Alternating field demagnetization level (mT) or alternative demagnetization approach	Average flow inclination and 95 percent uncertainty level for sample groupings (degrees)	Deviation corrected inclination for sample groupings (degrees)
760	-39.1	Therm	-39.1	
Sediment between 761 and 763 ft				
764	61.6	40	62.4 ± 0.9	
769	63.1	30		
774	60.7	40		
778	64.4	30		
783	63.8	30		
788	62.5	30		
792	60.6	30		
796	62.4	40		
798	61.8	40		
Sediment between 800 and 801 ft				
802	70.6	Therm	56.6 ± 1.1	
804	63.6	Therm		
806	61.4	40		
811	59.3	30		
817	56	30		
824	56.8	30		
829	57	30		
834	56.2	30		
840	56.2	40		
844	56.1	40		
848	57.6	30		
852	54.4	40		
Unrecovered core between 853 and 855 ft				
856	56.6	40	54.3	
859	51.4	40		
863	52.6	40		
866	54.2	30		
869	52.7	40		
872	54.7	30		
876	57	40		
Unrecovered core between 876 and 880 ft				
881	55.2	40		

Table A1. Paleomagnetic inclination values for basalt samples from coreholes at and near the Idaho National Laboratory, Idaho.—Continued

NAD 27					
N 43°26'58.79"					
W 112°58'26.34					
NGVD 29					
Alt 5,031.36 ft					
TD 1,218 ft					
Corehole USGS 108					
Sample depth (ft)	Characteristic remanent inclination (degrees)	Alternating field demagnetization level (mT) or alternative demagnetization approach	Average flow inclination and 95 percent uncertainty level for sample groupings (degrees)	Deviation corrected inclination for sample groupings (degrees)	
883	62.8	30	65.9 ± 4.3		
885	65.7	40			
886	70.9	40			
Unrecovered core between 888 and 889 ft					
892	65.6	40			
895	64.7	40			
899	54.3	30	52.6 ± 1.3		
904	48.4	30			
907	51.6	30			
910	50.5	40			
915	53.1	40			
918	55	40			
922	56	40			
926	51.9	40			
929	54.9	30			
931	51.1	30			
934	53.3	30			
936	51.6	30			
938	53.1	30			
Petrographic boundary at 938 ft					
939	54.9	403		54.7 ± 1.0	
942	53.5	40			
944	55.2	30			
947	55.5	30			
951	54.7	30			
954	54.3	40			
957	52.1	30			
962	55.2	30			
967	51.6	30			
972	56.0	30			
976	57.5	30			
980	56.7	30			
984	54.0	30			
988	46.7	40			
Petrographic boundary at 989 ft					
990	54.9	40	54.9 ± 1.1		
991	56.3	40			
992	55.2	40			
993	53.6	40			
995	55.5	40			
996	54.0	40			

Table A1. Paleomagnetic inclination values for basalt samples from coreholes at and near the Idaho National Laboratory, Idaho.—Continued

NAD 27				
N 43°26'58.79"				
W 112°58'26.34				
NGVD 29				
Alt 5,031.36 ft				
TD 1,218 ft				
Corehole USGS 108				
Sample depth (ft)	Characteristic remanent inclination (degrees)	Alternating field demagnetization level (mT) or alternative demagnetization approach	Average flow inclination and 95 percent uncertainty level for sample groupings (degrees)	Deviation corrected inclination for sample groupings (degrees)
Sediment and unrecovered core between 997 and 1,002 ft				
1,005	-59.4	40	-61.2 ± 0.8	
1,007	-60.0	40		
1,010	-59.1	30		
1,013	-61.4	40		
1,015	-63.8	40		
1,020	-63.3	40		
1,024	-64.4	40		
1,027	-61.6	30		
1,029	-56.9	30		
1,033	-61.7	40		
1,036	-59.5	40		
1,038	-59.2	40		
1,041	-62.2	40		
1,044	-64.1	40		
1,048	-62.8	40		
1,054	-61.6	40		
1,060	-62.3	30		
1,064	-61.0	30		
1,069	-61.7	40		
1,071	-53.6	40		Not included in average
1,074	-61.6	30		
1,077	-64.3	30		
1,080	-60.2	30		
1,082	-64.1	40		
1,084	-60.6	30		
1,089	-59.0	40		
1,092	-61.3	40		
1,096	-59.0	40		
1,100	-57.1	40		
Sediment between 1,100 and 1,103 ft				
1,103	-67.5	Therm	-70.2 ± 1.7	
1,108	-70	40		
1,114	-69.8	40		
1,120	-69.3	40		
1,124	-70.6	40		
1,129	-71.1	40		
1,135	-68.4	40		
1,140	-74.1	40		
1,146	-75.5	40		
1,151	-69.6	40		
1,159	-71	20		
1,161	-64.5	40		
1,165	-71.8	40		

Table A1. Paleomagnetic inclination values for basalt samples from coreholes at and near the Idaho National Laboratory, Idaho.—Continued

NAD 27				
N 43°26'58.79"				
W 112°58'26.34				
NGVD 29				
Alt 5,031.36 ft				
TD 1,218 ft				
Corehole USGS 108				
Sample depth (ft)	Characteristic remanent inclination (degrees)	Alternating field demagnetization level (mT) or alternative demagnetization approach	Average flow inclination and 95 percent uncertainty level for sample groupings (degrees)	Deviation corrected inclination for sample groupings (degrees)
Sediment between 1,166 and 1,168 ft				
1,169	-73.8	30	-70.4 ± 1.8	
1,172	-70.6	30		
1,174	-71.2	40		
1,175	-72.8	40		
1,178	-71	40		
1,179	-70.3	40		
1,181	-74.2	30		
1,186	-71.6	30		
1,189	-63.6	40		Not included in average
1,192	-66.1	40		
1,196	-66.9	40		
1,200	-68.4	40		
1,204	-66.2	40		
1,206	-65.7	30		
1,210	-76.2	30		
1,214	-70.2	30		

Table A1. Paleomagnetic inclination values for basalt samples from coreholes at and near the Idaho National Laboratory, Idaho.—
Continued

[See figure 1 and plate 1 for corehole locations. Sample depth measured to nearest 1 foot; shading delimits groups of samples used to determine the average flow inclination and 95 percent uncertainty level. For additional information see, appendix A text. **Characteristic remanent inclination:** In degrees down (negative value) or up (positive value) from the horizontal obtained by demagnetization. Petrographic boundary, indicates noted change in mineralogy. **Alternating-field:** Deviation corrected inclination, average inclination corrected for corehole deviation from vertical orientation, blank if not corrected. Li, values derived from a line fit from a vector component diagram. Therm, stepwise thermal demagnetization was applied to the sample. **Average flow inclination:** OP, overprint; NIA, the sample was not included in the group average inclination. **Abbreviations:** Alt, altitude above National Geodetic Vertical Datum of 1929 (NGVD 29); ft, foot; mT, milliTesla; N, north; N/A, not applicable; TO, sample was thermally overprinted by overlying flow; W, west; WL, water level below land surface, in feet, approximate]

NAD 27**N 43°30'36.28"****W 112°58'16.05"****Alt 4,977.30 ft****TD 1,239 ft****WL 548.86 ft**

Corehole USGS 131				
Sample depth (ft)	Characteristic remanent inclination (degrees)	Alternating field demagnetization level (mT) or alternative demagnetization approach	Average flow inclination and 95 percent uncertainty level for sample groupings (degrees)	Deviation corrected inclination for sample groupings (degrees)
14	64.2	10		
19	64.0	20		
24	66.5	20		
29	66.7	20		
35	66.7	20		
40	66.7	20		
44	59.7	20		
48	60.4	20		
49	59.6	20		
55	63.1	20		
57	63.4	20	63.9 ± 1.3	
60	58.9	20		
63	65.5	20		
66	68.6	20		
70	64.7	20		
75	62.2	20		
79	65.4	20		
84	61.6	20		
89	62.2	20		
93	66.0	20		
96	64.7	20		
97–134	Unrecovered core and sediment			
136	59.6	10		
139	61.5	10		
142	62.7	10		
146	59.4	20	60.5 ± 1.2	
151	60.5	20		
154	59.7	20		
157	61.8	20		
159	59.0	20		
160–161	Unrecovered core			
163	55.4	20		
164	58.4	10		
172	55.0	20		
177	55.4	20		
183	53.9	20		

44 Paleomagnetic Correlation of Basalt Flows in Coreholes, Idaho National Laboratory, Idaho

Table A1. Paleomagnetic inclination values for basalt samples from coreholes at and near the Idaho National Laboratory, Idaho.—
Continued

NAD 27				
N 43°30'36.28"				
W 112°58'16.05"				
Alt 4,977.30 ft				
TD 1,239 ft				
WL 548.86 ft				
Corehole USGS 131				
Sample depth (ft)	Characteristic remanent inclination (degrees)	Alternating field demagnetization level (mT) or alternative demagnetization approach	Average flow inclination and 95 percent uncertainty level for sample groupings (degrees)	Deviation corrected inclination for sample groupings (degrees)
188	52.8	20		
192	55.3	20		
195	54.0	20		
197	52.2	20	55.0 ± 1.2	
201	50.3	20		
203	52.8	20		
208	55.8	20		
213	53.9	20		
216	57.1	20		
218	55.9	20		
220	57.5	20		
223	58.8	20		
223–256	Unrecovered core and sediment			
257	49.5	20		
261	52.6	10		
263	52.3	20		
264	53.2	30	52.5 ± 1.4	
266	53.3	20		
268	54.2	20		
270	52.5	10		
272–287	Unrecovered core and sediment			
287	74.3	20		
293	69.1	20	72.5 ± 21.8	
297	74.1	20		
298–299	Unrecovered core			
300	62.2	20		
304	62.8	20		
307	60.2	20		
310	63.6	20	62.2 ± 1.6	
313	64.5	20		
317	62.0	20		
320	60.2	20		
320–322	Unrecovered core and sediment			
324	63.9	20		
325	63.8	20		
329	60.4	20		
331	58.3	20		
334	62.1	20		
336	57.6	20		
339	55.5	20		
344	62.3	20		
347	61.5	20		
350	62.0	20		
354	57.9	20		

Table A1. Paleomagnetic inclination values for basalt samples from coreholes at and near the Idaho National Laboratory, Idaho.—
Continued

NAD 27				
N 43°30'36.28"				
W 112°58'16.05"				
Alt 4,977.30 ft				
TD 1,239 ft				
WL 548.86 ft				
Corehole USGS 131				
Sample depth (ft)	Characteristic remanent inclination (degrees)	Alternating field demagnetization level (mT) or alternative demagnetization approach	Average flow inclination and 95 percent uncertainty level for sample groupings (degrees)	Deviation corrected inclination for sample groupings (degrees)
358	58.4	20		
360	59.4	20		
364	51.8	20	NIA	
366	58.5	20		
369	61.4	20		
371	61.0	20		
374	63.5	20	60.3 ± 0.8	
377	62.2	40		
380	59.1	20		
383	59.6	20		
388	61.3	20		
391	62.9	10		
394	63.2	20		
399	62.3	10		
402	55.8	20		
404	60.7	20		
414	59.2	20		
419	58.0	20		
421	55.5	20		
425	55.6	20		
427	59.6	20		
430	64.3	20		
434	60.5	Therm		
438	60.4	Therm		
440	59.0	Therm		
442	60.6	Therm		
443	Petrographic boundary			
445	65.1	Therm		
449	58.2	Therm		
453	-34.7	Therm		
456	-34.6	Therm		
459	-36.0	Therm		
463	-34.5	Therm		
467	-37.3	Therm		
472	-30.9	Therm		
475	-36.1	Therm		
479	-34.1	Therm		
482	-40.2	Therm		
485	-36.6	Therm	-35.1 ± 1.1	
488	-36.5	Therm		
492	-35.6	Therm		
494	-36.4	Therm		
497	-35.2	Therm		

Table A1. Paleomagnetic inclination values for basalt samples from coreholes at and near the Idaho National Laboratory, Idaho.—
Continued

NAD 27				
N 43°30'36.28"				
W 112°58'16.05"				
Alt 4,977.30 ft				
TD 1,239 ft				
WL 548.86 ft				
Corehole USGS 131				
Sample depth (ft)	Characteristic remanent inclination (degrees)	Alternating field demagnetization level (mT) or alternative demagnetization approach	Average flow inclination and 95 percent uncertainty level for sample groupings (degrees)	Deviation corrected inclination for sample groupings (degrees)
498	Petrographic boundary			
500	-35.6	Therm		
509	-32.0	Therm		
517	-33.5	Therm		
525	-31.3	Therm		
534	-40.6	Therm		
543	-41.7	Therm		
547	-46.9	Therm	-43.7 ± 3.7	
555	-44.4	Therm		
563	-45.1	Therm		
564–566	Unrecovered core and sediment			
568	-48.5	Therm		
571	-49.4	Therm	-47.4 ± 20.1	
573	-44.3	Therm		
575	Sediment and petrographic boundary			
576	63.5	Therm		
578	67.5	Therm		
582	67.7	20		
583	66.4	20		
587	64.4	20		
590	65.8	20		
594	65.7	20		
598	65.4	20		
603	64.7	20		
606	63.6	20		
608	67.4	20	65.6 ± 0.8	
611	64.1	20		
613	63.5	20		
617	67.3	20		
620	65.0	20		
625	67.1	20		
630	64.7	20		
635	65.9	20		
639	68.5	30		
642	63.4	10		
646	Petrographic boundary			
646	61.6	20	NIA	
648	58.7	20	NIA	
651	65.3	10		
655	66.0	20		
658	66.3	20		
661	64.4	20		
665	67.1	20	67.1 ± 1.1	

Table A1. Paleomagnetic inclination values for basalt samples from coreholes at and near the Idaho National Laboratory, Idaho.—
Continued

NAD 27				
N 43°30'36.28"				
W 112°58'16.05"				
Alt 4,977.30 ft				
TD 1,239 ft				
WL 548.86 ft				
Corehole USGS 131				
Sample depth (ft)	Characteristic remanent inclination (degrees)	Alternating field demagnetization level (mT) or alternative demagnetization approach	Average flow inclination and 95 percent uncertainty level for sample groupings (degrees)	Deviation corrected inclination for sample groupings (degrees)
670	67.4	20		
677	67.5	20		
683	67.0	20		
689	68.5	20		
696	68.3	20		
702	70.3	20		
703–707	Unrecovered core and sediment			
708	68.6	20		
716	64.7	10		
722	65.1	20		
728	66.4	20	66.3 ± 1.7	
732	68.7	20		
737	66.0	20		
740	64.8	20		
741–742	Sediments			
744	68.8	20		
746	63.7	20		
748	65.2	20	65.2 ± 2.8	
750	63.7	20		
752	62.2	20		
753	67.3	20		
754–762	Unrecovered core and sediment			
764	67.5	20		
766	69.0	20		
767	68.6	10		
771	67.3	20		
774	68.3	20		
776	67.9	20		
780	66.2	20		
781	66.7	20		
783	65.8	20	67.6 ± 0.9	
785	66.7	20		
787	63.7	20		
790	70.5	20		
793	68.5	20		
795	68.4	20		
797	67.0	20		
798	Petrographic boundary			
800	69.8	20		
802	60.3	20	NIIA	
804	53.2	20		
806	52.2	20		
808	55.2	20	54.0 ± 2.4	

Table A1. Paleomagnetic inclination values for basalt samples from coreholes at and near the Idaho National Laboratory, Idaho.—
Continued

NAD 27				
N 43°30'36.28"				
W 112°58'16.05"				
Alt 4,977.30 ft				
TD 1,239 ft				
WL 548.86 ft				
Corehole USGS 131				
Sample depth (ft)	Characteristic remanent inclination (degrees)	Alternating field demagnetization level (mT) or alternative demagnetization approach	Average flow inclination and 95 percent uncertainty level for sample groupings (degrees)	Deviation corrected inclination for sample groupings (degrees)
810	53.3	Li		
812	57.6	Li		
815	52.3	Li		
816–819	Unrecovered core and sediment			
820	-65.7	Therm		
822	-64.3	Therm		
824	-68.6	Therm	-65.2 ± 3.5	
826	-65.5	Therm		
828	-61.9	Li		
828–830	Unrecovered core			
831	-61.3	Li		
834	-59.5	Li		
837	-58.0	Li		
840	-60.7	Li		
842	-61.3	Li		
844	-58.0	Li		
847	-60.9	Li		
850	-64.4	Li		
852	-58.1	Li		
854	-58.1	Li		
855	-54.9	Li		
858	-60.9	Li		
862	-58.0	Li		
864	-59.2	Li		
868	-60.4	Li		
871	-61.4	Li	-60.5 ± 0.8	
874	-60.1	Li		
876	-62.5	Li		
878	-66.6	Li		
879	-63.9	Li		
881	-60.0	Li		
883	-62.4	Li		
885	-60.0	Li		
888	-59.3	Li		
890	-60.5	Li		
891	-62.1	Li		
895	-59.2	Li		
898	-61.3	Li		
901	-61.2	Li		
903	-62.1	Li		
906	-60.0	Li		
907–909	Sediments			
909	-69.6	Therm		
911	-72.9	Li		

Table A1. Paleomagnetic inclination values for basalt samples from coreholes at and near the Idaho National Laboratory, Idaho.—
Continued

NAD 27				
N 43°30'36.28"				
W 112°58'16.05"				
Alt 4,977.30 ft				
TD 1,239 ft				
WL 548.86 ft				
Corehole USGS 131				
Sample depth (ft)	Characteristic remanent inclination (degrees)	Alternating field demagnetization level (mT) or alternative demagnetization approach	Average flow inclination and 95 percent uncertainty level for sample groupings (degrees)	Deviation corrected inclination for sample groupings (degrees)
913	-74.7	Li		
915	-74.3	Li		
916	-70.6	Li		
919	-75.1	Li		
921	-68.1	Li	-71.7 ± 2.1	
923	-64.0	Li		
925	-72.3	Li		
928	-72.5	Li		
930	-73.1	Li		
932	-72.8	Li		
934–936	Unrecovered core and sediment			
937	52.6	Therm		
939	48.3	Li		
944	47.8	Li		
946	51.3	Li		
948	50.3	Li		
950	53.2	Li		
953	50.6	Li		
955	52.3	Li		
957	50.2	Li		
959	45.6	Li		
961	49.3	Li		
963	48.6	Li		
967	53.9	Li		
970	52.3	Li	51.4 ± 1.0	
972	55.1	Li		
974	44.3	Li		
978	54.5	Li		
982	45.2	Li		
984	52.9	Li		
987	53.8	Li		
989	53.6	Li		
992	52.1	Li		
994	52.7	Li		
996	52.4	Li		
999	50.6	Li		
1,001	54.1	Li		
1,004	50.2	Li		
1,006	46.3	Li		
1,008	46.0	Li		
1,009–1,010	Unrecovered core			
1,011	50.8	Li		
1,013	51.2	Li		
1,016	50.9	Li		

Table A1. Paleomagnetic inclination values for basalt samples from coreholes at and near the Idaho National Laboratory, Idaho.—
Continued

NAD 27				
N 43°30'36.28"				
W 112°58'16.05"				
Alt 4,977.30 ft				
TD 1,239 ft				
WL 548.86 ft				
Corehole USGS 131				
Sample depth (ft)	Characteristic remanent inclination (degrees)	Alternating field demagnetization level (mT) or alternative demagnetization approach	Average flow inclination and 95 percent uncertainty level for sample groupings (degrees)	Deviation corrected inclination for sample groupings (degrees)
1,020	51.0	Li		
1,023	51.4	Li		
1,026	50.1	Li		
1,029	50.9	Li		
1,032	53.3	Li		
1,034	53.3	Li		
1,037	52.4	Li		
1,038	53.4	Li		
1,041	47.2	Li		
1,043	51.6	Li	51.2 ± 0.7	
1,046	51.1	Li		
1,050	54.6	Li		
1,051	52.1	Li		
1,055	51.5	Li		
1,058	51.8	Li		
1,061	51.7	Li		
1,064	51.0	Li		
1,066	49.3	Li		
1,068	51.9	Li		
1,070	47.3	Li		
1,073	49.4	Li		
1,076	51.6	Li		
1,079	49.7	Li		
1,083	50.5	Li		
1,083	Oxidation and petrographic boundary			
1,085	57.9	Li		
1,087	56.7	Li		
1,089	56.0	Li		
1,092	53.0	Li		
1,098	56.4	Li		
1,102	54.2	Li		
1,105	54.6	Li		
1,110	54.3	Li		
1,114	56.2	Li		
1,118	53.1	Li		
1,123	52.5	Li		
1,127	54.8	Li		
1,129	55.5	Li		
1,132	56.7	Li		
1,135	55.6	Li		
1,139	53.7	Li		
1,141	53.3	Li		
1,146	53.7	Li		
1,149	54.9	Li		

Table A1. Paleomagnetic inclination values for basalt samples from coreholes at and near the Idaho National Laboratory, Idaho.—
Continued

NAD 27				
N 43°30'36.28"				
W 112°58'16.05"				
Alt 4,977.30 ft				
TD 1,239 ft				
WL 548.86 ft				
Corehole USGS 131				
Sample depth (ft)	Characteristic remanent inclination (degrees)	Alternating field demagnetization level (mT) or alternative demagnetization approach	Average flow inclination and 95 percent uncertainty level for sample groupings (degrees)	Deviation corrected inclination for sample groupings (degrees)
1,153	50.2	Li		
1,156	55.9	Li		
1,159	60.1	Li		
1,162	56.0	Li	54.2 ± 0.9	
1,165	54.2	Li		
1,170	49.8	Li		
1,173	53.1	Li		
1,176	52.3	Li		
1,180	56.8	Li		
1,182	53.4	Li		
1,184	53.9	Li		
1,187	54.0	Li		
1,191	55.4	Li		
1,195	49.8	Li		
1,200	46.1	Li		
1,202	43.1	Li		
1,204	50.2	Li		
1,207	56.4	Li		
1,209	54.2	Li		
1,211	58.3	Li		
1,213	52.3	Li		
1,215	54.0	Li		
1,218	54.6	Li		
1,220	55.1	Li		
1,222	54.7	Li		
1,226	53.1	Li		
1,229	53.3	Li		
1,232	55.2	Li		
1,236	58.2	Li		
1,239	58.4	Li		

Table A1. Paleomagnetic inclination values for basalt samples from coreholes at and near the Idaho National Laboratory, Idaho.—Continued

[See figure 1 and plate 1 for corehole locations. Sample depth measured to nearest 1 foot; shading delimits groups of samples used to determine the average flow inclination and 95 percent uncertainty level. For additional information see, appendix A text. **Characteristic remanent inclination:** In degrees down (negative value) or up (positive value) from the horizontal obtained by demagnetization. Petrographic boundary, indicates noted change in mineralogy. **Alternating-field:** Deviation corrected inclination, average inclination corrected for corehole deviation from vertical orientation, blank if not corrected. Li, values derived from a line fit from a vector component diagram. Therm, stepwise thermal demagnetization was applied to the sample. **Average flow inclination:** OP, overprint; NIIA, the sample was not included in the group average inclination. **Abbreviations:** Alt, altitude above National Geodetic Vertical Datum of 1929 (NGVD 29); ft, foot; mT, milliTesla; N, north; N/A, not applicable; TO, sample was thermally overprinted by overlying flow; W, west; WL, water level below land surface, in feet, approximate]

NAD 27
N 43°34'47.72",
W 112°58'12.00"
NGVD 29
Alt 4,935.00 ft
TD 1,048 ft
WL 490.55 ft

Corehole USGS 136				
Sample depth (ft)	Characteristic remanent inclination (degrees)	Alternating-field demagnetization level (mT) or alternative demagnetization approach	Average flow inclination and 95 percent uncertainty level for sample groupings (degrees)	Deviation corrected inclination for sample groupings (degrees)
49	51.9	Li	NIIA	
53	58.3	Li		
56	63.7	Li		
58	62.8	Li		
63	62.9	Li		
67	58.4	Li		
73	59.6	Li	60.1 ± 1.8	
78	59.8	Li		
81	53.6	Li	NIIA	
85	52.7	Li	NIIA	
89	55.7	Li		
93	60.3	Li		
95–99	Unrecovered core and sediment			
101	77.4	Therm	59.5 - OP	
105	74.1	Therm		
109	75.4	Li		
112	76.7	Li		
117	74.7	Li		
121	78.9	Li		
123	74.9	Li		
129	78.1	Li	77.4 ± 1.3	
133	75.8	Li		
138	79.6	Li		
143	77.5	Li		
145	81.8	Li		
147	79.7	Li		
149–156	Unrecovered core and sediment			
157	79.3	Li		
158–181	Unrecovered core and sediment			
182	73.2	Li		
185	71.7	Li		
193	73.6	Li		
195	75.1	Li		
198	65.3	Li	72.9 ± 1.4	
201	73.8	Li		

Table A1. Paleomagnetic inclination values for basalt samples from coreholes at and near the Idaho National Laboratory, Idaho.—
Continued

Corehole USGS 136				
Sample depth (ft)	Characteristic remanent inclination (degrees)	Alternating-field demagnetization level (mT) or alternative demagnetization level for sample groupings approach	Average flow inclination and 95 percent uncertainty (degrees)	Deviation corrected inclination for sample groupings (degrees)
NAD 27				
N 43°34'47.72"				
W 112°58'12.00"				
NGVD 29				
Alt 4,935.00 ft				
TD 1,048 ft				
WL 490.55 ft				
Corehole USGS 136				
203	70.6	Li		
206	74.5	Li		
209	71.0	Li		
210–217	Unrecovered core and sediment			
218	55.5	Li		
223	57.5	Li		
229	56.0	Li		
234	56.4	Li		
239	54.1	Li	55.5 ± 0.9	
241	56.0	Li		
245	54.7	Li		
248	55.3	Li		
251	53.7	Li		
252–254	Unrecovered core and sediment			
256	54.1	Li		
263	55.7	Li		
270	54.5	Li		
277	53.2	Li		
284	57.1	Li		
289	56.7	Li	52.9 ± 1.6	
295	54.1	Li		
302	48.3	Li		
309	50.1	Li		
317	51.5	Li		
322	51.1	Li		
328	49.3	Li		
329–330	Sediments			
333	65.4	Therm	51.3 - OP	
338	56.0	Therm	NIA 53.1 - OP	
342	64.8	Therm		
346	64.8	Li		
348	62.5	Li		
352	63.3	Li		
355	63.6	Li		
359	62.6	Li		
364	61.8	Li		
366	63.1	Li		
369	64.5	Li	65.3 ± 1.3	
372	66.4	Li		
377	66.0	Li		
381	66.7	Li		
386	62.0	Li		
391	68.7	Li		

54 Paleomagnetic Correlation of Basalt Flows in Coreholes, Idaho National Laboratory, Idaho

Table A1. Paleomagnetic inclination values for basalt samples from coreholes at and near the Idaho National Laboratory, Idaho.—
Continued

NAD 27				
N 43°34'47.72",				
W 112°58'12.00"				
NGVD 29				
Alt 4,935.00 ft				
TD 1,048 ft				
WL 490.55 ft				
Corehole USGS 136				
Sample depth (ft)	Characteristic remanent inclination (degrees)	Alternating-field demagnetization level (mT) or alternative demagnetization level for sample groupings approach	Average flow inclination and 95 percent uncertainty (degrees)	Deviation corrected inclination for sample groupings (degrees)
396	69.7	Li		
402	69.2	Li		
408	71.8	Li		
415	65.6	Li		
421	62.1	Li		
Petrographic boundary				
424	69.1	Therm	66.3 - OP	
428	69.4	Li		
432	68.7	Li		
435	69.9	Li		
439	62.3	Li		NIIA
443	69.4	Li		
446	65.0	Li		
448	67.4	Li		
452	60.7	Li		NIIA
456	70.7	Li		
461	69.2	Li		
466	71.8	Li	69.3 ± 1.3	
471	66.8	Li		
475	70.5	Li		
478	72.6	Li		
481	68.8	Li		
485	62.7	Li		
489	69.9	Li		
493	68.8	Li		
498	72.8	Li		
500–501	Sediments			
503	72.9	Therm		
506	56.8	Therm		
511	57.6	Li		
518	56.8	Li		
520	54.5	Li		
524	56.3	Li		
528	54.6	Li		
532	54.7	Li		
536	56.2	Li		
541	58.2	Li		
545	56.4	Li		
548	55.1	Li		
552	56.4	Li		
555	53.5	Li	56.3 ± 0.9	
558	53.5	Li		

Table A1. Paleomagnetic inclination values for basalt samples from coreholes at and near the Idaho National Laboratory, Idaho.—
Continued

NAD 27 N 43°34'47.72" , W 112°58'12.00" NGVD 29 Alt 4,935.00 ft TD 1,048 ft WL 490.55 ft				
Corehole USGS 136				
Sample depth (ft)	Characteristic remanent inclination (degrees)	Alternating-field demagnetization level (mT) or alternative demagnetization approach	Average flow inclination and 95 percent uncertainty for sample groupings (degrees)	Deviation corrected inclination for sample groupings (degrees)
560	54.2	Li		
563	55.0	Li		
566	57.8	Li		
572	62.9	Li		
578	62.6	Li		
583	56.1	Li		
588	57.7	Li		
594	54.7	Li		
598	55.2	Li		
603	57.0	Li		
603–604	Sediments			
606	56.0	Therm		
611	58.5	Therm	54.6 - OP	
616	61.5	Li		
621	63.5	Li		
627	59.6	Li		
632	60.4	Li		
639	61.8	Li		
644	60.8	Li	60.7 ± 1.4	
650	56.4	Li		
655	58.2	Li		
658	Petrographic boundary			
662	62.1	Therm		
667	62.7	Therm		
673	62.5	Li		
679	65.7	Li		
684	67.6	Li		
691	69.0	Li		
695	67.9	Li	66.9 ± 2.3	
699	66.2	Li		
701	Petrographic boundary			
703	62.5	Therm		
705	69.6	Therm		
708	56.7	Li		
711	57.9	Li		
713	62.1	Li	57.2 ± 3.4	
716	57.7	Li		
720	52.8	Li		
722–726	Sediments			
727	-73.2	Therm	56.2 - OP	
731	-68.0	Therm		

Table A1. Paleomagnetic inclination values for basalt samples from coreholes at and near the Idaho National Laboratory, Idaho.—
Continued

NAD 27				
N 43°34'47.72",				
W 112°58'12.00"				
NGVD 29				
Alt 4,935.00 ft				
TD 1,048 ft				
WL 490.55 ft				
Corehole USGS 136				
Sample depth (ft)	Characteristic remanent inclination (degrees)	Alternating-field demagnetization level (mT) or alternative demagnetization level for sample groupings approach	Average flow inclination and 95 percent uncertainty (degrees)	Deviation corrected inclination for sample groupings (degrees)
736	-70.1	Therm		
739	-69.4	Therm		
744	-69.1	Li	-70.2 ± 1.5	
748	-69.4	Li		
752	-72.0	Li		
756	-70.3	Li		
757	Sediment and petrographic boundary			
760	-71.1	Li		
765	-71.7	Li		
771	-69.1	Li		
778	-73.4	Li		
785	-70.3	Li		
790	-71.6	Li		
795	-69.1	Li		
798	-66.3	Li		
799	-70.9	Li		
800	-71.7	Li	-70.2 ± 0.8	
804	-70.7	Li		
807	-70.0	Li		
811	-70.6	Li		
816	-70.1	Li		
822	-70.5	Li		
827	-68.6	Li		
832	-68.7	Li		
835	-70.8	Li		
839	-68.2	Li		
840	Caliche found on petrographic boundary			
841	-68.0	Li		
843	-70.7	Li		
846	-69.0	Li		
848	-68.7	Li	-69.3 ± 1.0	
851	-68.9	Li		
852	Caliche and thin sediment			
855	-70.7	Therm		
861	-68.8	Therm		
865	-64.6	Li		
870	-65.1	Li		
874	-65.7	Li		
878	-65.5	Li		
884	-65.2	Li		
888	-67.1	Li	-65.6 ± 0.8	
892	-66.7	Li		

Table A1. Paleomagnetic inclination values for basalt samples from coreholes at and near the Idaho National Laboratory, Idaho.—
Continued

NAD 27				
N 43°34'47.72",				
W 112°58'12.00"				
NGVD 29				
Alt 4,935.00 ft				
TD 1,048 ft				
WL 490.55 ft				
Corehole USGS 136				
Sample depth (ft)	Characteristic remanent inclination (degrees)	Alternating-field demagnetization level (mT) or alternative demagnetization level for sample groupings approach	Average flow inclination and 95 percent uncertainty (degrees)	Deviation corrected inclination for sample groupings (degrees)
895	-64.6	Li		
900	-64.1	Li		
902	-65.4	Li		
904	-68.6	Li		
905	Oxidation, caliche and petrographic boundary			
907	52.0	Therm	-64.7 - OP	
911	55.6	Li		
916	59.0	Li		
920	55.1	Li		
924	55.0	Li		
928	47.4	Li	NIA	
931	52.9	Li		
935	54.5	Li		
940	55.1	Li		
944	54.7	Li		
949	55.6	Li		
953	50.7	Li		
957	55.1	Li		
961	56.8	Li	55.2 ± 0.8	
964	58.0	Li		
967	54.5	Li		
971	55.8	Li		
975	54.8	Li		
978	52.4	Li		
981	54.7	Li		
985	56.2	Li		
988	56.0	Li		
992	56.1	Li		
997	57.0	Li		
1,001	56.0	Li		
1,004	56.0	Li		
1,007	56.5	Li		
1,011	61.3	Li		
1,016	60.8	Li		
1,021	59.5	Li		
1,026	60.5	Li	59.6 ± 1.7	
1,031	60.8	Li		
1,036	57.0	Li		
1,042	57.5	Li		
1,043–1,048	Sediments			

Table A1. Paleomagnetic inclination values for basalt samples from coreholes at and near the Idaho National Laboratory, Idaho.—Continued

[See figure 1 and plate 1 for corehole locations. Sample depth measured to nearest 1 foot; shading delimits groups of samples used to determine the average flow inclination and 95 percent uncertainty level. For additional information see, appendix A text. **Characteristic remanent inclination:** In degrees down (negative value) or up (positive value) from the horizontal obtained by demagnetization. Petrographic boundary, indicates noted change in mineralogy. **Alternating-field:** Deviation corrected inclination, average inclination corrected for corehole deviation from vertical orientation, blank if not corrected. Li, values derived from a line fit from a vector component diagram. Therm, stepwise thermal demagnetization was applied to the sample. **Average flow inclination:** OP, overprint; NIIA, the sample was not included in the group average inclination. **Abbreviations:** Alt, altitude above National Geodetic Vertical Datum of 1929 (NGVD 29); ft, foot; mT, milliTesla; N, north; N/A, not applicable; TO, sample was thermally overprinted by overlying flow; W, west; WL, water level below land surface, in feet, approximate]

NAD 27
N 43°27'03.07"
W 113°02'55.62"
Alt 5,053.81 ft
NGVD 29
TD 1,317 ft
WL 627.25 ft

Corehole USGS 137A				
Sample depth (ft)	Characteristic remanent inclination (degrees)	Alternating field demagnetization level (mT) or alternative demagnetization approach	Average flow inclination and 95 percent uncertainty level for sample groupings (degrees)	Deviation corrected inclination for sample groupings (degrees)
9	66.3	Li		
13	65.5	Li		
15	66.3	Li		
16	64.3	Li	64.7 ± 1.6	
19	61.5	Li		
23	64.2	Li		
29	64.6	Li		
34	Petrographic boundary			
37	65.4	Li		
46	61.7	Li		
52	66.6	Li		
60	64.1	Li		
68	67.4	Li		
76	66.1	Li	65.1 ± 1.4	
84	67.4	Li		
93	63.4	Li		
100	64.8	Li		
108	68.8	Li		
112	62.3	Li		
121	63.3	Li		
123	Oxidation and petrographic boundary			
129	63.0	Li		
132	62.6	Li		
137	63.1	Li		
141	63.3	Li		
145	63.0	Li		
149	68.0	Li		
154	61.9	Li		
158	61.7	Li	64.4 ± 1.3	
161	64.0	Li		
164	63.5	Li		
166	67.9	Li		
170	67.5	Li		
174	62.4	Li		

Table A1. Paleomagnetic inclination values for basalt samples from coreholes at and near the Idaho National Laboratory, Idaho.—
Continued

NAD 27				
N 43°27'03.07"				
W 113°02'55.62"				
Alt 5,053.81 ft				
NGVD 29				
TD 1,317 ft				
WL 627.25 ft				
Corehole USGS 137A				
Sample depth (ft)	Characteristic remanent inclination (degrees)	Alternating field demagnetization level (mT) or alternative demagnetization approach	Average flow inclination and 95 percent uncertainty level for sample groupings (degrees)	Deviation corrected inclination for sample groupings (degrees)
179	66.1	Li		
181	67.6	Li		
183–190	Unrecovered core and sediment			
191	60.9	Li		
194	63.2	Li		
197	62.5	Li		
200	61.8	Li		
203	63.1	Li	62.7 ± 0.7	
207	62.1	Li		
211	62.6	Li		
214	62.2	Li		
215–320	Interval of rhyolitic ash becomes welded with depth - Big Southern Butte			
322	64.4	Therm	NIIA	
327	55.6	Therm	63.8 - OP	
332	57.6	Li		
336	59.0	Li		
339	56.6	Li		
342	53.3	Li		
345	53.5	Li		
349	55.1	Li		
354	54.6	Li	55.6 ± 0.8	
359	55.4	Li		
364	54.3	Li		
368	55.0	Li		
373	52.6	Li		
374	Sediments, oxidation and petrographic boundary			
376	55.9	Therm		
378	54.7	Therm		
381	56.1	Therm		
385	73.2	Therm	56.1 - OP	
389	72.1	Therm	56.7 - OP	
391	73.7	Therm	58.0 - OP	
393	69.9	Therm	56.4 - OP	
397	72.9	Therm		
401	71.7	Li		
403	72.3	Li		
406	72.8	Li	72.4 ± 0.7	
410	71.5	Li		

Table A1. Paleomagnetic inclination values for basalt samples from coreholes at and near the Idaho National Laboratory, Idaho.—
Continued

Corehole USGS 137A				
Sample depth (ft)	Characteristic remanent inclination (degrees)	Alternating field demagnetization level (mT) or alternative demagnetization approach	Average flow inclination and 95 percent uncertainty level for sample groupings (degrees)	Deviation corrected inclination for sample groupings (degrees)
NAD 27 N 43°27'03.07" W 113°02'55.62" Alt 5,053.81 ft NGVD 29 TD 1,317 ft WL 627.25 ft				
415	73.9	Li		
420	72.3	Li		
421–426	Sediments			
427	72.8	Therm		
432	69.8	Therm	NIIA	
437	68.9	Therm	NIIA	
445	64.9	Therm		
452	63.7	Li		
460	59.0	Li		
468	60.8	Li		
476	60.9	Li		
482	59.2	Li		
489	62.4	Li	62.6 ± 1.3	
497	65.7	Li		
504	66.1	Li		
511	62.1	Li		
516	65.3	Li		
522	62.5	Therm		
522	Petrographic boundary			
526	61.7	Therm		
529	61.8	Li		
532	65.9	Li		
537	65.9	Li		
542	65.4	Li	66.6 ± 2.6	
547	65.9	Li		
552	69.8	Li		
553	Oxidation and petrographic boundary			
555	68.0	Li		
557	67.3	Li		
560	69.3	Li		
564	69.9	Li		
566	69.4	Li		
568	71.1	Li	69.2 ± 0.9	
571	68.8	Li		
573	Petrographic boundary			
575	71.9	Therm		
579	67.8	Therm		
583	68.9	Therm		
587	69.2	Therm		

Table A1. Paleomagnetic inclination values for basalt samples from coreholes at and near the Idaho National Laboratory, Idaho.—
Continued

NAD 27				
N 43°27'03.07"				
W 113°02'55.62"				
Alt 5,053.81 ft				
NGVD 29				
TD 1,317 ft				
WL 627.25 ft				
Corehole USGS 137A				
Sample depth (ft)	Characteristic remanent inclination (degrees)	Alternating field demagnetization level (mT) or alternative demagnetization approach	Average flow inclination and 95 percent uncertainty level for sample groupings (degrees)	Deviation corrected inclination for sample groupings (degrees)
590	18.6	Therm	NIIA	
595	-24.4	Therm		
598	-25.7	Therm		
602	-23.5	Therm		
607	-29.2	Therm		
612	-28.7	Therm		
616	-22.4	Therm	-26.0 ± 1.5	
620	-26.7	Therm		
624	-24.5	Therm		
626	-28.3	Therm		
629	-26.6	Therm		
634	-25.7	Therm		
641	-16.8	Therm	NIIA	
641–643	Sediments			
644	59.5	Therm		
647	59.4	Li		
649	57.3	Li		
652	62.2	Li	59.5 ± 2.0	
656	56.5	Li		
659	60.0	Li		
663	61.5	Li		
664–667	Unrecovered core and sediment			
668	65.4	Therm		
672	64.8	Therm		
676	65.7	Li		
681	65.8	Li		
684	64.8	Li		
688	62.7	Li		
691	65.5	Li		
694	62.9	Li		
697	56.9	Li	NIIA	
699	68.9	Li	65.1 ± 0.9	
703	66.7	Li		
706	66.5	Li		
710	66.4	Li		
714	63.1	Li		
717	64.8	Li		
722	54.9	Li	NIIA	
725	62.5	Li		
728	64.8	Li		

62 Paleomagnetic Correlation of Basalt Flows in Coreholes, Idaho National Laboratory, Idaho

Table A1. Paleomagnetic inclination values for basalt samples from coreholes at and near the Idaho National Laboratory, Idaho.—
Continued

Corehole USGS 137A				
Sample depth (ft)	Characteristic remanent inclination (degrees)	Alternating field demagnetization level (mT) or alternative demagnetization approach	Average flow inclination and 95 percent uncertainty level for sample groupings (degrees)	Deviation corrected inclination for sample groupings (degrees)
NAD 27 N 43°27'03.07" W 113°02'55.62" Alt 5,053.81 ft NGVD 29 TD 1,317 ft WL 627.25 ft				
729	Petrographic boundary			
732	65.8	Therm		
735	53.9	Therm		
738	55.5	Therm		
742	46.8	Li		
745	48.4	Li		
748	48.4	Li		
750	56.8	Li		
754	51.1	Li		
758	49.6	Li		
763	52.7	Li		
766	51.5	Li		
769	55.6	Li	52.1 ± 1.3	
774	52.1	Li		
779	52.2	Li		
785	53.6	Li		
790	50.8	Li		
796	51.7	Li		
799	49.1	Li		
802	51.5	Li		
806	54.8	Li		
810	55.4	Li		
810–814	Unrecovered core and sediment			
816	-63.1	Therm		
819	-62.7	Therm		
821	-63.9	Li		
824	-65.9	Li		
831	-63.6	Li		
833	-63.5	Li		
837	-59.2	Li		
840	-63.5	Li		
843	-62.8	Li		
846	-64.8	Li		
851	-60.3	Li		
854	-65.2	Li		
858	-60.2	Li		
861	-59.8	Li		
865	-62.3	Li		
870	-60.0	Li	-62.0 ± 1.0	
872	-64.8	Li		

Table A1. Paleomagnetic inclination values for basalt samples from coreholes at and near the Idaho National Laboratory, Idaho.—
Continued

Corehole USGS 137A				
Sample depth (ft)	Characteristic remanent inclination (degrees)	Alternating field demagnetization level (mT) or alternative demagnetization approach	Average flow inclination and 95 percent uncertainty level for sample groupings (degrees)	Deviation corrected inclination for sample groupings (degrees)
NAD 27				
N 43°27'03.07"				
W 113°02'55.62"				
Alt 5,053.81 ft				
NGVD 29				
TD 1,317 ft				
WL 627.25 ft				
874	-61.1	Li		
877	-63.7	Li		
880	-61.9	Li		
884	-60.6	Li		
887	-66.2	Li		
893	-60.7	Li		
897	-57.9	Li		
899	-55.9	Li		
902	-61.8	Li		
906	-59.5	Li		
909	-64.8	Li		
912	-56.7	Li		
912	Petrographic boundary			
914	-62.7	Li		
917	-57.6	Li		
920	-61.9	Li		
923	-60.0	Li		
926	-57.8	Li		
931	-58.1	Li		
937	-57.5	Li		
943	-57.0	Li		
949	-59.1	Li	-58.5 ± 0.7	
954	-57.4	Li		
960	-58.5	Li		
963	-59.7	Li		
967	-58.7	Li		
970	-58.8	Li		
976	-58.3	Li		
979	-57.3	Li		
980–982	Sediments			
983	-66.7	Therm	-57.0 - OP	
986	-63.0	Therm	-59.0 - OP	
988	-64.8	Therm		
991	-68.3	Li		
994	-67.0	Li	-65.1 ± 2.7	
988	-63.4	Li		
992	-68.4	Li		
995	-59.4	Li		
1,001	Petrographic boundary			
1,002	-65.5	Li		

Table A1. Paleomagnetic inclination values for basalt samples from coreholes at and near the Idaho National Laboratory, Idaho.—
Continued

Corehole USGS 137A				
Sample depth (ft)	Characteristic remanent inclination (degrees)	Alternating field demagnetization level (mT) or alternative demagnetization approach	Average flow inclination and 95 percent uncertainty level for sample groupings (degrees)	Deviation corrected inclination for sample groupings (degrees)
NAD 27				
N 43°27'03.07"				
W 113°02'55.62"				
Alt 5,053.81 ft				
NGVD 29				
TD 1,317 ft				
WL 627.25 ft				
1,005	-65.6	Li		
1,009	-66.6	Li		
1,012	-65.7	Li		
1,016	-66.7	Li		
1,020	-65.4	Li		
1,024	-65.9	Li		
1,027	-62.6	Li		
1,030	-75.6	Li	NIA	
1,032	-64.5	Li		
1,036	-66.5	Li		
1,040	-66.2	Li		
1,044	-68.1	Li	-65.4 ± 0.6	
1,048	-64.7	Li		
1,051	-63.8	Li		
1,053	-63.1	Li		
1,057	-63.2	Li		
1,062	-64.3	Li		
1,066	-64.1	Li		
1,071	-64.6	Li		
1,075	-67.4	Li		
1,079	-63.7	Li		
1,082	-67.3	Li		
1,085	-66.3	Li		
1,087	-67.2	Li		
1,088	Sediments			
1,090	-71.2	Therm	-66.0 - OP	
1,094	-67.4	Therm	NIA	
1,097	-72.3	Therm		
1,101	-71.7	Li		
1,103	-73.2	Li		
1,105	-73.3	Li		
1,108	-76.4	Li		
1,111	-74.3	Li		
1,114	-73.0	Li		
1,119	-74.2	Li		
1,123	-72.6	Li		
1,128	-73.1	Li		
1,132	-71.6	Li		
1,135	-71.9	Li		
1,138	-72.6	Li		
1,141	-73.8	Li	-73.6 ± 0.9	

Table A1. Paleomagnetic inclination values for basalt samples from coreholes at and near the Idaho National Laboratory, Idaho.—
Continued

Corehole USGS 137A				
Sample depth (ft)	Characteristic remanent inclination (degrees)	Alternating field demagnetization level (mT) or alternative demagnetization approach	Average flow inclination and 95 percent uncertainty level for sample groupings (degrees)	Deviation corrected inclination for sample groupings (degrees)
1,146	-75.2	Li		
1,149	-75.2	Li		
1,153	-70.1	Li		
1,157	-68.3	Li		
1,161	-70.7	Li		
1,165	-72.2	Li		
1,169	-77.0	Li		
1,173	-76.5	Li		
1,178	-74.8	Li		
1,184	-74.3	Li		
1,190	-77.6	Li		
1,198	-76.3	Li		
1,200	Petrographic boundary			
1,201	-73.9	Therm		
1,203	-77.3	Therm		
1,207	-71.5	Li		
1,211	-70.8	Li		
1,216	-72.2	Li		
1,219	-68.9	Li		
1,222	-68.8	Li		
1,224	-70.5	Li		
1,227	-72.4	Li		
1,232	-75.3	Li		
1,238	-78.4	Li		
1,242	-72.1	Li		
1,248	-73.2	Li		
1,253	-69.5	Li		
1,258	-69.8	Li	-71.0 ± 1.0	
1,263	-71.9	Li		
1,267	-69.6	Li		
1,271	-72.2	Li		
1,276	-68.4	Li		
1,281	-71.3	Li		
1,286	-72.2	Li		
1,290	-70.7	Li		
1,296	-70.8	Li		
1,301	-69.9	Li		
1,306	-68.0	Li		
1,312	-67.3	Li		
1,317	-68.9	Li		

Publishing support provided by the U.S. Geological Survey
Science Publishing Network, Tacoma Publishing Service Center
For more information concerning the research in this report, contact the
Director, Idaho Water Science Center
U.S. Geological Survey
230 Collins Road
Boise, Idaho 83702
<http://id.water.usgs.gov>

